Electronic Supplementary Material (ESI) for Chemical Communications.

Supporting Information

Dual Catalysis for the Copolymerisation of Epoxides and Lactones

Naomi E. Clayman,[a,†] Lilliana S. Morris,[b,†] Anne M. LaPointe,[b] Ivan Keresztes,[b] Robert M. Waymouth,[a,*] and Geoffrey W. Coates[b,*]

[a]*Department of Chemistry, Stanford University, Stanford, California 94305-5080, United States*
[b]*Department of Chemistry and Chemical Biology, Cornell University, Ithaca, New York, 14853-1301, United States*

Table of Contents

General Experimental Description

All reactions and subsequent manipulations were performed under N_2 using a glovebox or Schlenk line. Flash column chromatography was performed using silica gel (particle size 40–64 μm, 230–400 mesh). All reagents were purchased from commercial vendors and were used as received unless otherwise noted. 1,2-Dimethoxyethane (DME) was purchased from Fisher Scientific and dried by stirring over calcium hydride for 24 hours or over Na/benzophenone for 3 days, followed by distillation under vacuum into a Straus storage flask. The solvent was then degassed through three freeze-pump-thaw cycles. All monomers were purchased from Sigma Aldrich and were dried by stirring over excess calcium hydride for three days and distilled under vacuum before being taken through three freeze-pump-thaw cycles. 1,8-Diazabicyclo[5.4.0]undece-7-ene was dried by stirring over excess calcium hydride for 3 days, distilled under vacuum, and taken through three freeze-pump-thaw cycles. SalcyCrCl was purchased from Strem and recrystallized from a super-saturated solution in acetonitrile. Deuterated solvents were purchased from Cambridge Isotope Laboratory.

NMR spectra were acquired on Varian Inova spectrometers (^{1}H, 500 or 600 MHz), or a Bruker AV III HD spectrometer with broadband Prodigy Cryoprobe (^{1}H, 500 MHz). All NMR spectra were taken in $CDCl_3$ at 25 °C. ^{1}H NMR spectra were referenced using residual solvent shifts ($CHCl_3$ = 7.26 ppm). ^{13}C NMR spectra were referenced by solvent shifts ($CDCl_3$ = 77.16 ppm). All NMR spectra were processed using MestReNova software package. Gel permeation chromatography (GPC) analyses were carried out using an Agilent 1260 Infinity GPC System equipped with an Agilent 1260 Infinity autosampler and a refractive index detector. The Agilent GPC system was equipped with two Agilent PolyPore columns (5 micron, 4.6 mm ID) which were eluted with THF at 30 °C at 0.3 mL/min and calibrated using monodisperse polystyrene standards. Differential scanning calorimetry (DSC) measurements were carried out using a Mettler-Toledo Polymer DSC instrument equipped with a chiller and autosampler. Polymers were prepared in aluminum pans with the heating program: -70 °C for 10 min, -70 °C to 200 °C at 10 °C/min, 200 °C to -70 °C at 10 °C/min, -70 °C for 10 min, and -70 °C to 200 °C at 10 °C/min. Data were processed with StarE software. All reported melting temperatures and enthalpies were observed on the second heat.

Calculation of M_n Theoretical

Theoretical molecular weights were calculated according to the following equation:

$$M_n theo. = \frac{\left((g\ lactone) \times \left(\frac{\%\ conversion\ lactone}{100}\right)\right) + \left((g\ PO) \times \left(\frac{\%\ conversion\ PO}{100}\right)\right)}{(mmol\ 1,6-hexanediol) + (mmol\ Cr\ cat)}$$

Determination of Polymer Tacticity

Polymer tacticity was determined by integration of the triad signals in the ^{13}C NMR spectrum of purified polymer, according to previously published equations.[1] As incorporation of lactone increased and crystallinity decreased, the triad signal disappeared from the ^{13}C NMR spectra (Figure S1). When applicable, these samples have been noted as having an unresolvable triad region.

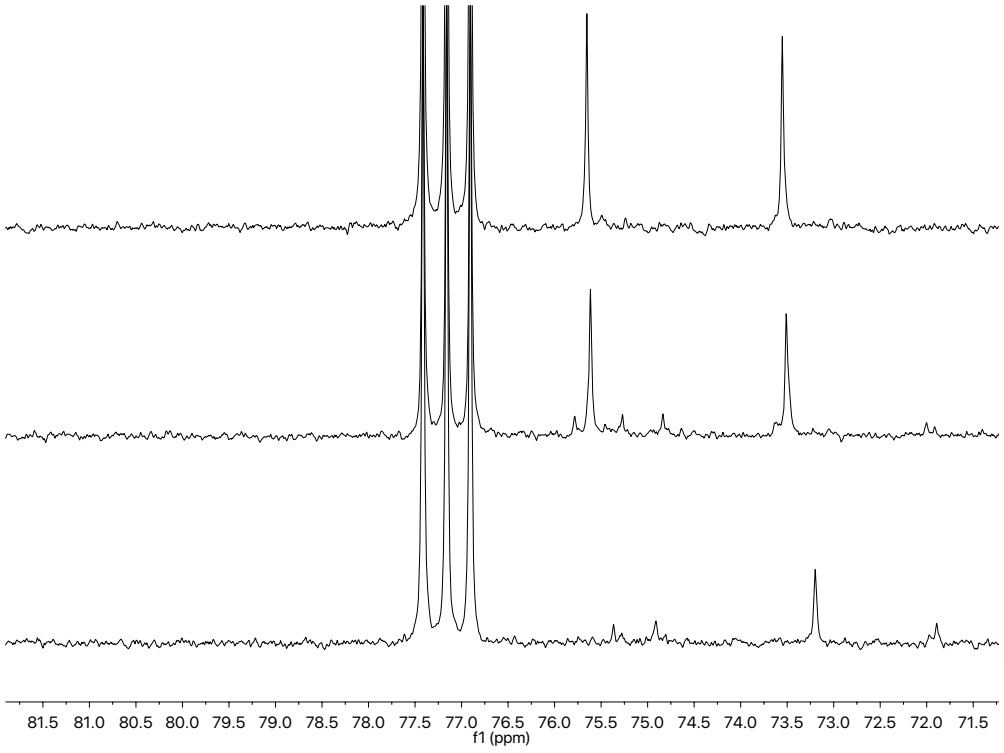

Figure S1. Expanded region of the ^{13}C NMR spectrum of purified PO-VL copolymers with a feed ratio of $[PO]_0$:$[VL]_0$ 100:1 (top), 10:1 (middle), and 1:1 (bottom). Peak at 75.65 ppm indicative of the [*mm*] triad of isotactic PPO, this peak disappears at a feed ratio of 1:1 due to high lactone incorporation.

Determination of VL-PO Sequence by ^{1}H NMR

A COSY spectrum was taken of a VL-PO copolymer with a 1:1 monomer feed ratio to assist with assignment of the peaks arising from crossover between one homopolymer to the other (Figure S2). Using this information, the peaks of the ^{1}H NMR spectrum were assigned, with unique peaks present for specific polymer sequences (Figure S3).

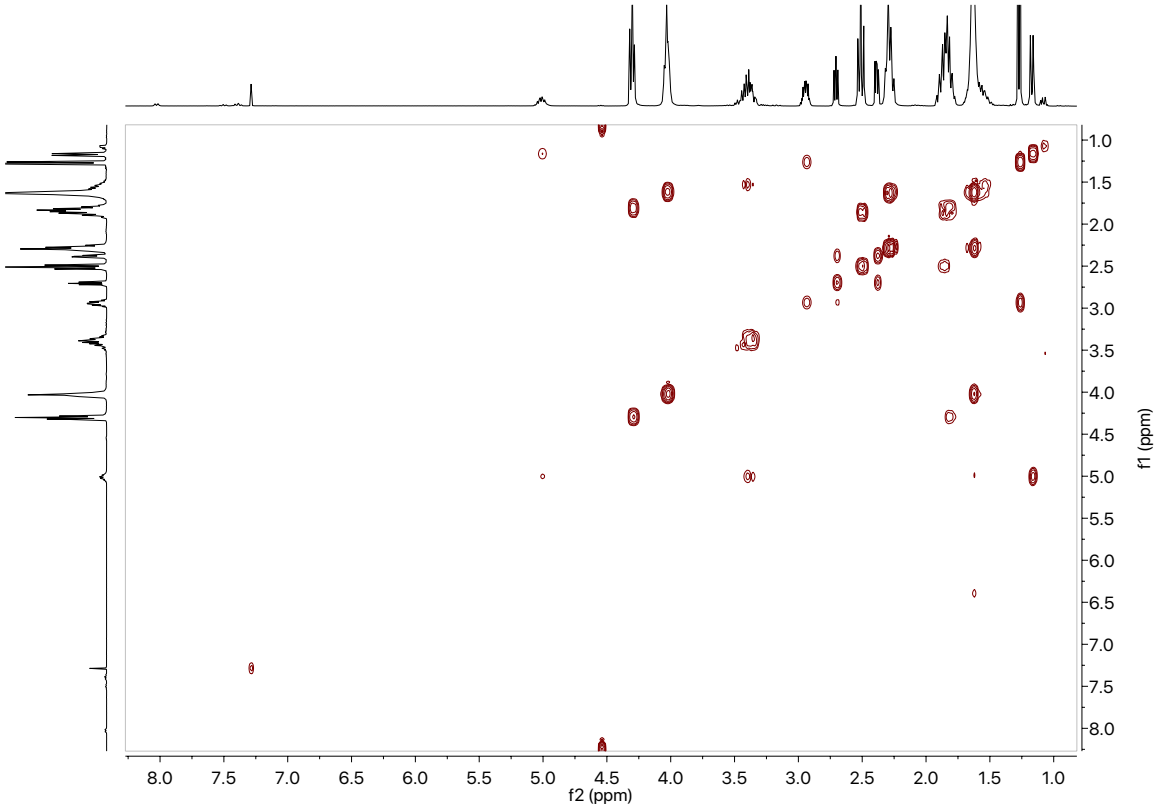

Figure S2. COSY Spectrum of a PO:VL copolymer with a feed ratio of 1:1. Cross peaks allow assignment of monomer sequence (see Figure S3).

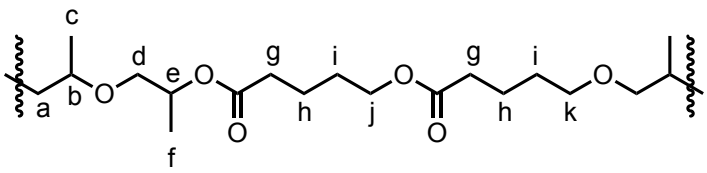

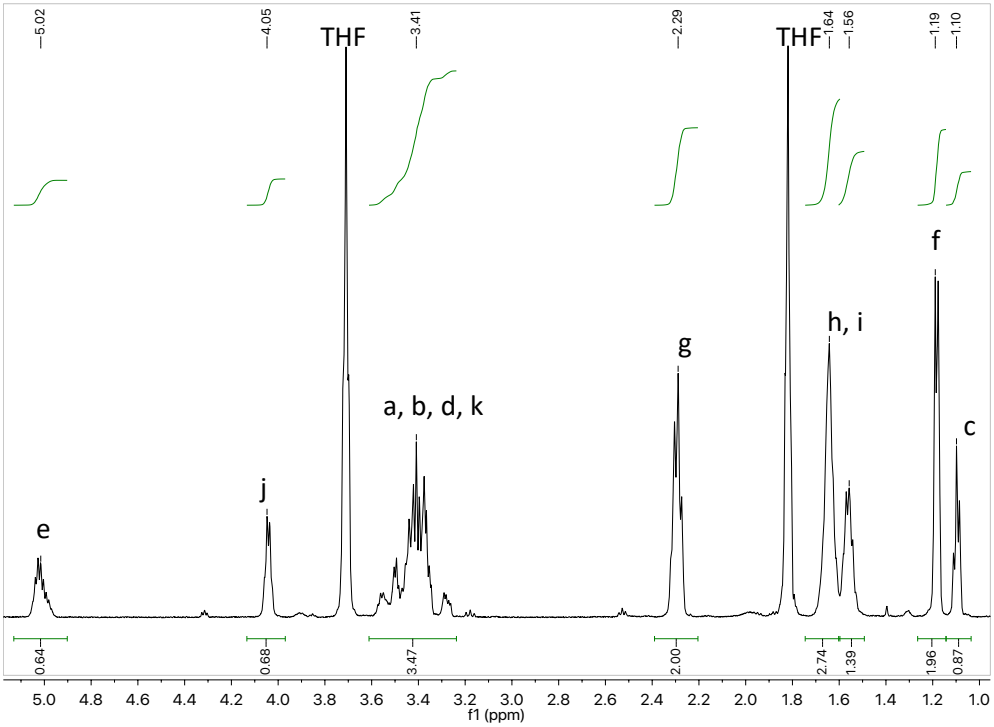

Figure S3. Expanded region of the ^{1}H NMR spectrum of PO-VL copolymer with a monomer feed ratio of $[PO]_0$:$[VL]_0$ = 1:1 after purification by dialysis against THF, with peak assignments. Structure of molecule represents the molecule with all possible two monomer sequences (PO-VL [peaks d, e, f], PO-PO [peaks a, b, c], VL-VL [peaks g, h, i, j], VL-PO [peaks not distinct, determined by subtraction from other possible sequences]) responsible for different signals in the spectrum. Ratio of PO-VL to PO-PO determined by comparison of integrations of peaks f and c. Ratio of VL-PO and VL-VL determined by comparison of integrations of j and g. Small peaks at 3.9 ppm and 1.3 ppm are from the hexanediolate midsegment.

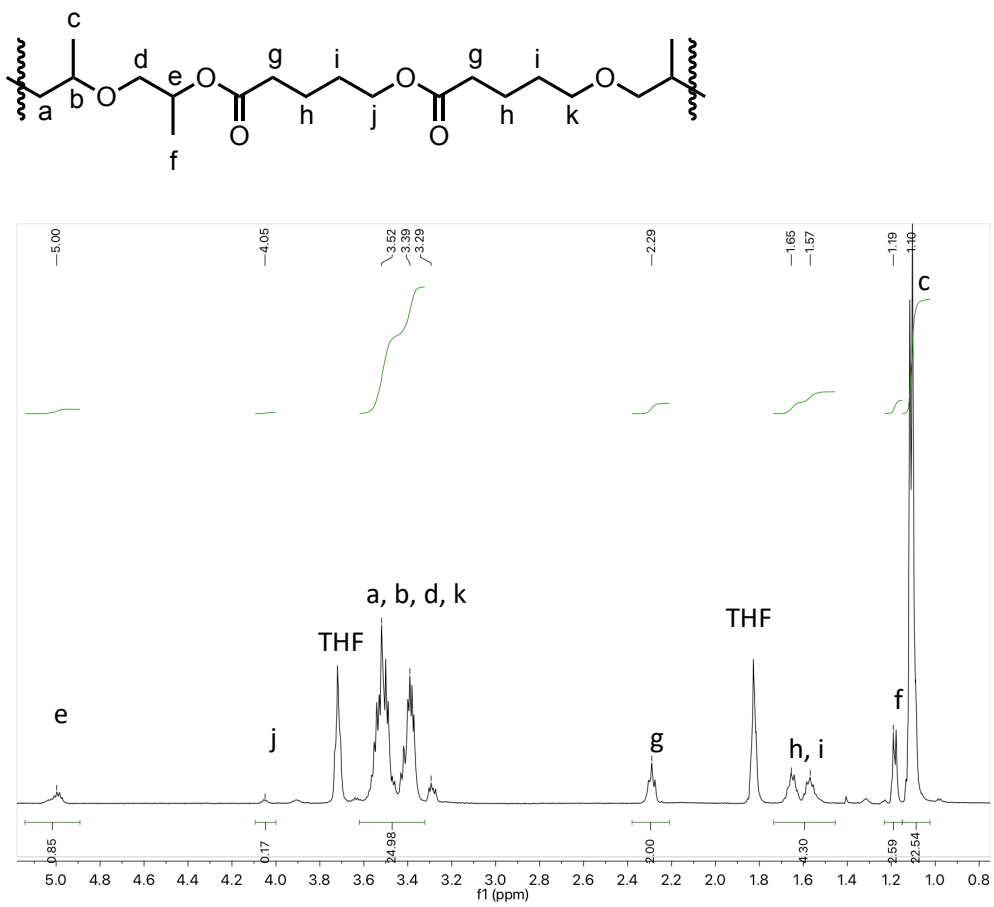

Figure S4. Expanded region of the ^{1}H NMR spectrum of PO-VL copolymer with a monomer feed ratio of $[PO]_0$:$[VL]_0$ = 10:1 after purification by dialysis against THF with peak assignments.

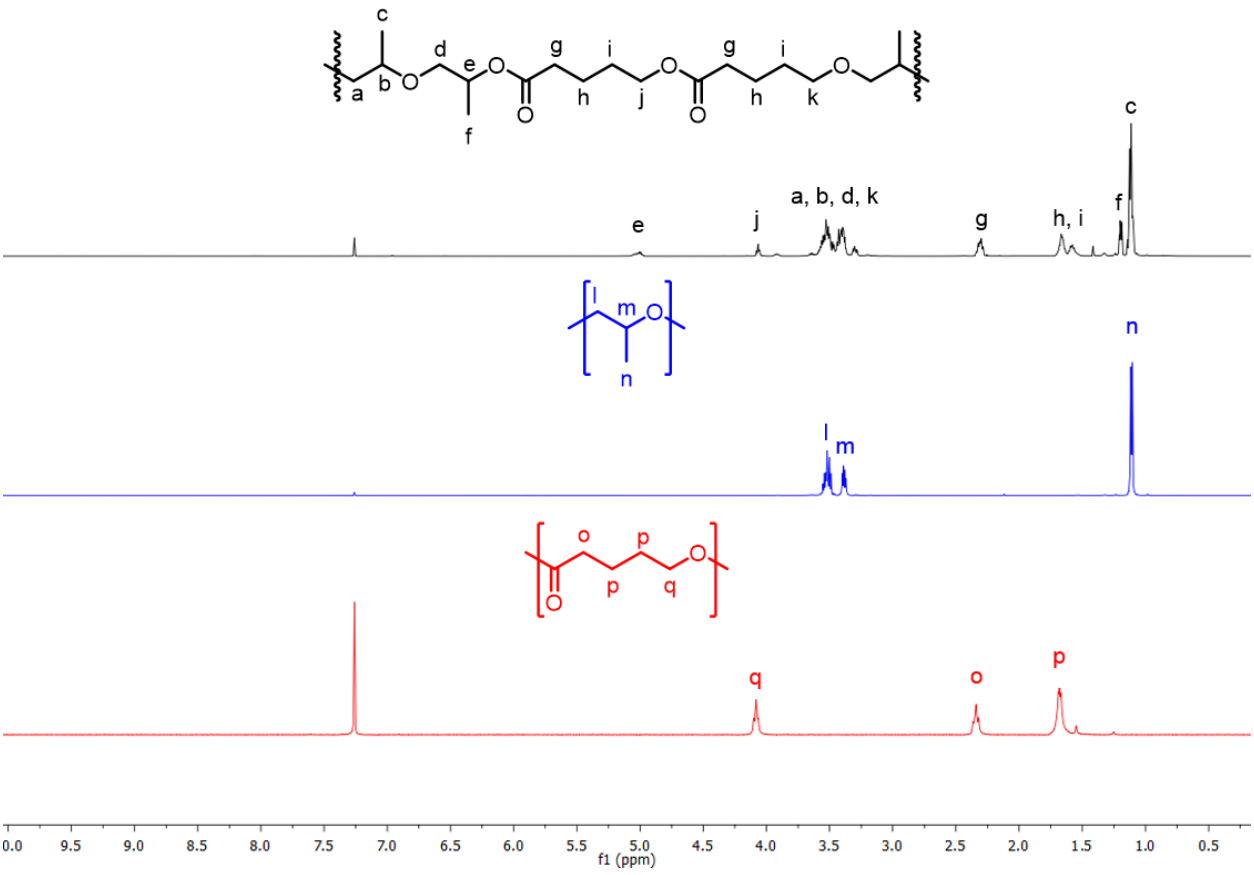

Figure S5. Stacked ^{1}H NMR spectra of PO-VL copolymer, *i*PPO homopolymer, and VL homopolymer.

Assignment of Peaks in BL-PO Copolymer

The peaks of the BL-PO copolymer were assigned based on the assignment of copolymer peaks in the ^{1}H NMR of the VL-PO copolymer.

Assignment of Peaks in CL-PO Copolymer

The peaks of the CL-PO polymer were assigned based on the assignment of copolymer peaks in the ^{1}H NMR of the VL-PO copolymer.

Synthetic Procedures

Bimetallic chromium catalyst (**1**) and [PPN][OAc^{F3}] were synthesized according to reported procedures.[2]

Compatibility studies: Compatibility of 1,8-diazabicyclo[5.4.0]undec-7-ene (DBU) with a monometallic chromium salen complex (Figure S6) was assessed with a polymerisation of *L*-lactide. Two polymerisations were set up in tandem: two 20 mL vials were each charged with *L*-lactide (200 mg, 1.39 mmol), DBU (2.1 uL, 0.014 mmol), pyrene butanol (3.8 mg, 0.014 mmol) in 3 mL DME. To one vial was added Cr-salen complex (5.7 mg, 0.014 mmol). Time point aliquots were removed and quenched with excess benzoic acid. *L*-Lactide conversion to polylactide was determined by ^{1}H NMR. Final conversion of the polylactide without Cr additive was 88.6%, with Cr was 71.2%.

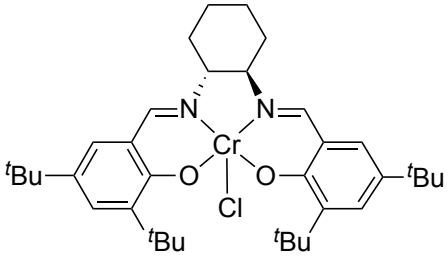

Figure S6. Monomeric Cr-salen (SalcyCrCl) that was used to assess compatibility of DBU polymerisation with **1**.

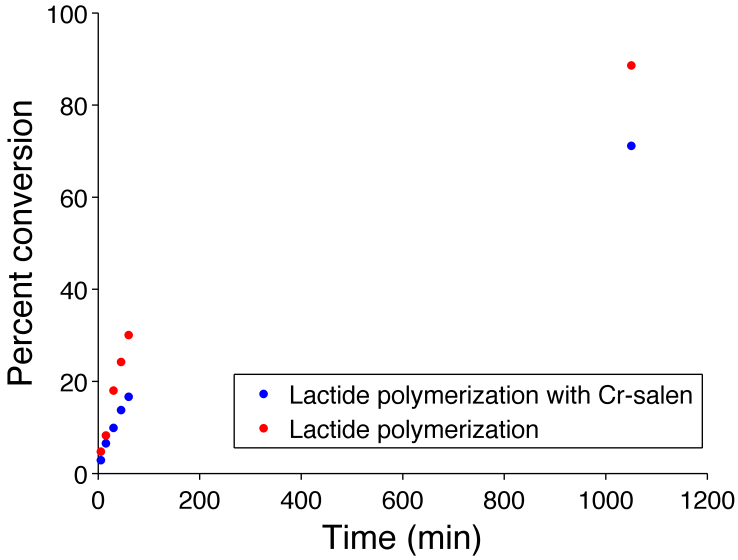

Figure S7. Conversion of *L*-lactide to polylactide in the presence and absence of Cr-salen.

The compatibility of the bimetallic chromium catalyst polymerisation to the addition of DBU was evaluated. To 20 mL vials with a septum cap, chromium catalyst (0.4 mg, $0.3x10^{-3}$ mmol), [PPN][OAc^{F3}] (0.2 mg, $0.3x10^{-3}$ mmol), 1,6-hexanediol (0.7 mg, $0.6x10^{-3}$ mmol), propylene oxide (PO) (279 mg, 4.8 mmol), DME (0.95 mL), and DBU (0 mmol or $0.8x10^{-3}$ mmol) were added. The polymerisations were sealed and allowed to stir. The polymerisations were quenched by removal of volatiles *in vacuo*. Conversion was evaluated by mass. Time points were evaluated by separate polymerisations. Conversion of PO without DBU present was 17% while the polymerisation went to 12% conversion in the presence of DBU with the same reaction time (Figure S8).

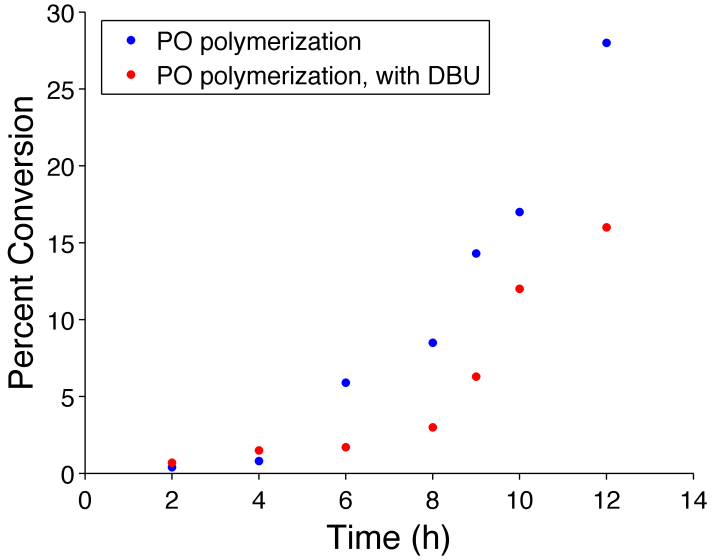

Figure S8. Conversion of PO to *i*PPO in the presence and absence of DBU.

General polymerisation procedure for propylene oxide-δ-valerolactone copolymers:

A 20 mL scintillation vial with a stir bar was charged with chromium catalyst (2.0 mg, $1.4x10^{-3}$ mmol), [PPN][OAc^{F3}] (0.9 mg, $1.4x10^{-3}$ mmol), 1,6-hexanediol (1.6 mg, 0.014 mmol), and DBU (1.0 mg, $6.9x10^{-3}$ mmol). Propylene oxide (PO) and valerolactone (VL) were added in ratios of PO:VL = 1:1 (0.81 mL, 8.9 mmol VL; 0.62 mL, 8.9 mmol PO), 10:1 (0.08 mL, 0.89 mmol VL; 0.62 mL 8.9 mmol PO), or 100:1 (0.0080 mL, 0.089 mmol VL; 0.62 mL, 8.9 mmol PO). Reactions were stirred in an N_2 filled glovebox. Time point aliquots of 200 uL for kinetics

measurements were removed and quenched with excess benzoic acid, and volatiles were removed *in vacuo*. Conversion was determined by NMR integration relative to residual VL monomer. Polymers were purified by dialysis against tetrahydrofuran (THF) in Spectra/Por3 3.5k dialysis tubing.

General Polymerisation procedure for propylene oxide-γ-butyrolactone copolymers:

An 8 mL scintillation vial with a stir bar and septum cap was charged with chromium catalyst (2.0 mg, $1.4x10^{-3}$ mmol), [PPN][OAc^{F3}] (0.9 mg, $1.4x10^{-3}$ mmol), 1,6-hexanediol (1.6 mg, 0.014 mmol) and DBU (1.0 mg, $6.9x10^{-3}$ mmol). Propylene oxide (480 mg, 8.3 mmol) and γ-butyrolactone (0.083, 0.83, or 8.3 mmol) were added and the vial was sealed and allowed to stir. The reaction was quenched with excess benzoic acid and an aliquot was taken to evaluate conversion via ^{1}H NMR peaks. Excess propylene oxide was removed from the reaction mixture *in vacuo* before the polymer was purified by dialysis against tetrahydrofuran (THF) in Spectra/Por3 3.5k dialysis tubing.

General Polymerisation procedure for propylene oxide-ε-caprolactone copolymers:

An 8 mL scintillation vial with a stir bar and septum cap was charged with chromium catalyst (2 mg, $1.4x10^{-3}$ mmol), [PPN][OAc^{F3}] (0.9 mg, $1.4x10^{-3}$ mmol), 1,6-hexanediol (1.6 mg, 0.014 mmol) and DBU (1.0 mg, $6.9x10^{-3}$ mmol). Propylene oxide (480 mg, 8.3 mmol) and ε-caprolactone (0.083, 0.83, or 8.3 mmol) were added and the vial was sealed and allowed to stir. The reaction was quenched with excess benzoic acid and excess propylene oxide was removed from the reaction mixture *in vacuo*. Conversion of PO was evaluated by mass and conversion of lactone was evaluated by integration of a crude ^{1}H NMR spectrum before the polymer was purified by dialysis against tetrahydrofuran (THF) in Spectra/Por3 3.5k dialysis tubing.

Variation of CSA and Lactone Loading

The loading of δ-valerolactone (VL), γ-butyrolactone (BL), and ε-caprolactone (CL) were varied against the loading of propylene oxide (PO) (Table S1). Additionally, the loading of 1,6-hexanediol (HD) was varied against each of these monomer loadings to yield a library of copolymers with a range of ester contents and crystallinities.

Table S1. Effect of lactone (L), $[PO]_0$:$[L]_0$ feed ratios, and 1,6-hexanediol CTA loading on copolymerisation

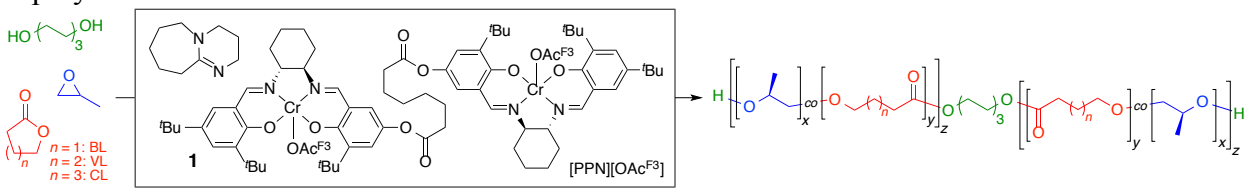

Entry	L	PO:L	HD:1	Conv. L[b] (%)	Conv. PO[c] (%)	% Ester[b]	M_n theo.[d] (kDa)	M_n exp.[e] (kDa)	$Đ$[e]	[*mm*][f]	T_m[g] (°C)	ΔH_{fus} (J/g)
1	VL	10:1	5	12	11	8.8	8.9	7.9	1.26	97	35, 45	-60
2	VL	1:1	5	8	5	47.8	10.8	5.6	1.19	-[h]	27	33
3	VL	10:1	20	28	11	15.2	2.8	4.6	1.09	-[h]	18	0.1
4	VL	1:1	20	17	14	48.9	7.7	7.3	1.13	-[h]	18	9
5	CL	100:1	5	19	30	0.4	20.4	18.9	1.10	93	59	64
6	CL	10:1	5	5	28	1.4	18.8	4.6	1.09	94	58	71
7	CL	1:1	5	2	3	22.2	3.6	-[i]	-[i]	-[h]	46, 51	44
8	CL	100:1	10	12	24	0.2	6.8	13.7	1.08	94	58	74
9	CL	1:1	10	3	1	43.6	2.0	-[i]	-[i]	-[h]	30, 38	56
10	CL	100:1	20	9	16	0.2	3.0	4.6	1.06	95	51	31
11	CL	10:1	20	22	12	13.6	2.9	4.4	1.19	98	40	49
12	CL	1:1	20	4	11	38.7	3.0	-[i]	-[i]	-[h]	31	12
13	BL	100:1	5	11	4[b]	3.2	3.0	2.9	1.07	95	37	53
14	BL	10:1	5	3	4[b]	8.7	2.3	-[i]	-[i]	92	13	23
15	BL	1:1	5	1	3[b]	18.2	2.2	-[k]	-[k]	-[k]	-[k]	-[k]
16	BL	100:1	10	9	13[b]	1.2	4.3	10.5	1.11	94	58	90
17	BL	1:1	10	1	2[b]	17.9	1.0	-[k]	-[k]	-[k]	-[k]	-[k]
18	BL	100:1	20	10	8[b]	2.3	1.3	2.7	1.16	94	34	66
19	BL	10:1	20	4	4[b]	11.8	0.7	-[i]	-[i]	-[h]	-[l]	-[l]
20	BL	1:1	20	1	4[b]	19.2	1.0	-[k]	-[k]	-[k]	-[k]	-[k]

[a] Polymerisation conditions: 2.0 mg **1**; $[PO]_0$:$[\mathbf{1}]_0$:$[[PPN][OAc^{F3}]]_0$:$[DBU]_0$ = 6000:1:1:5; t_{rxn} = 6h. [b] Determined by ^{1}H NMR spectroscopy. [c] Determined gravimetrically. [d] See Supplementary Equation 1. [e] Determined by GPC relative to polystyrene standards at 30 °C in THF. [f] Determined by ^{13}C NMR spectroscopy. [g] Determined by DSC. [h] no [*mm*] peaks resolvable. [i] Due to low molecular weight of the sample, this peak fell outside the calibration region. [k] Not determined due to the small size of the sample. [l] No T_m determined for this sample.

The trends for these copolymers mirror those observed in the main text. For all loadings of hexanediol, as VL loading increases, ester content of the final polymer also increases (Table S1, Entries 1–4). However, the higher loading of chain shuttling agent in these polymerisations leads to increased lactone conversion and decreased melting temperatures. For ε-caprolactone derived copolymers, overall ester content is lower than in valerolactone analogues (Table S1, Entries 5–

12). These polymers exhibited increased ester content with increased lactone loading, and decreased melting point with increased lactone or 1,6-hexanediol loading. Finally, γ-butyrolactone derived polymers were small, and therefore could not be characterized with all methodologies (Table S1, Entries 13–20). Ester content increased with increased lactone or chain shuttling agent loading, with T_m loss observed earlier than in other copolymers. Overall, all copolymers showed increased ester content and decreased melting point with increases in lactone or 1,6-hexanediol loading.

Extension of Reaction Times to Achieve Higher Conversions

To achieve higher conversions and ensure chains were not terminating early, copolymerisations were run for longer periods of time while conversions of both VL and PO were monitored (Figures S9 – 11). These reactions used the kinetics conditions from the main text of $[PO]_0$:$[1]_0$: $[[PPN][OAc^{F3}]]_0$:$[DBU]_0$:$[HD]_0$ = 6000:1:1:5:10.

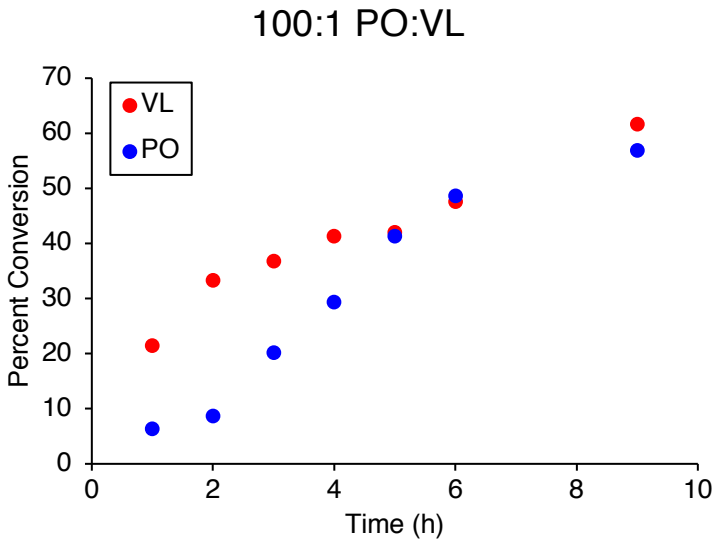

Figure S9. Conversion of PO and VL to copolymer at $[PO]_0$:$[VL]_0$ = 100:1.

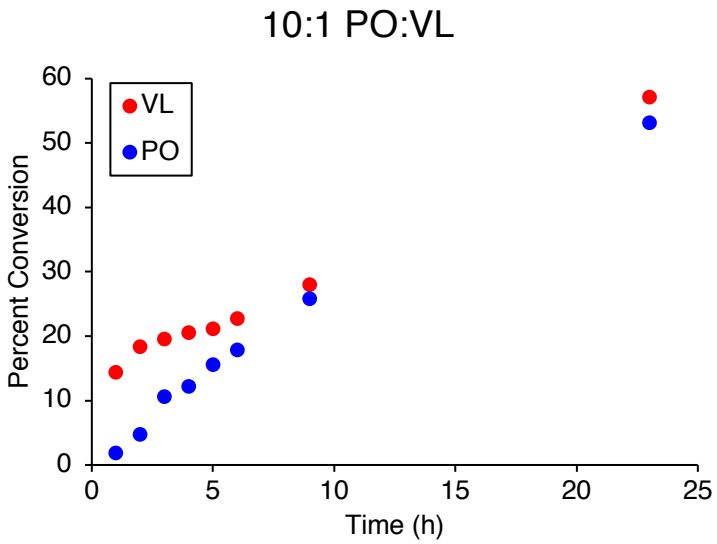

Figure S10. Conversion of PO and VL to copolymer at $[PO]_0$:$[VL]_0$ = 10:1.

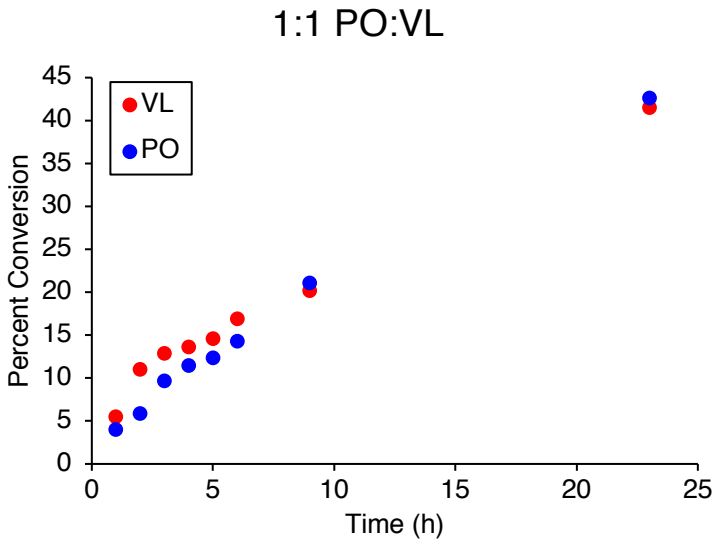

Figure S11. Conversion of PO and VL to copolymer at $[PO]_0$:$[VL]_0$ = 1:1.

Copolymer Degradation

To confirm the presence of ester units throughout the backbone of the polymer, 20 mg of a PO-VL copolymer with 50% ester content and an M_n of 10.8 kDa was added to a 4 mL of a 0.5 M NaOH solution that was prepared with 50% (v/v) MeOH in H_2O. Aliquots were taken, extracted with dichloromethane, and dried with sodium sulfate before being analyzed be GPC. Within 7

hours, the polymer had degraded outside the calibration region of the GPC and within 24 hours a significant decrease in molecular weight and broadening of the peak had occurred (Figure S12). The rapid degradation of the copolymer and broadening of dispersity confirm the presence of ester units throughout the polymer backbone. The ester enrichment early in the polymerisation likely contributes to the significant broadening of the peak observed during degradation.

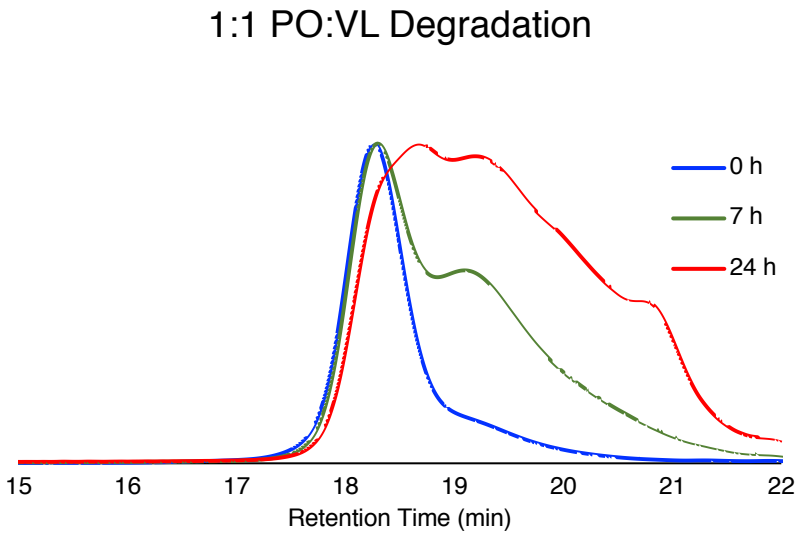

Figure S12. GPC chromatograms of a PO-VL copolymer before and after 7 and 24 hours of degradation in basic solution.

DECRA Experiments to Confirm Lack of Contamination

To confirm that the polymer formed in the copolymerization system was exclusively copolymer with no homopolymer contaminant, several diffusion NMR experiments were performed on a Varian INOVA 600 MHz spectrometer equipped with a 5mm inverse, triple-resonance probehead. Experiments were performed in $CDCl_3$ at 25°C with the "DgcsteSL_cc" pulse sequence as provided in VnmrJ 3.2A. Square diffusion gradients were used with strength varying from 3 to 76 G/cm in 16 quadratic increments. Diffusion gradient duration (δ = 1.5 ms) and diffusion delay (Δ = 200 ms) were adjusted to collect three half-lives of exponential decay (~87% maximum polymer signal attenuation). The experiments were analyzed using direct exponential curve resolution algorithm (DECRA)[3] as implemented in the General NMR Analysis Toolbox (GNAT).[4] DECRA was recently shown to detect minor homopolymer impurities in block copolymer samples.[5]

A diffusion NMR experiment was performed on a VL-PO copolymer sample (PO:VL 10:1, Table 1, Entry 4). DECRA analysis with three components produced two spectra with clean, exponential decay profiles: the expected copolymer (Figure S13, middle) and $CDCl_3$ (Figure S13, bottom). The spectrum of the third component (Figure S13, top) was similar to the copolymer but showed phase errors and very little decay, indicating that it arose from spectral artifacts in the diffusion dataset. To confirm that DECRA would have identified homopolymer contaminants, another diffusion experiment was performed on a sample of CL-PO (Table S1, Entry 7) dosed with 10 % *i*PPO homopolymer. DECRA analysis with four components (Figure S14) resulted in three components with clean, exponential decays: the copolymer(top), homopolymer (second from top), and $CDCl_3$ (bottom). The spectra of the co- and homopolymers were distinguishable by the presence of minor resonances corresponding to the ester component in the former. The spectrum for the fourth component consisted entirely of noise. These results confirm that a homopolymer contaminant would have been detected in the VL-PO sample.

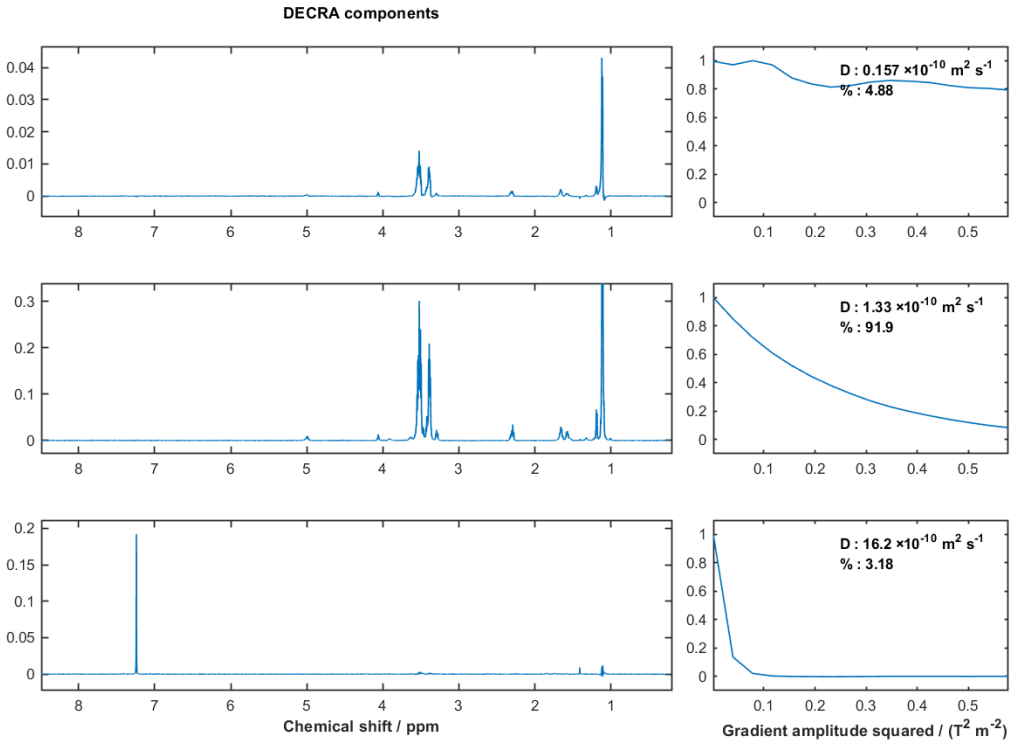

Figure S13. DECRA analysis of VL-PO copolymer (PO:VL 10:1, Table 1, Entry 4) fitted to 3 components showing noise (top), copolymer (middle), and chloroform (bottom).

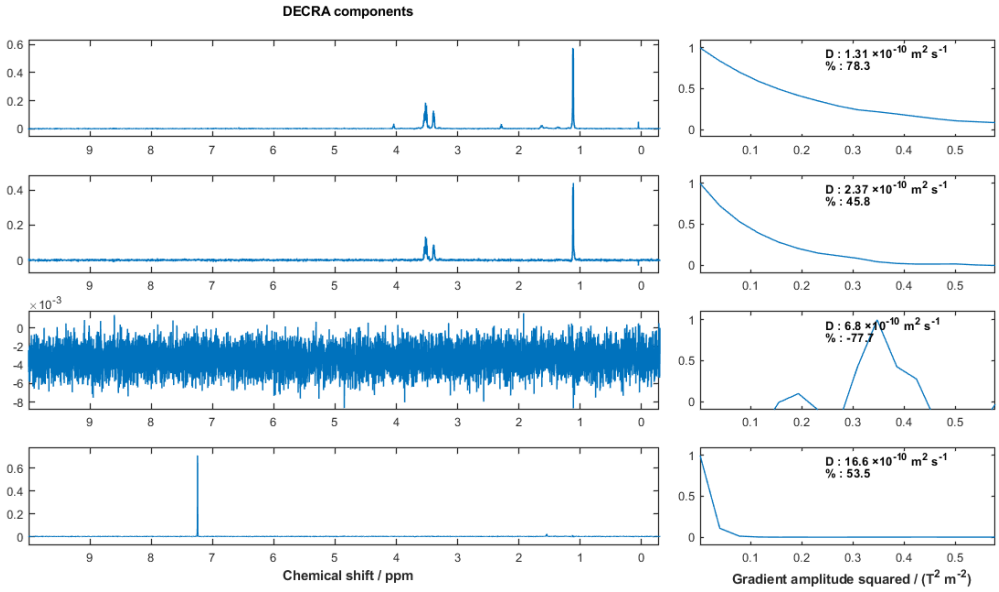

Figure S14. DECRA analysis of a CL-PO copolymer (Table S1, Entry 7) with added *i*PPO homopolymer fitted to 4 components, showing copolymer (top), *i*PPO homopolymer (second), noise (third), and chloroform (bottom).

^{1}H and ^{13}C NMR Spectra, GPC Chromatograms, and DSC Thermograms

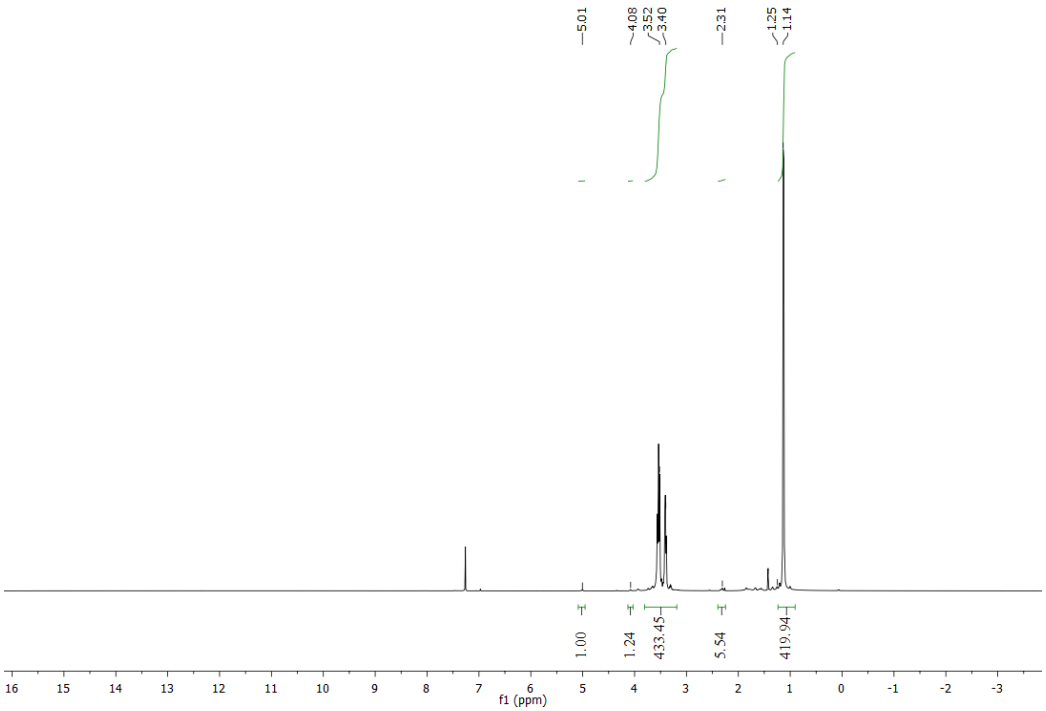

Figure S15. ^{1}H NMR spectrum of PO-VL copolymer from Table 1, Entry 1.

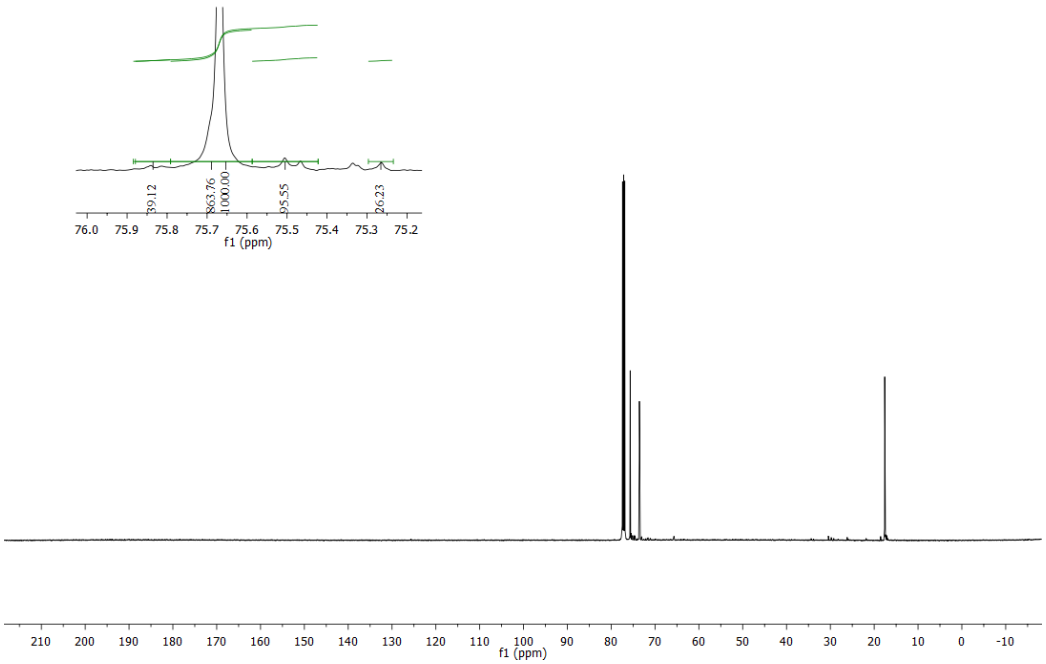

Figure S16. ^{13}C NMR spectrum of PO-VL copolymer from Table 1, Entry 1.

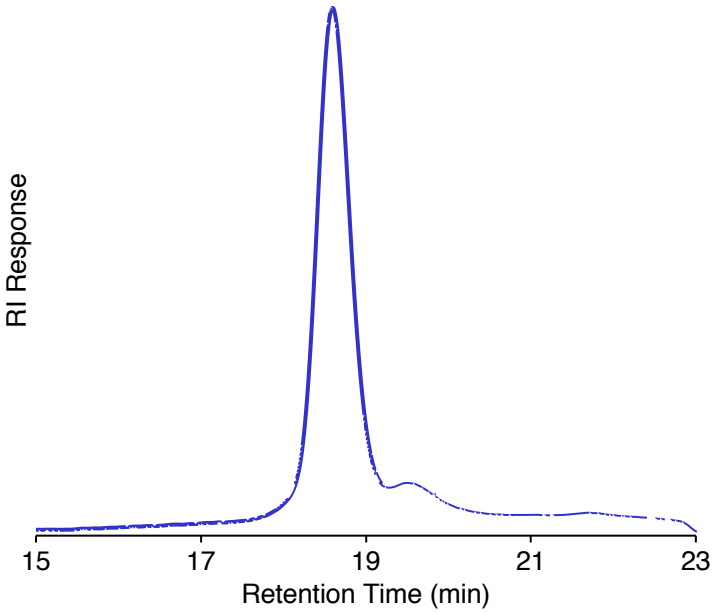

Figure S17. GPC chromatogram of PO-VL copolymer from Table 1, Entry 1.

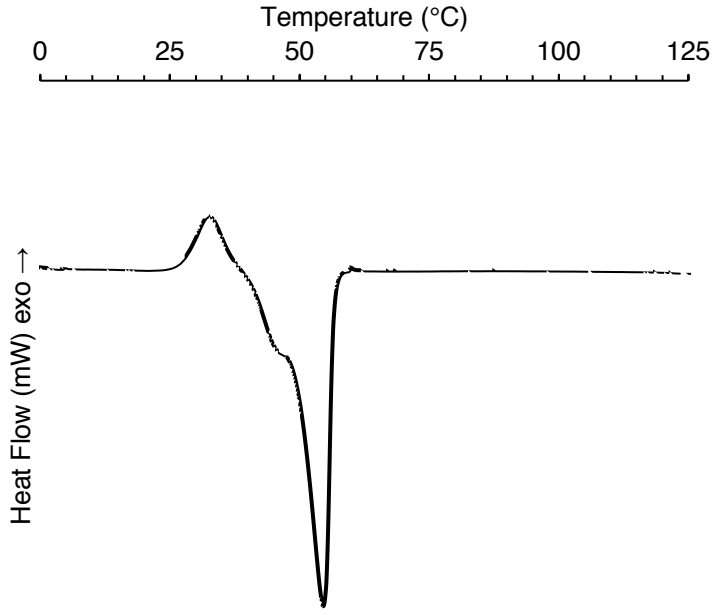

Figure S18. DSC thermogram of PO-VL copolymer from Table 1, Entry 1.

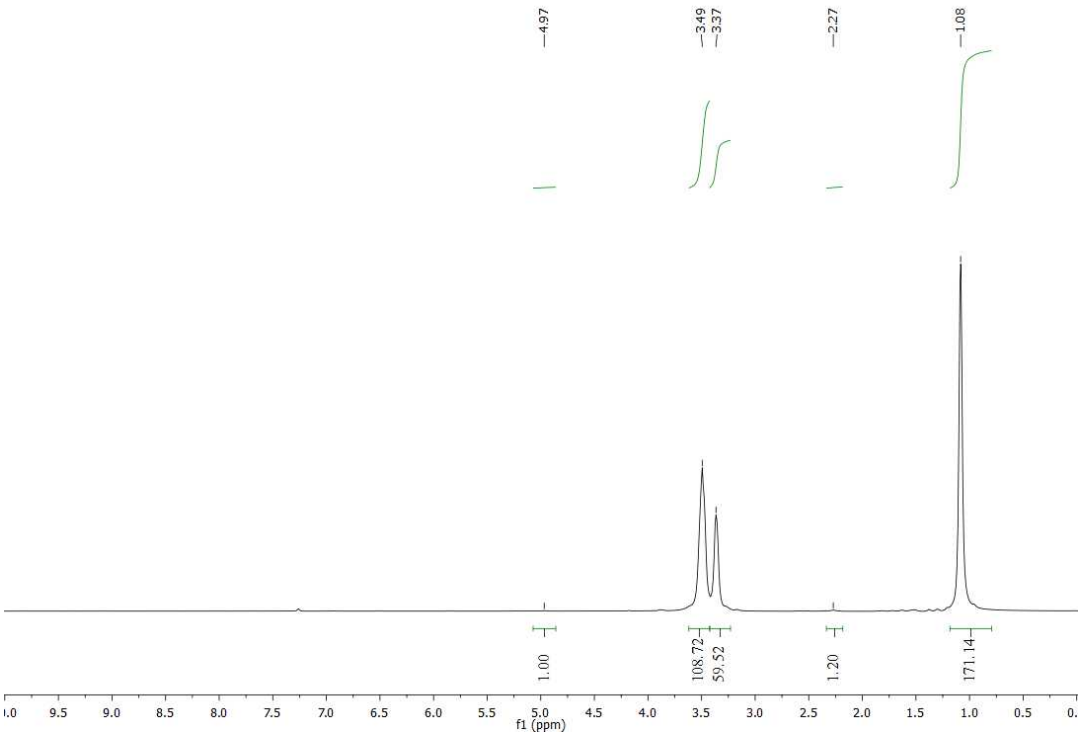

Figure S19. ^{1}H NMR spectrum of PO-VL copolymer from Table 1, Entry 2.

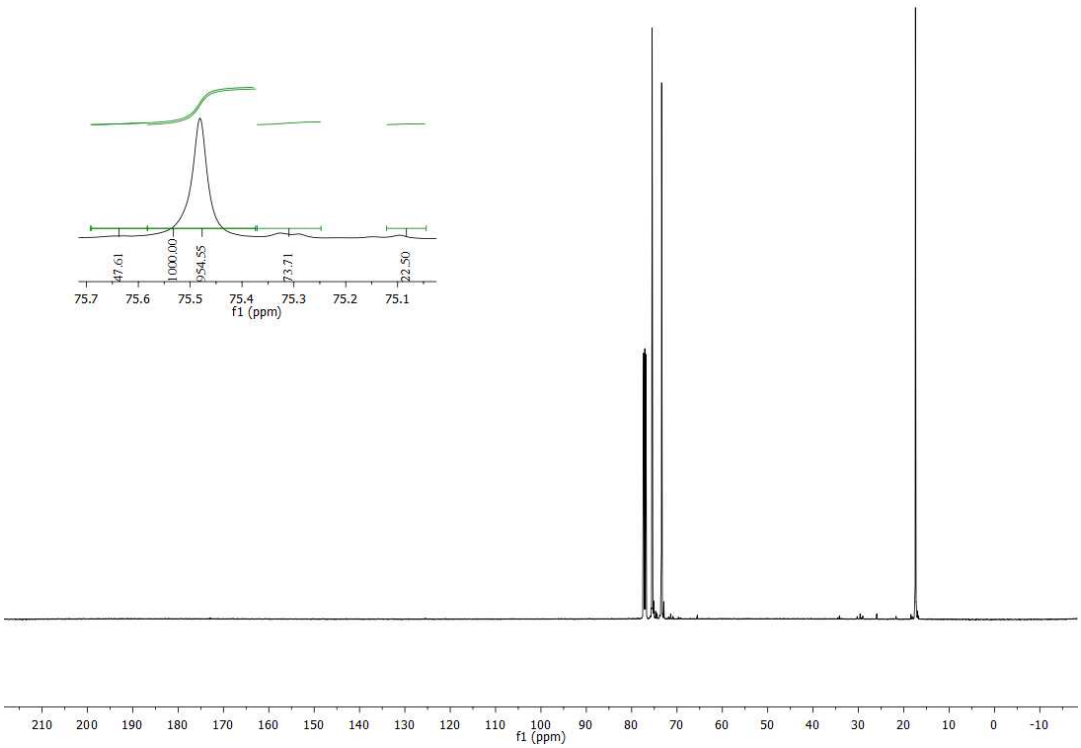

Figure S20. ^{13}C NMR spectrum of PO-VL copolymer from Table 1, Entry 2.

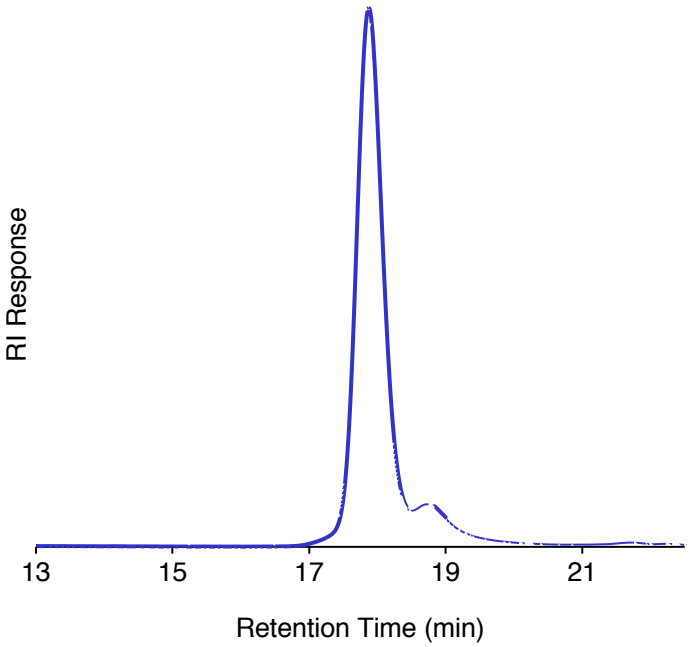

Figure S21. GPC chromatogram of PO-VL copolymer from Table 1, Entry 2.

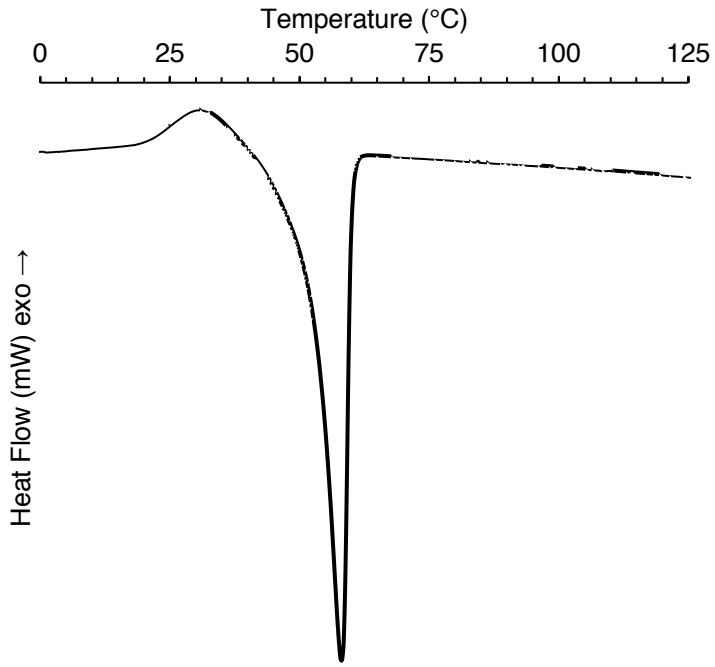

Figure S22. DSC thermogram of PO-VL copolymer from Table 1, Entry 2.

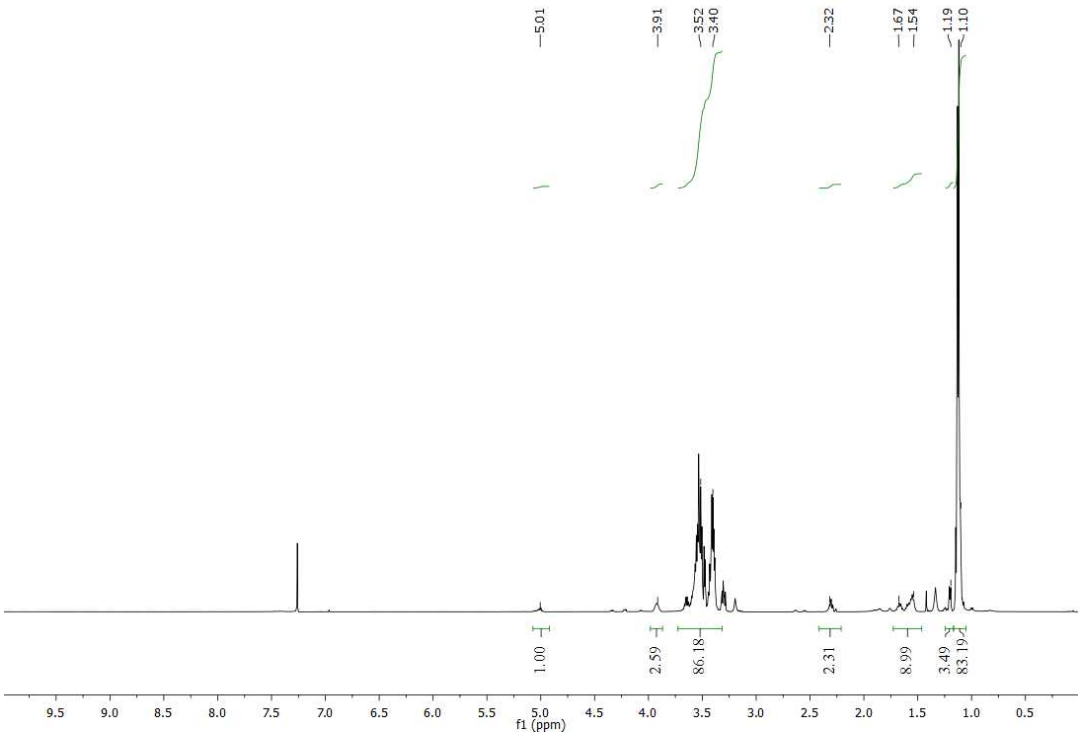

Figure S23. ^{1}H NMR spectrum of PO-VL copolymer from Table 1, Entry 3.

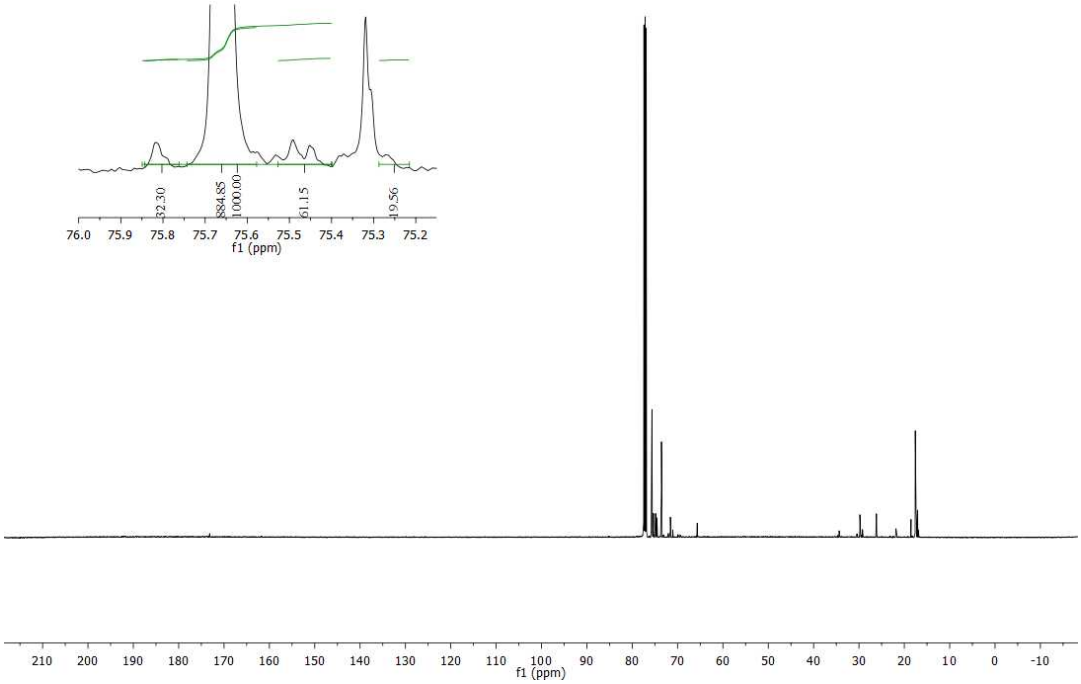

Figure S24. ^{13}C NMR spectrum of PO-VL copolymer from Table 1, Entry 3.

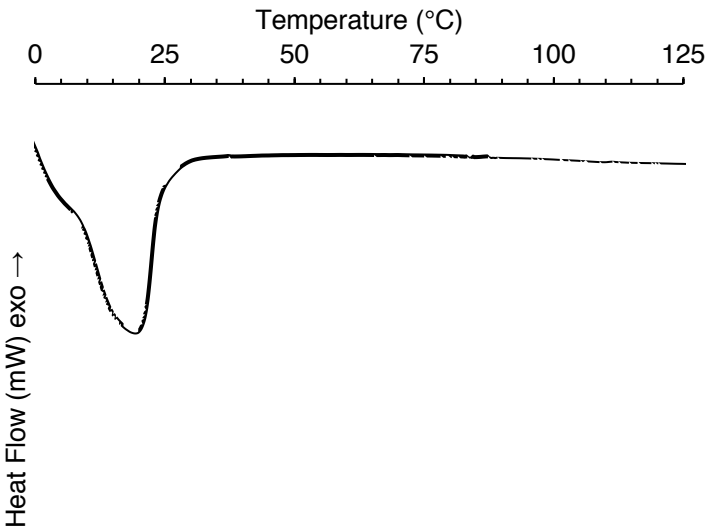

Figure S25. DSC thermogram of PO-VL copolymer from Table 1, Entry 3.

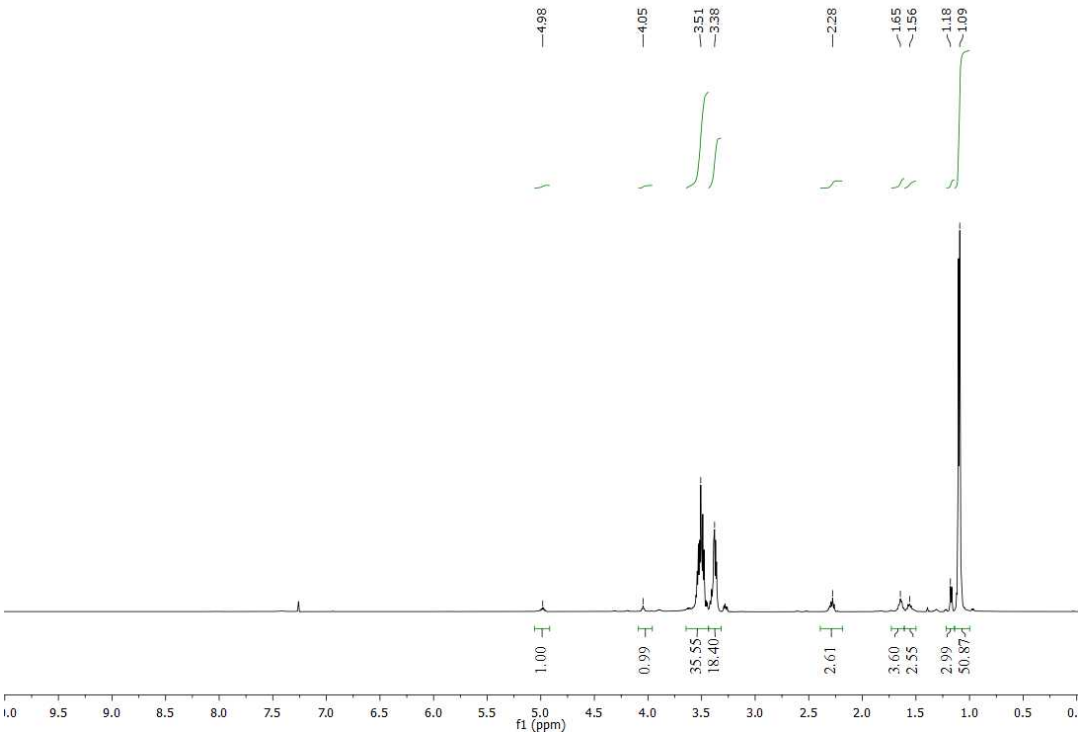

Figure S26. ^{1}H NMR spectrum of PO-VL copolymer from Table 1, Entry 4.

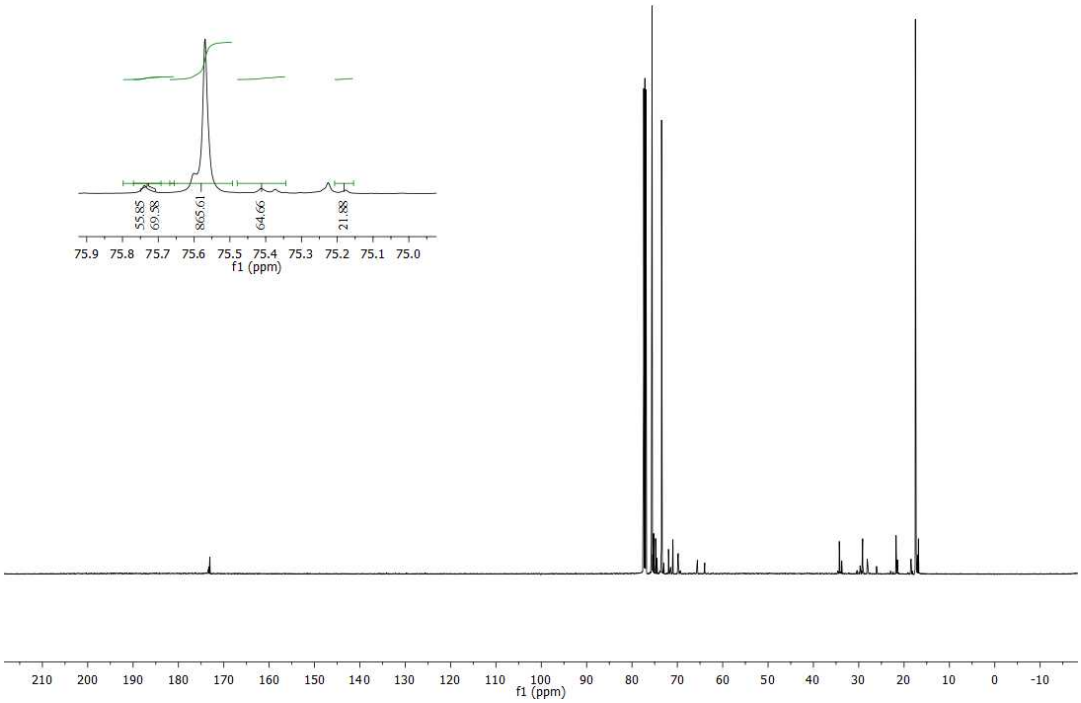

Figure S27. ^{13}C NMR spectrum of PO-VL copolymer from Table 1, Entry 4.

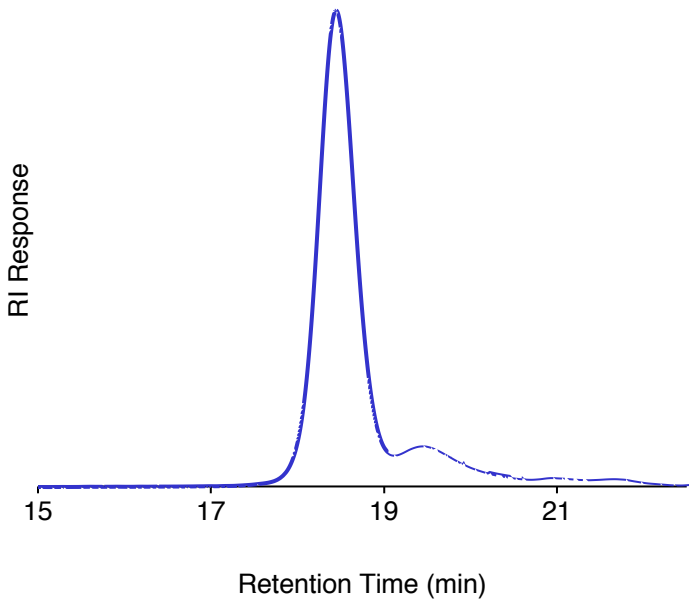

Figure S28. GPC chromatogram of PO-VL copolymer from Table 1, Entry 4.

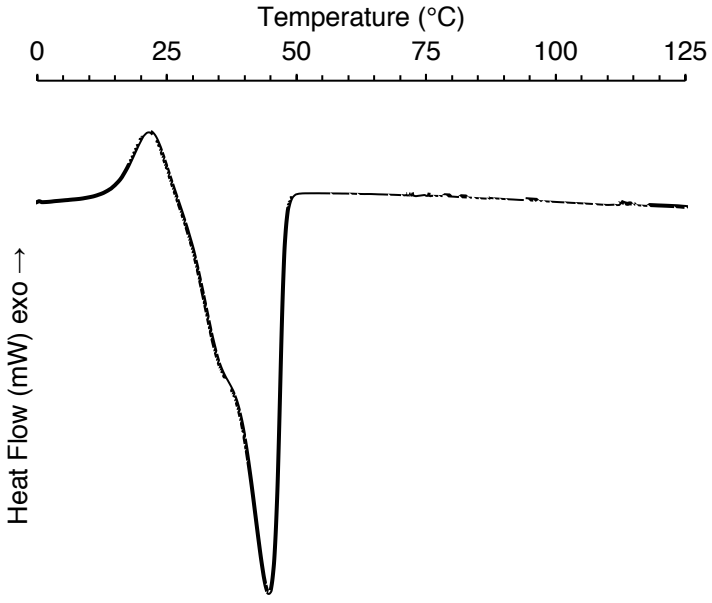

Figure S29. DSC thermogram of PO-VL copolymer from Table 1, Entry 4.

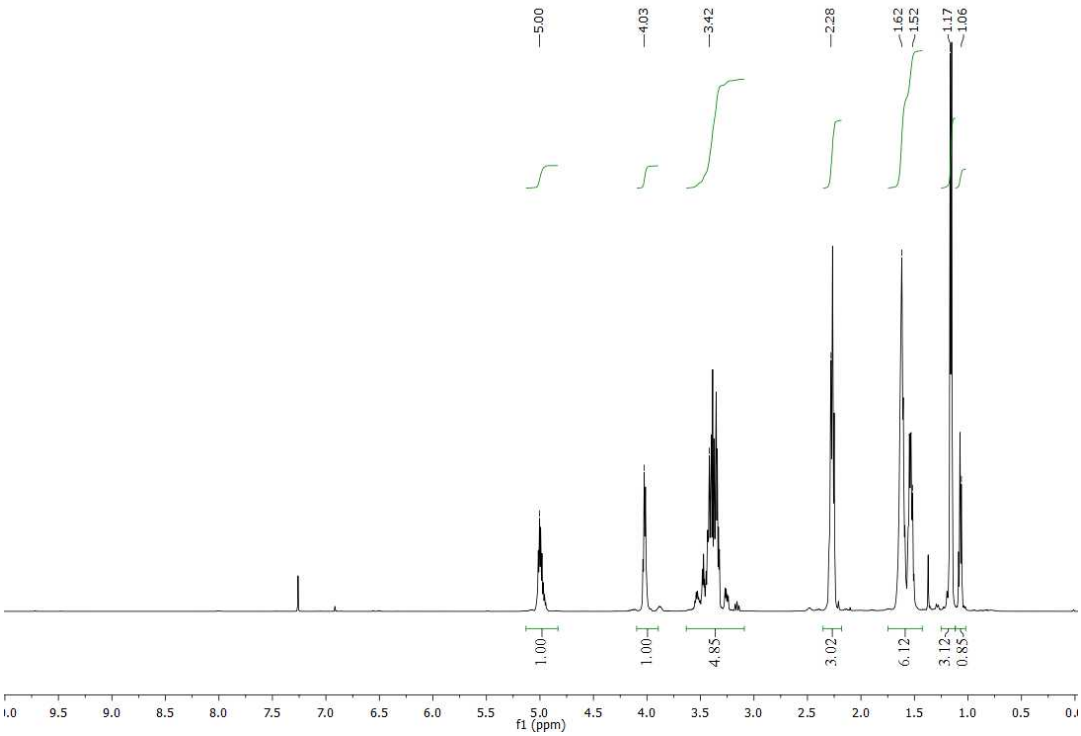

Figure S30. [1]H NMR spectrum of PO-VL copolymer from Table 1, Entry 5.

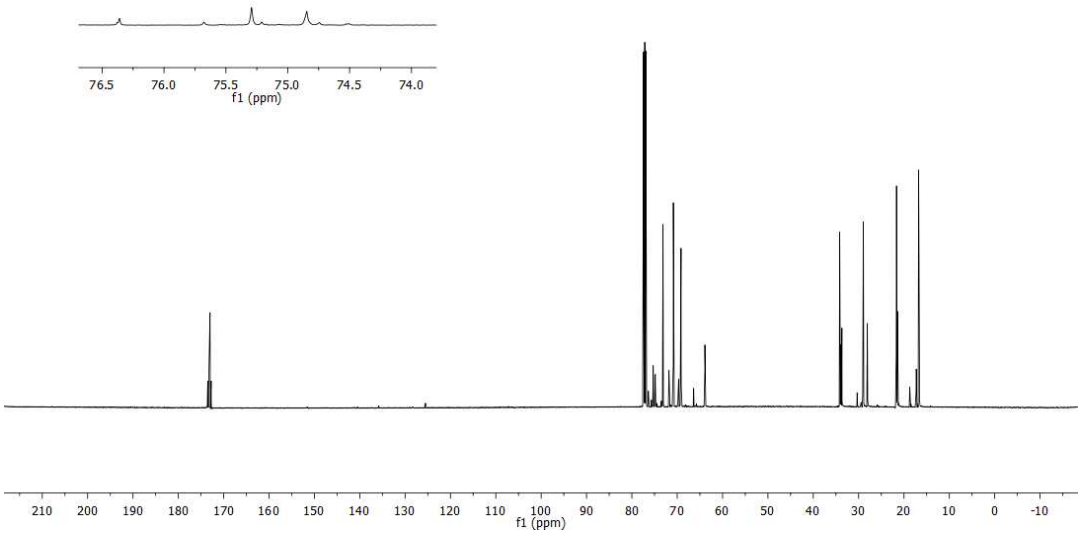

Figure S31. [13]C NMR spectrum of PO-VL copolymer from Table 1, Entry 5.

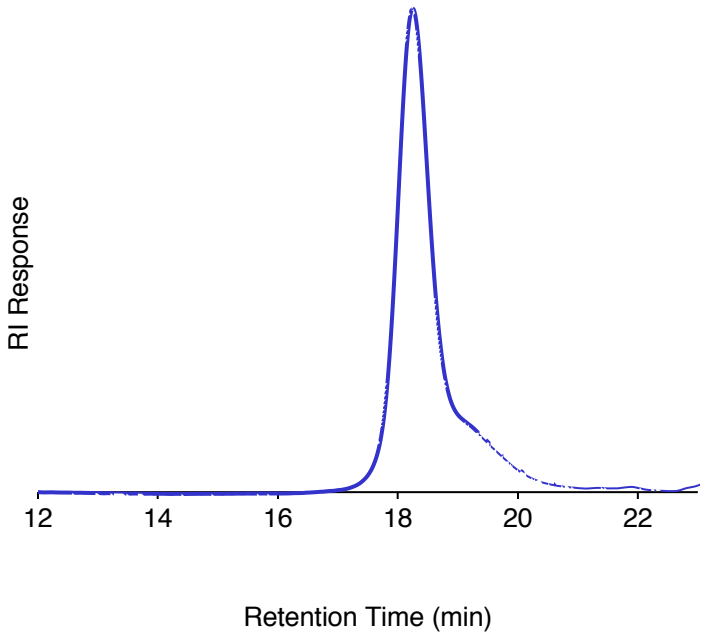

Figure S32. GPC chromatogram of PO-VL copolymer from Table 1, Entry 5.

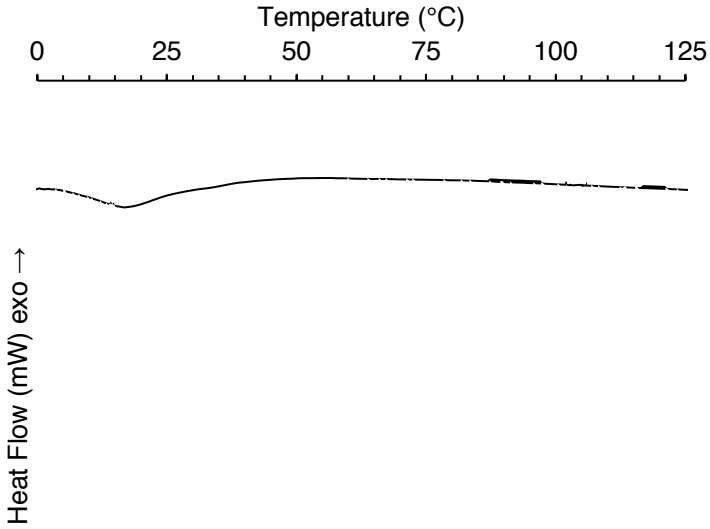

Figure S33. DSC thermogram of PO-VL copolymer from Table 1, Entry 5.

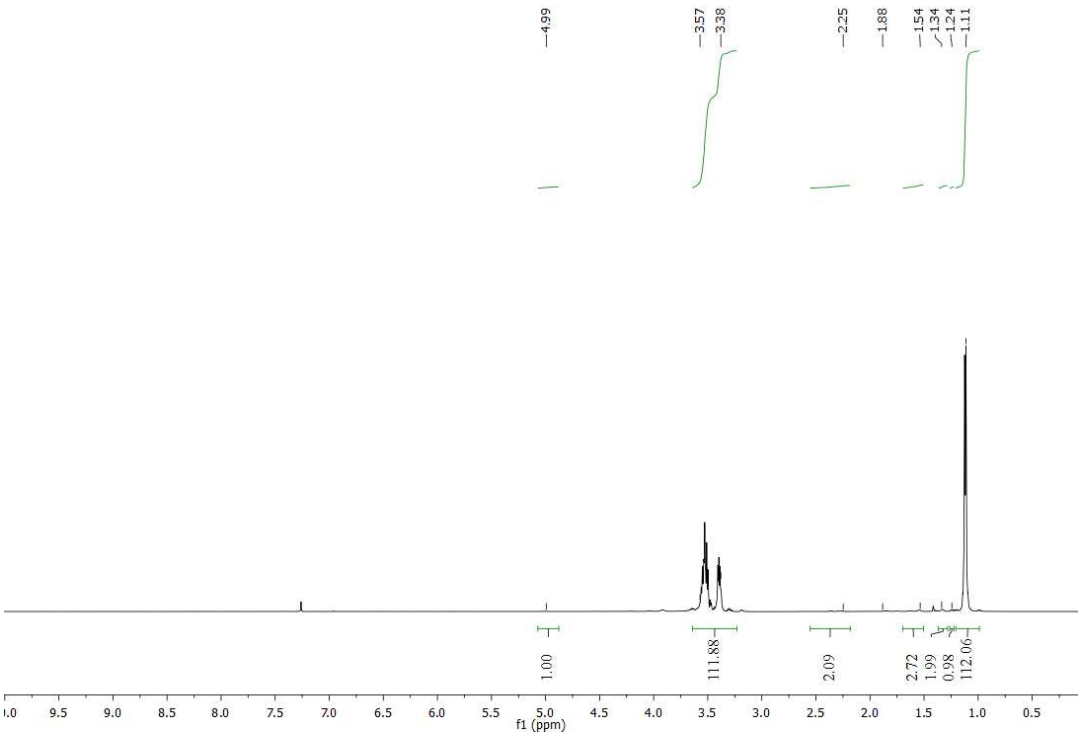

Figure S34. [1]H NMR spectrum of PO-BL copolymer from Table 1, Entry 6.

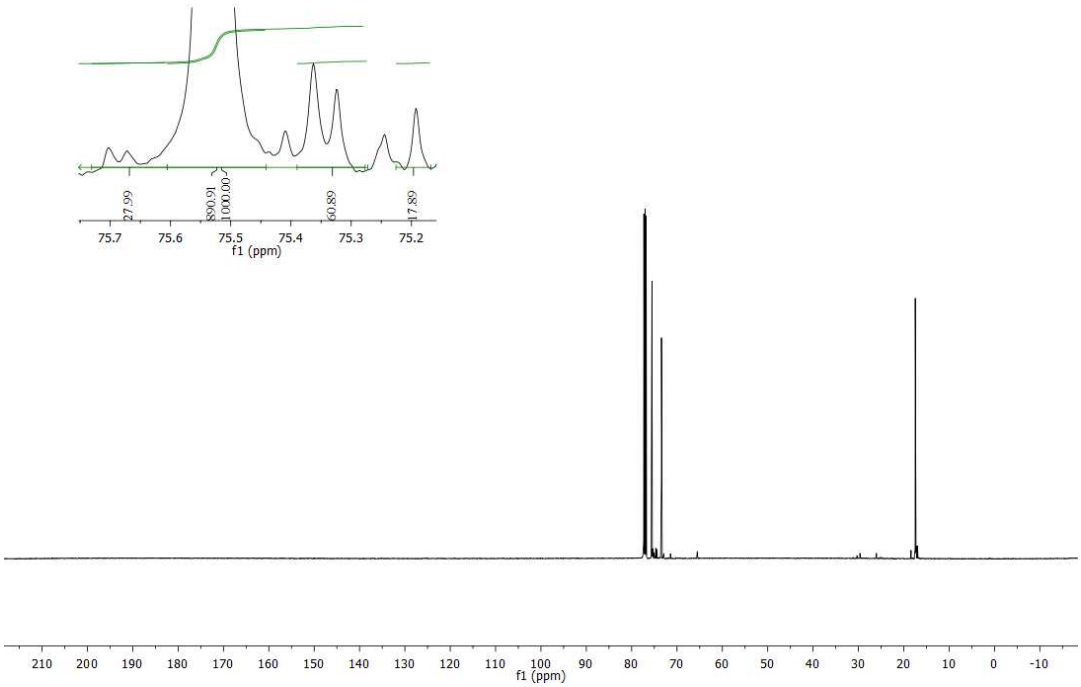

Figure S35. [13]C NMR spectrum of PO-BL copolymer from Table 1, Entry 6.

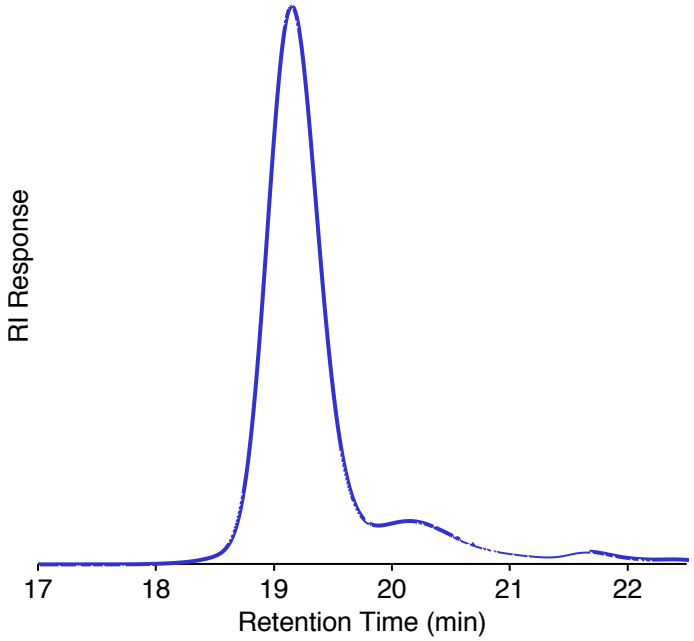

Figure S36. GPC chromatogram of PO-BL copolymer from Table 1, Entry 6.

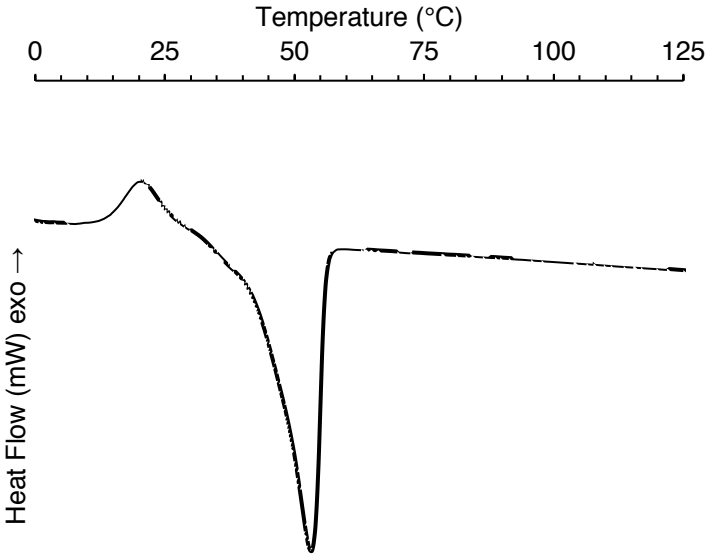

Figure S37. DSC thermogram of PO-BL copolymer from Table 1, Entry 6.

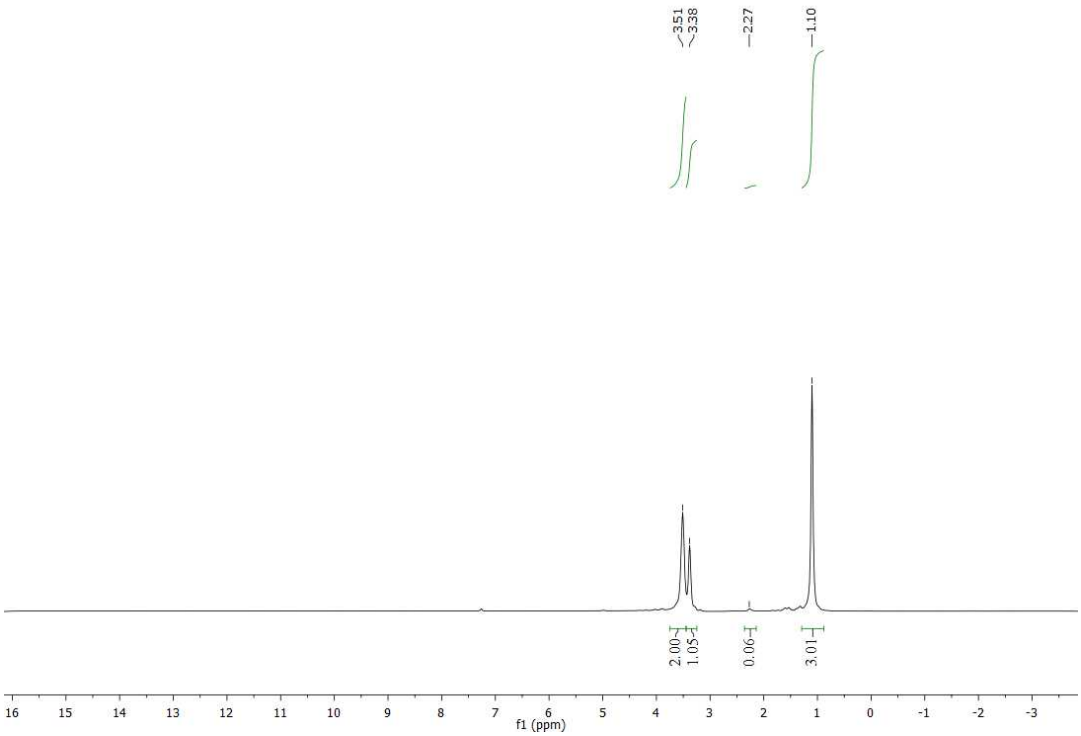

Figure S38. ^{1}H NMR spectrum of PO-CL copolymer from Table 1, Entry 7.

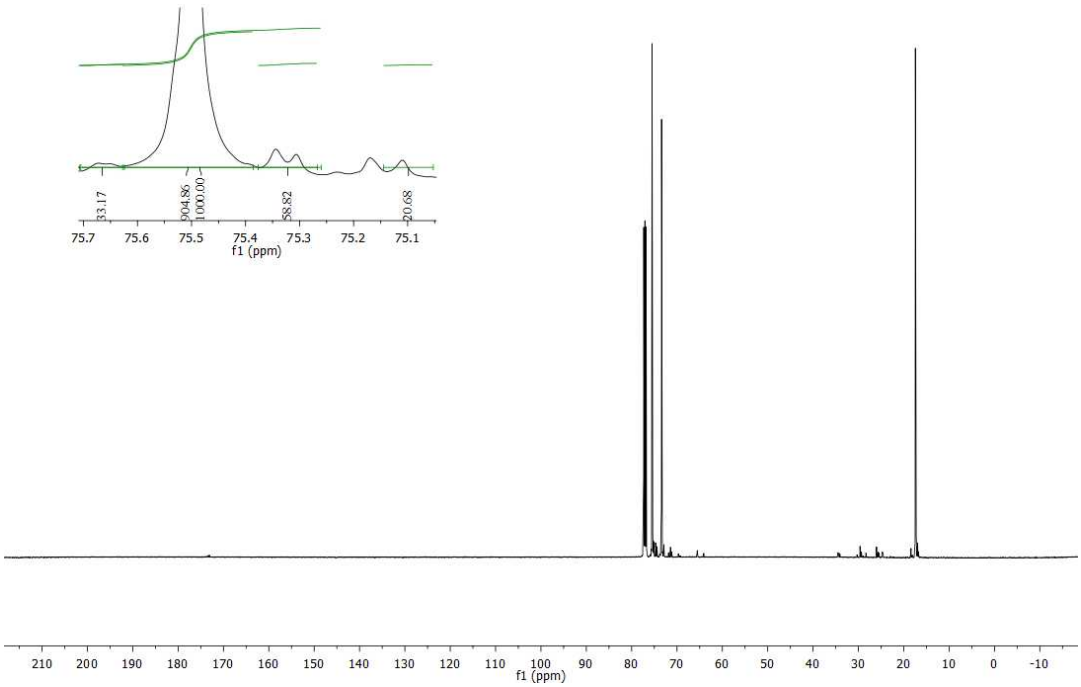

Figure **S39.** ^{13}C NMR spectrum of PO-CL copolymer from Table 1, Entry 7.

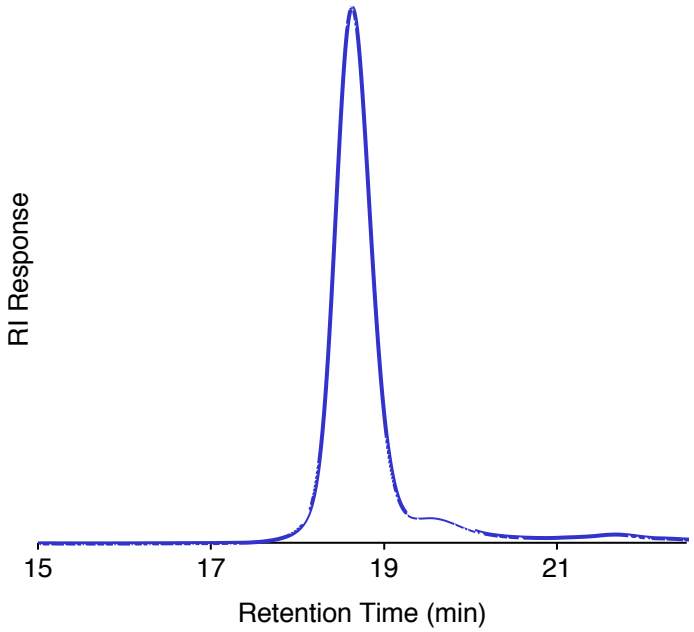

Figure S40. GPC chromatogram of PO-CL copolymer from Table 1, Entry 7.

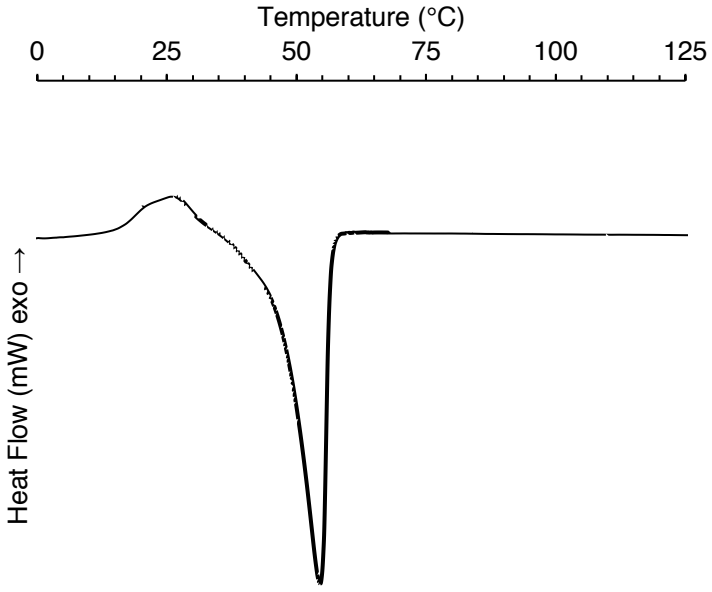

Figure S41. DSC thermogram of PO-CL copolymer from Table 1, Entry 7.

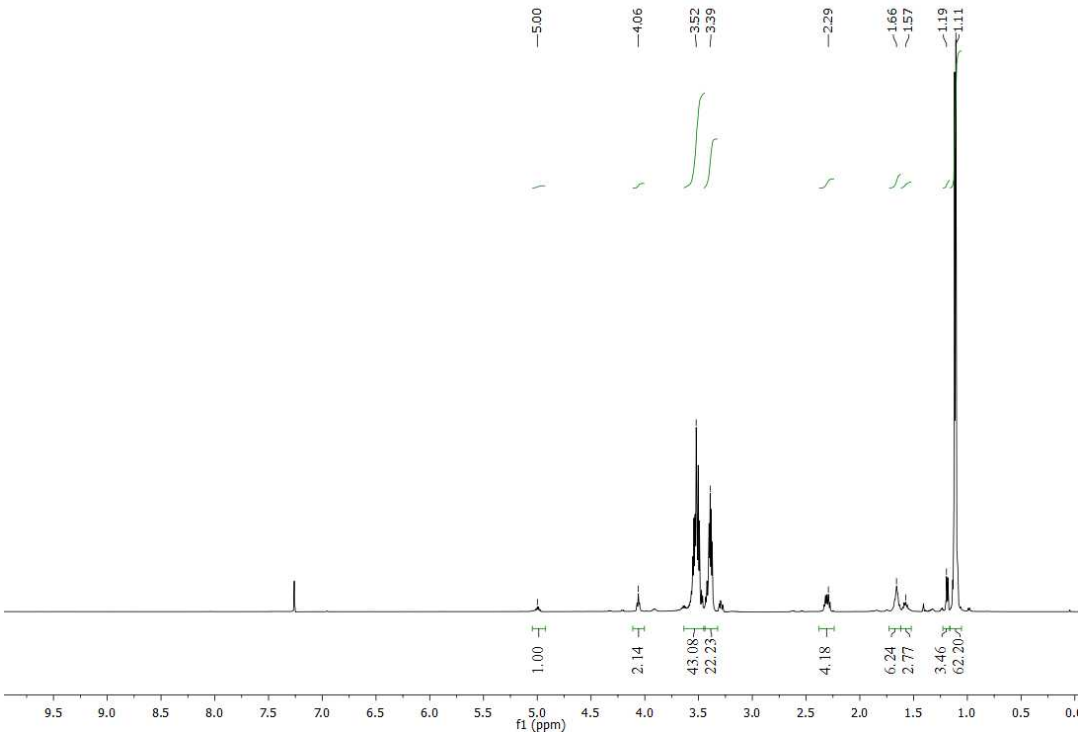

Figure S42. [1]H NMR spectrum of PO-VL copolymer from Supplementary Table 1, Entry 1.

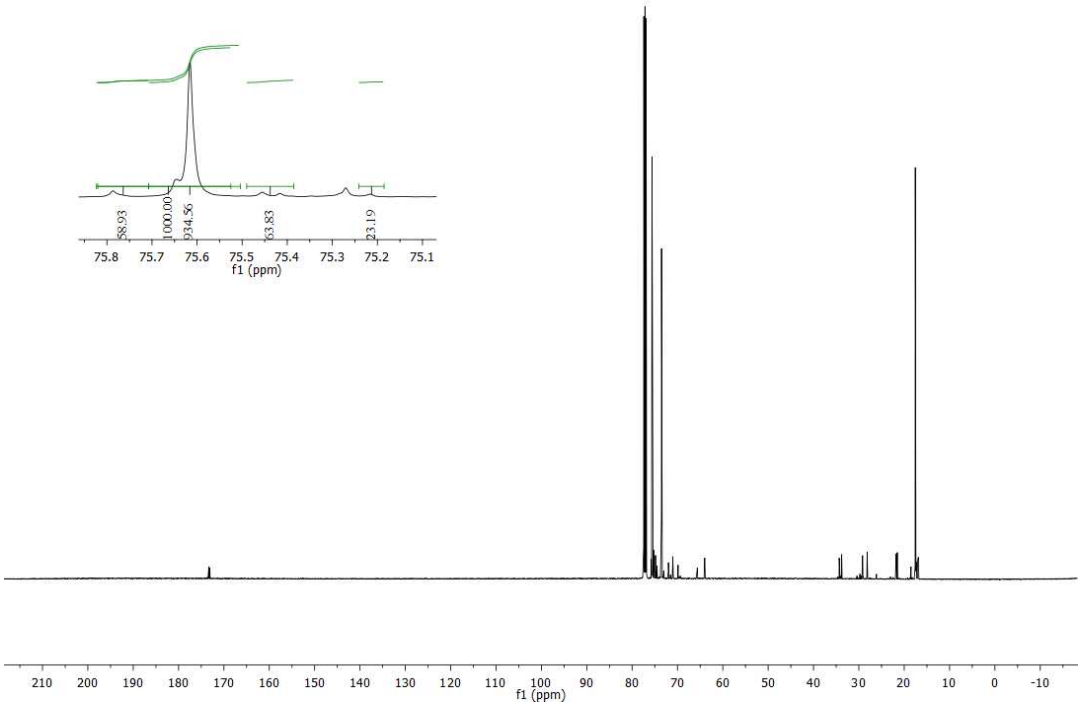

Figure S43. [13]C NMR spectrum of PO-VL copolymer from Supplementary Table 1, Entry 1.

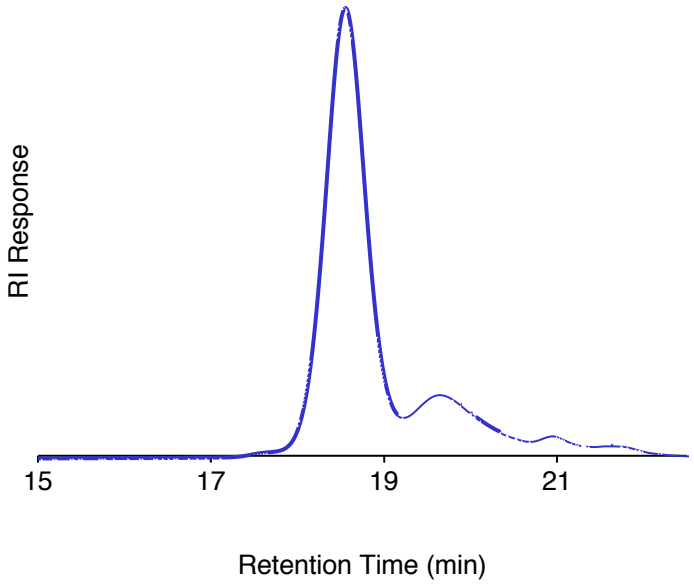

Figure S44. GPC chromatogram of PO-VL copolymer from Supplementary Table 1, Entry 1.

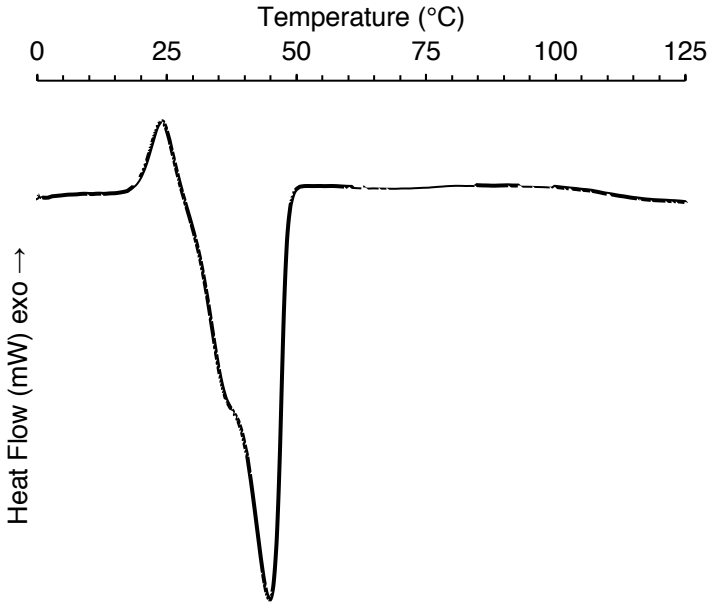

Figure S45. DSC thermogram of PO-VL copolymer from Supplementary Table 1, Entry 1.

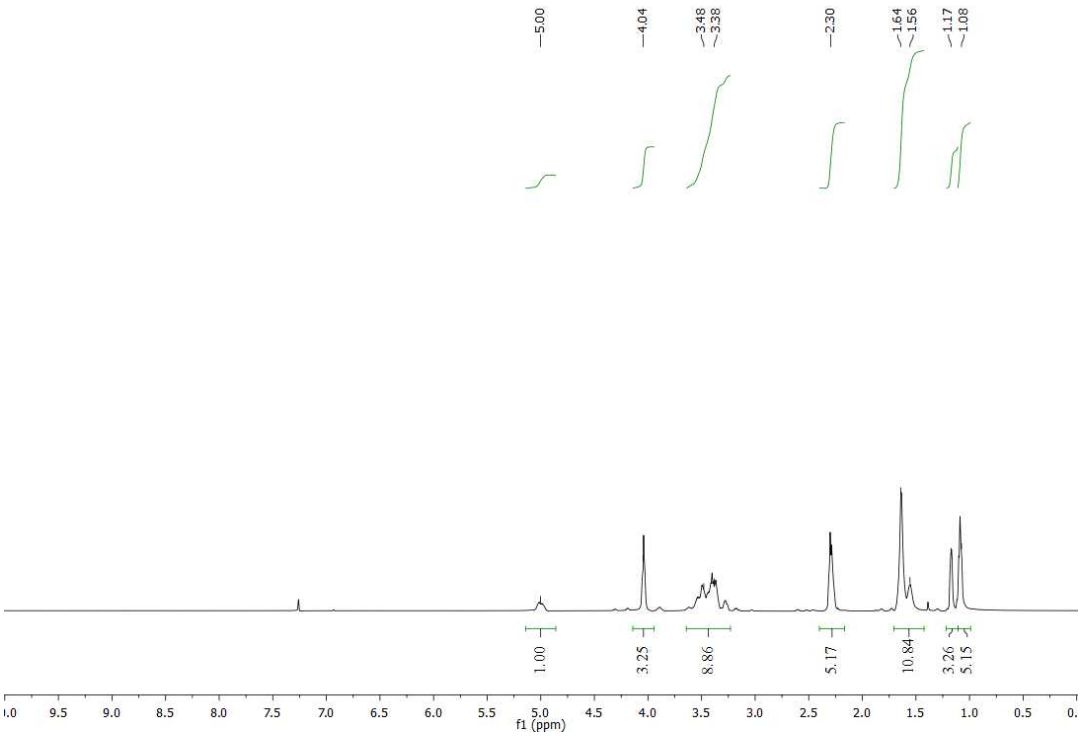

Figure S46. [1]H NMR spectrum of PO-VL copolymer from Supplementary Table 1, Entry 2.

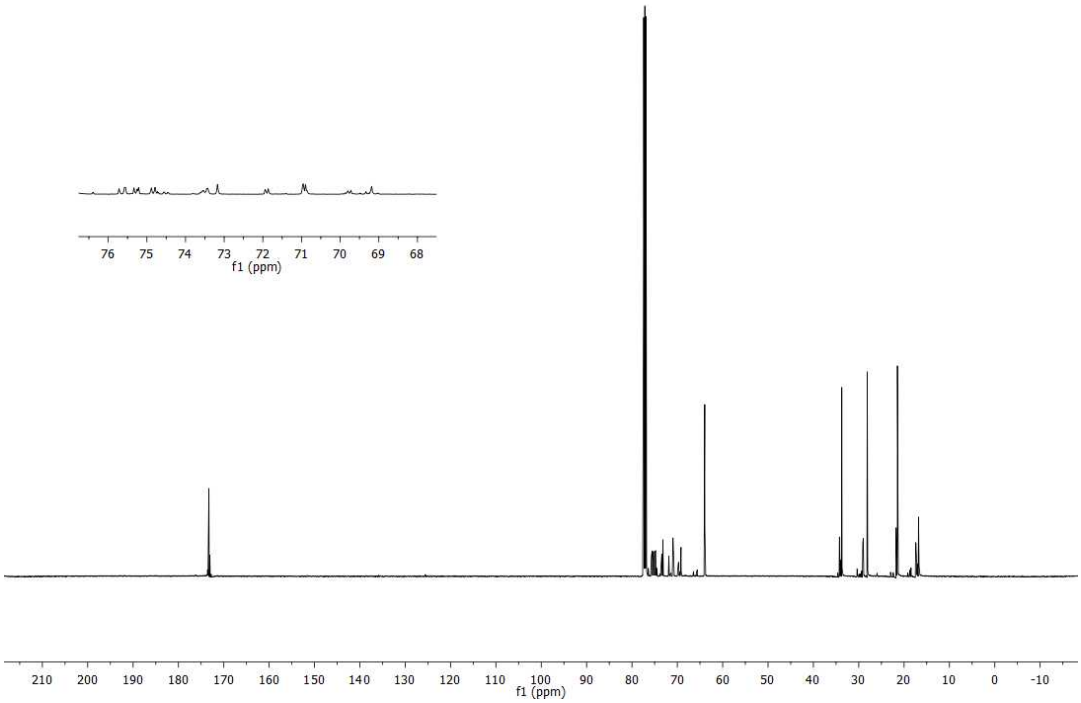

Figure S47. [13]C NMR spectrum of PO-VL copolymer from Supplementary Table 1, Entry 2.

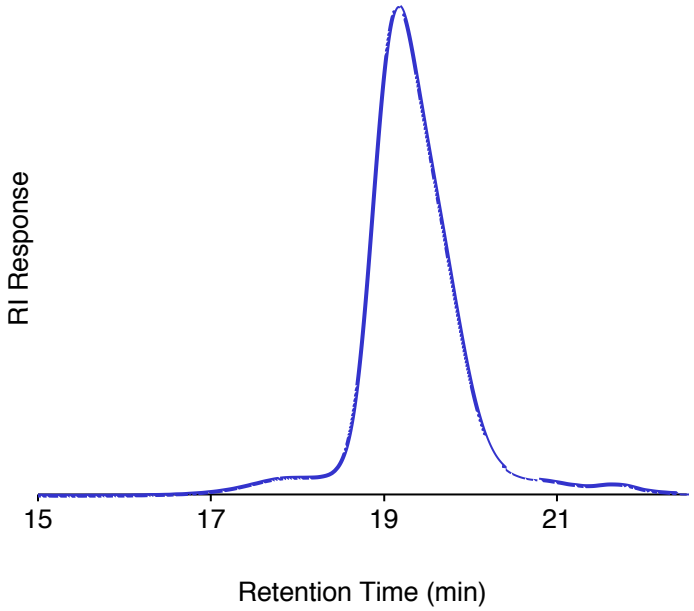

Figure S48. GPC chromatogram of PO-VL copolymer from Supplementary Table 1, Entry 2.

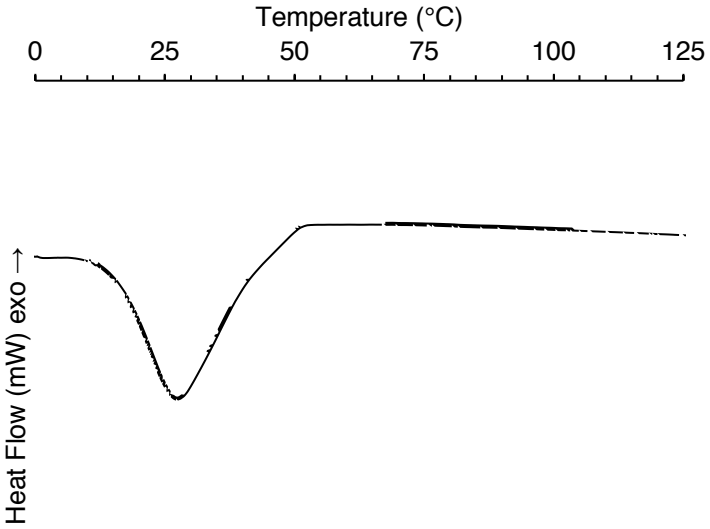

Figure S49. DSC thermogram of PO-VL copolymer from Supplementary Table 1, Entry 2.

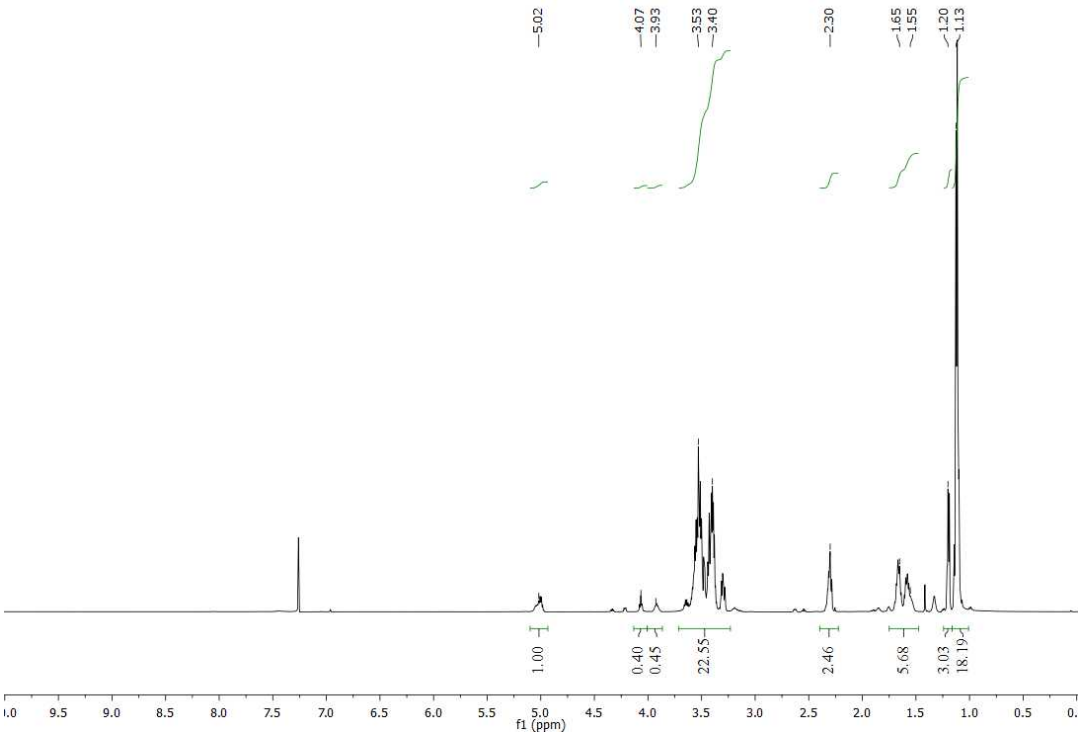

Figure S50. ^{1}H NMR spectrum of PO-VL copolymer from Supplementary Table 1, Entry 3.

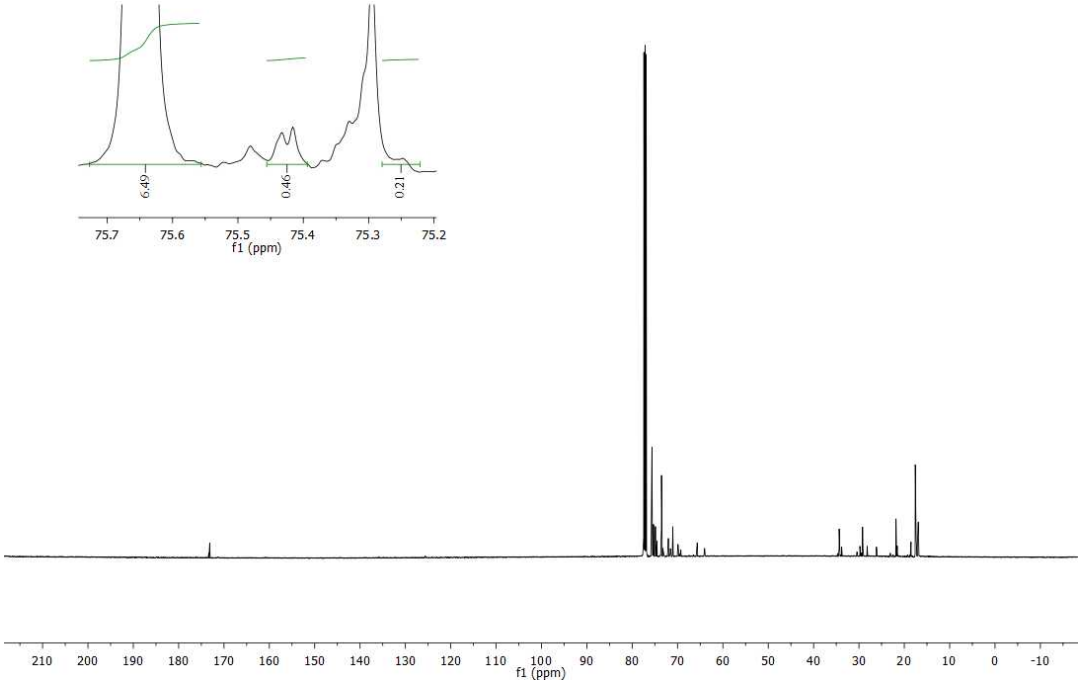

Figure S51. ^{13}C NMR spectrum of PO-VL copolymer from Supplementary Table 1, Entry 3.

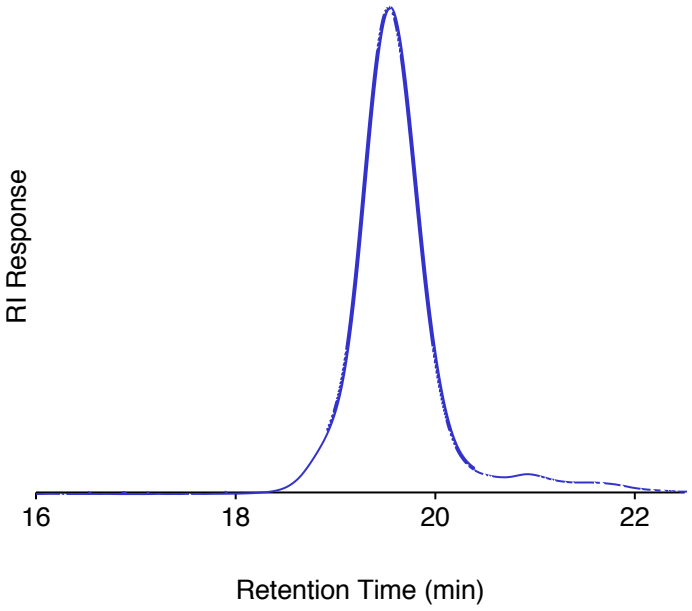

Figure S52. GPC chromatogram of PO-VL copolymer from Supplementary Table 1, Entry 3.

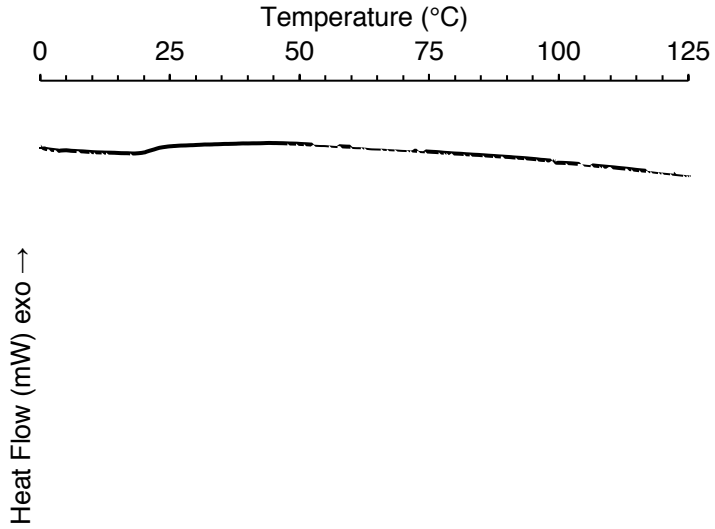

Figure S53. DSC thermogram of PO-VL copolymer from Supplementary Table 1, Entry 3.

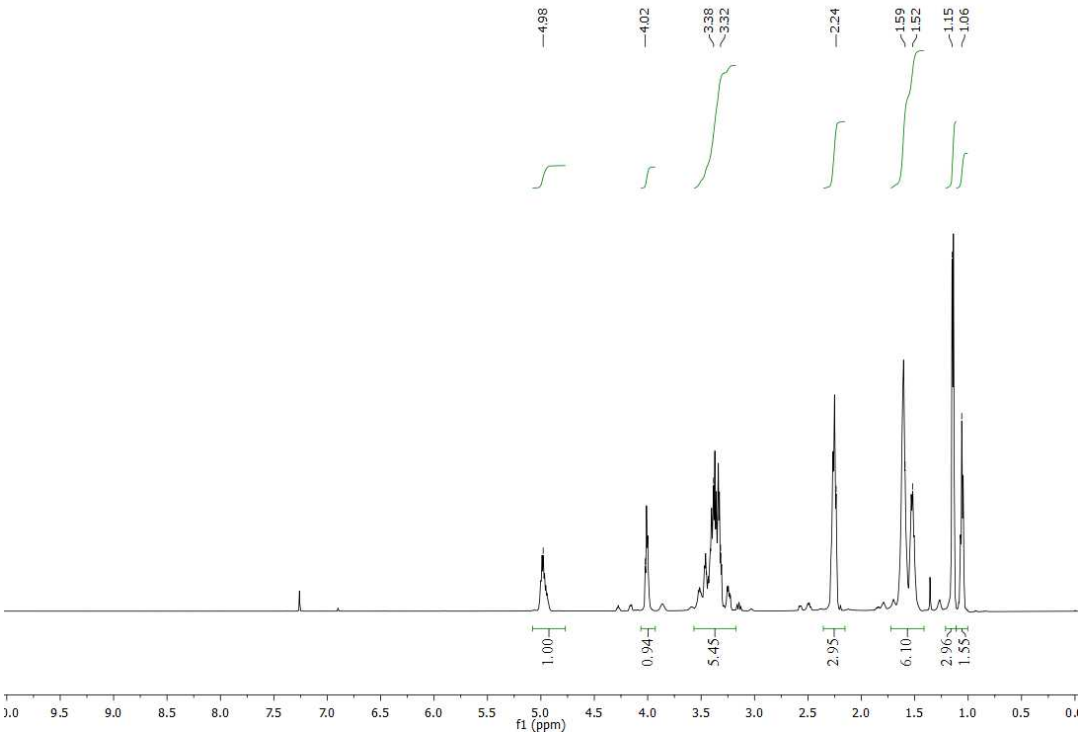

Figure S54. ^{1}H NMR spectrum of PO-VL copolymer from Supplementary Table 1, Entry 4.

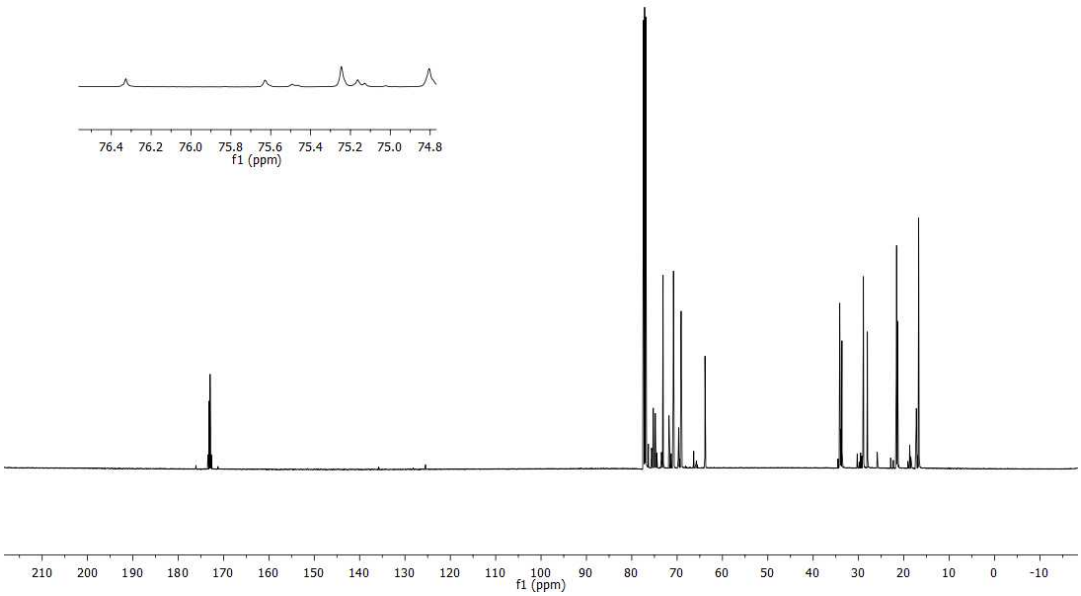

Figure S55. ^{13}C NMR spectrum of PO-VL copolymer from Supplementary Table 1, Entry 4.

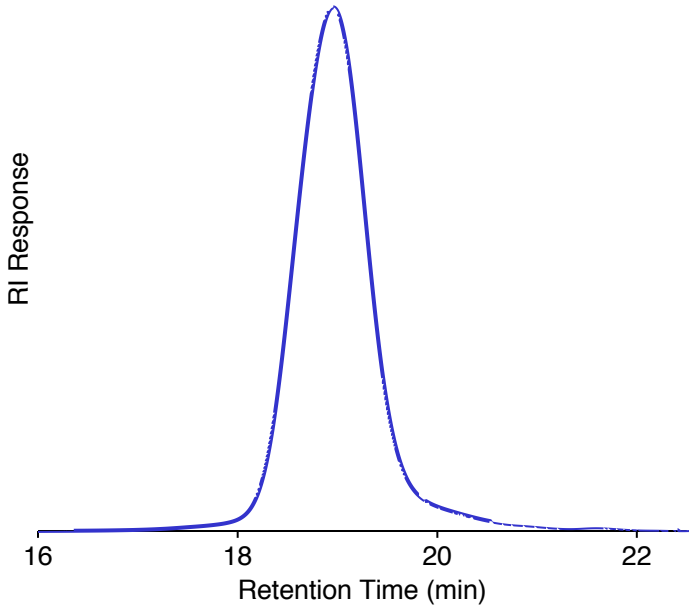

Figure S56. GPC chromatogram of PO-VL copolymer from Supplementary Table 1, Entry 4.

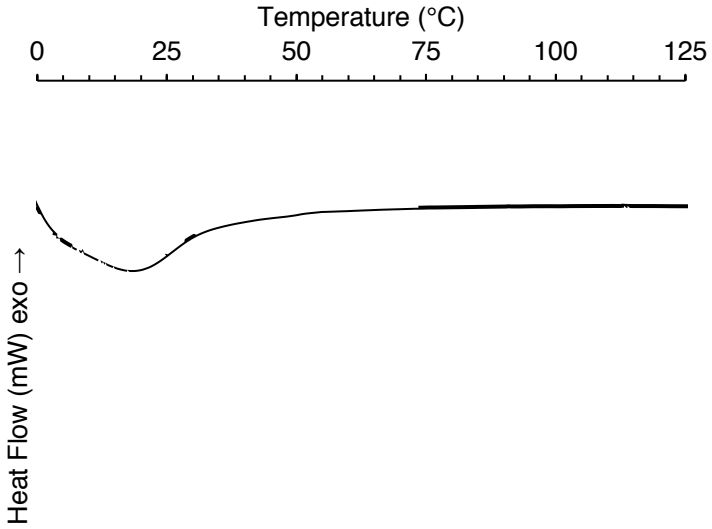

Figure S57. DSC thermogram of PO-VL copolymer from Supplementary Table 1, Entry 4.

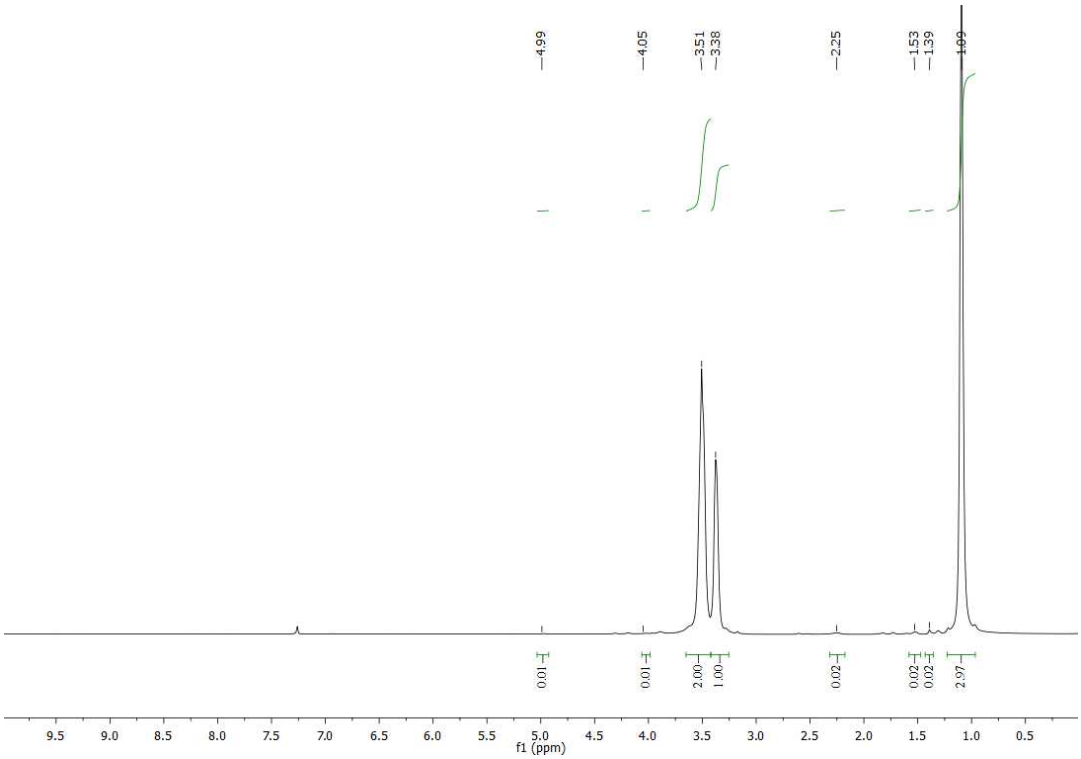

Figure S58. ^{1}H NMR spectrum of PO-CL copolymer from Supplementary Table 1, Entry 5.

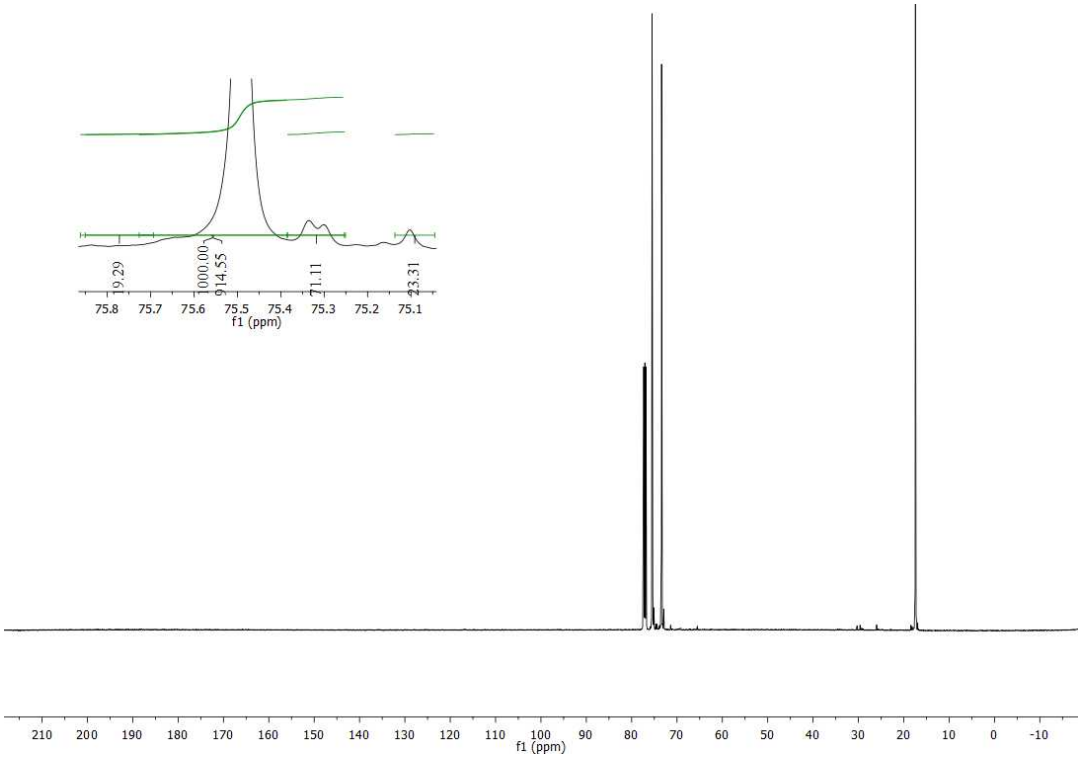

Figure S59. ^{13}C NMR spectrum of PO-CL copolymer from Supplementary Table 1, Entry 5.

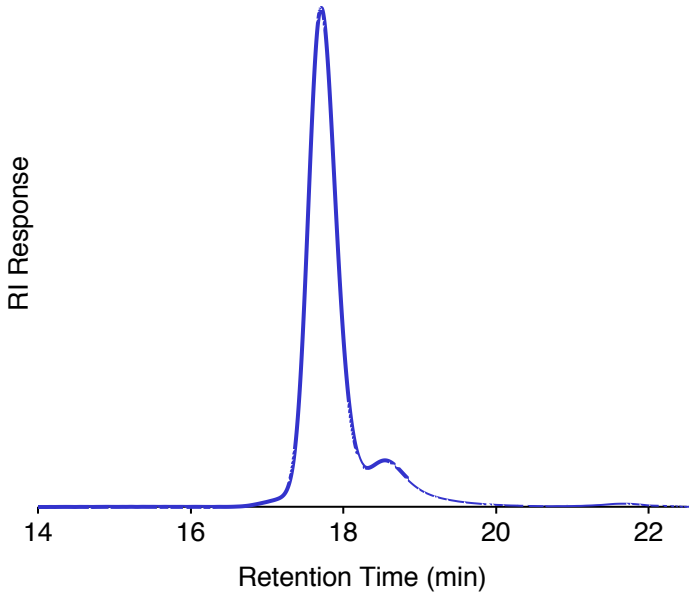

Figure S60. GPC chromatogram of PO-CL copolymer from Supplementary Table 1, Entry 5.

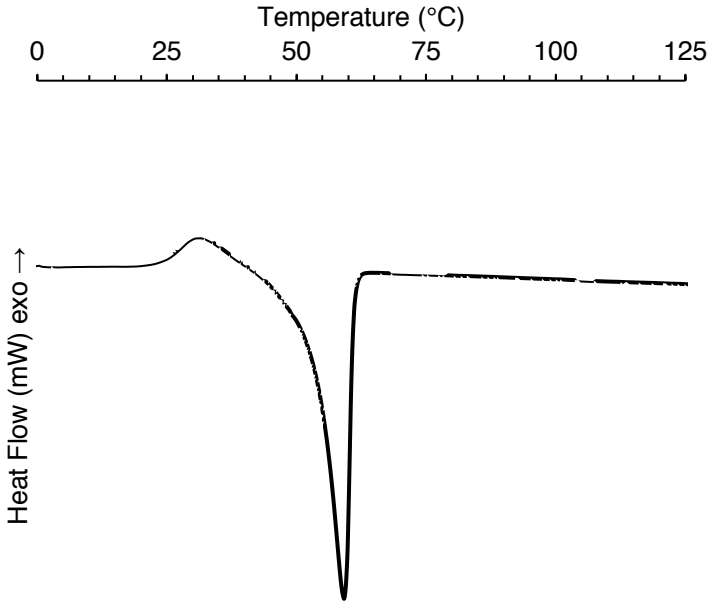

Figure S61. DSC thermogram of PO-CL copolymer from Supplementary Table 1, Entry 5.

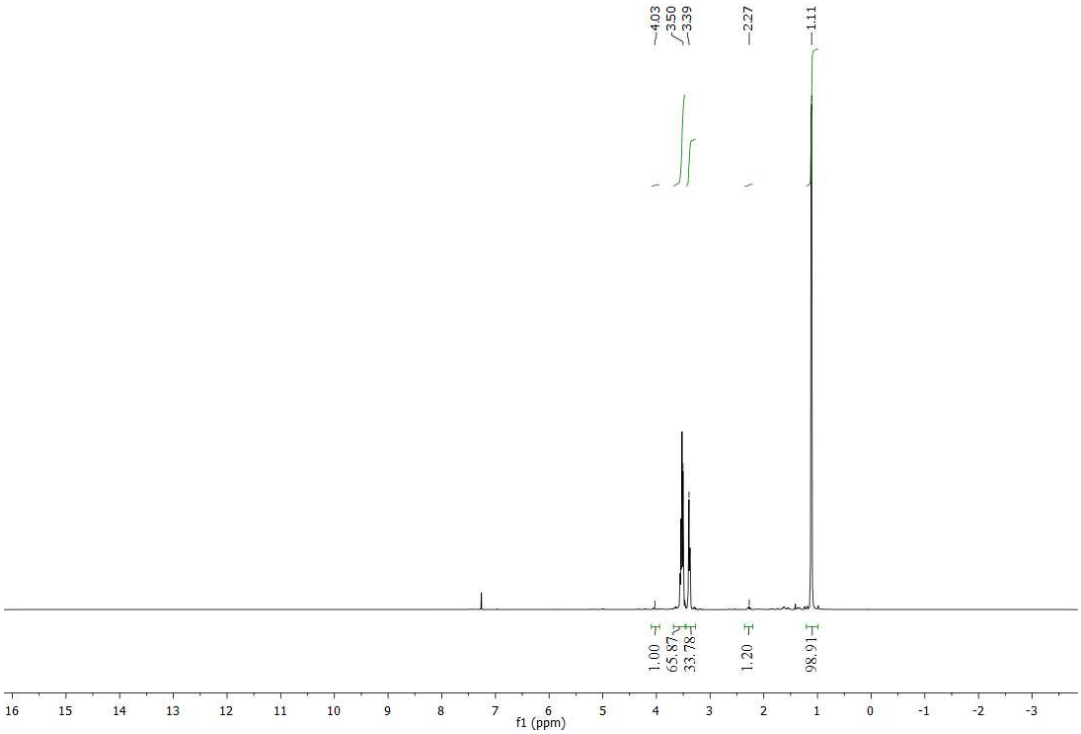

Figure S62. ^{1}H NMR spectrum of PO-CL copolymer from Supplementary Table 1, Entry 6.

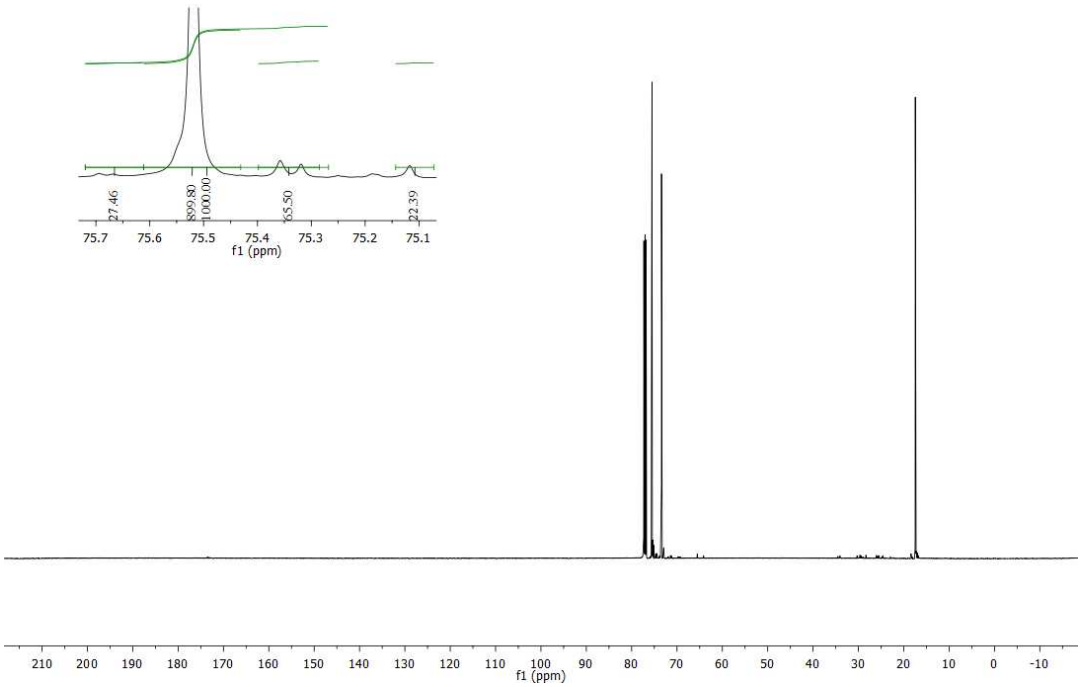

Figure S63. ^{13}C NMR spectrum of PO-CL copolymer from Supplementary Table 1, Entry 6.

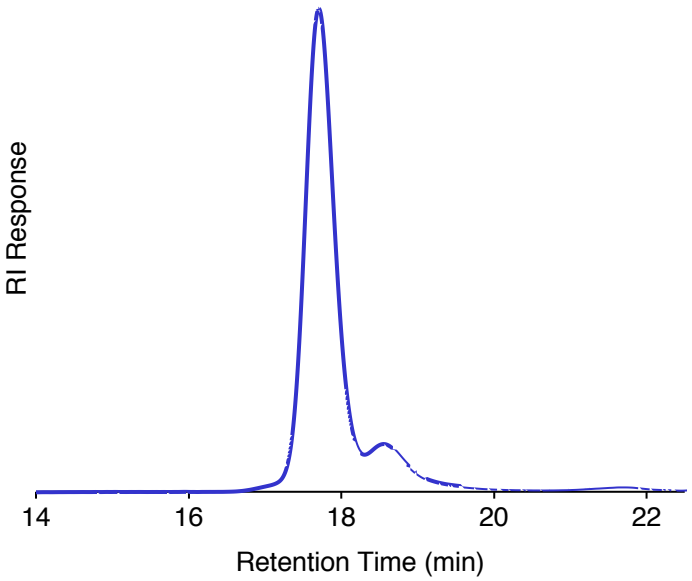

Figure S64. GPC chromatogram of PO-CL copolymer from Supplementary Table 1, Entry 6.

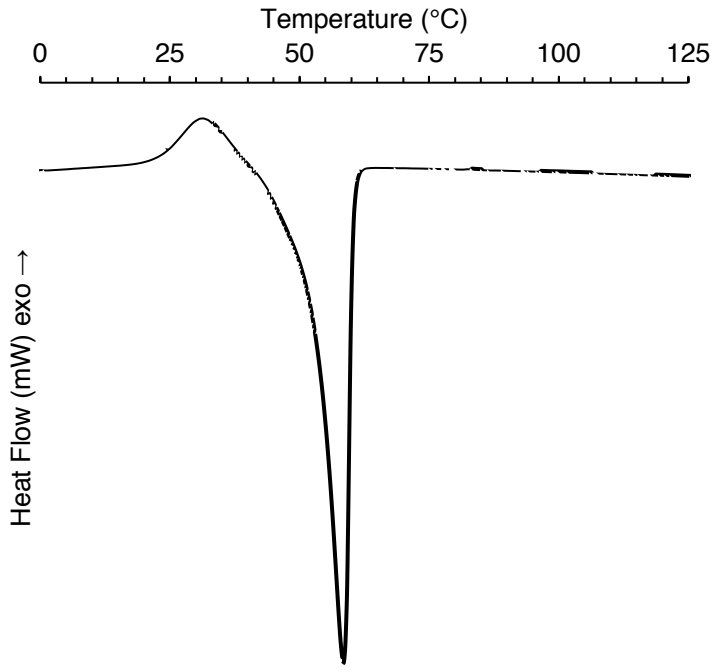

Figure S65. DSC thermogram of PO-CL copolymer from Supplementary Table 1, Entry 6.

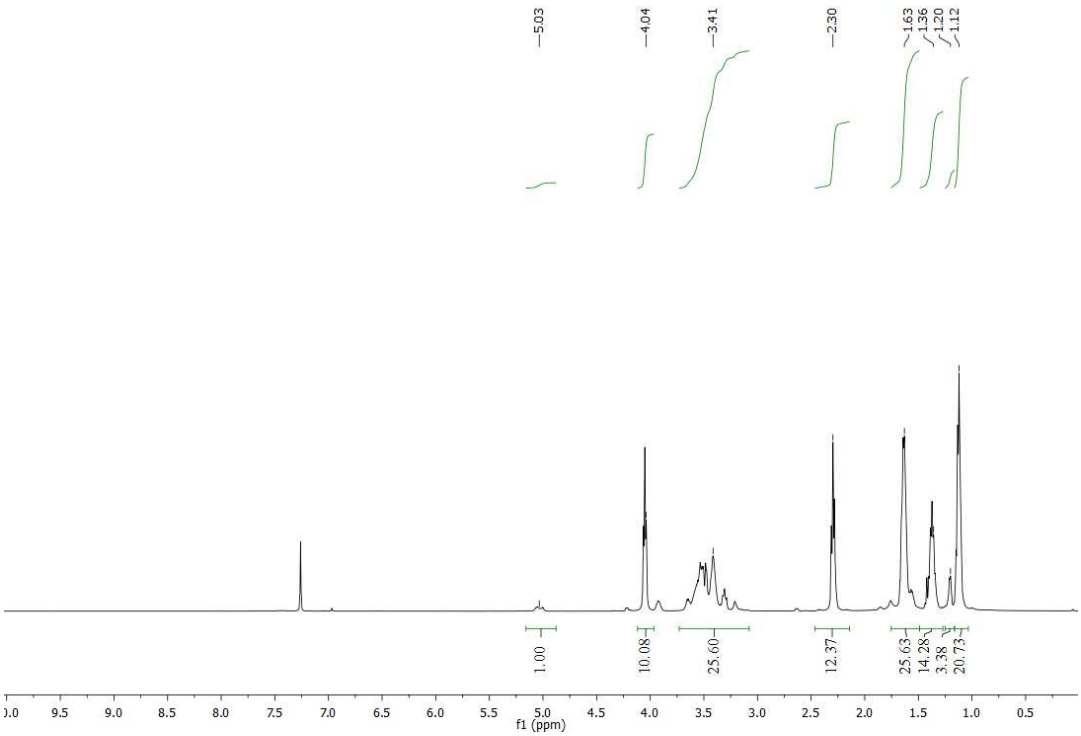

Figure S66. [1]H NMR spectrum of PO-CL copolymer from Supplementary Table 1, Entry 7.

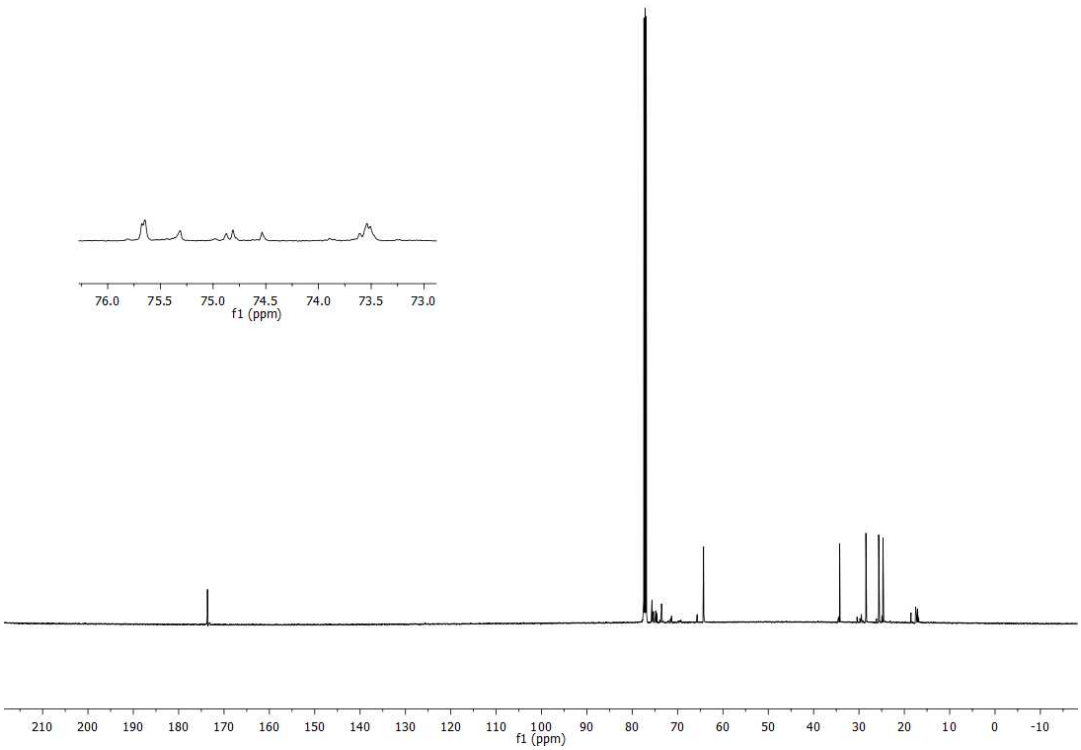

Figure S67. [13]C NMR spectrum of PO-CL copolymer from Supplementary Table 1, Entry 7.

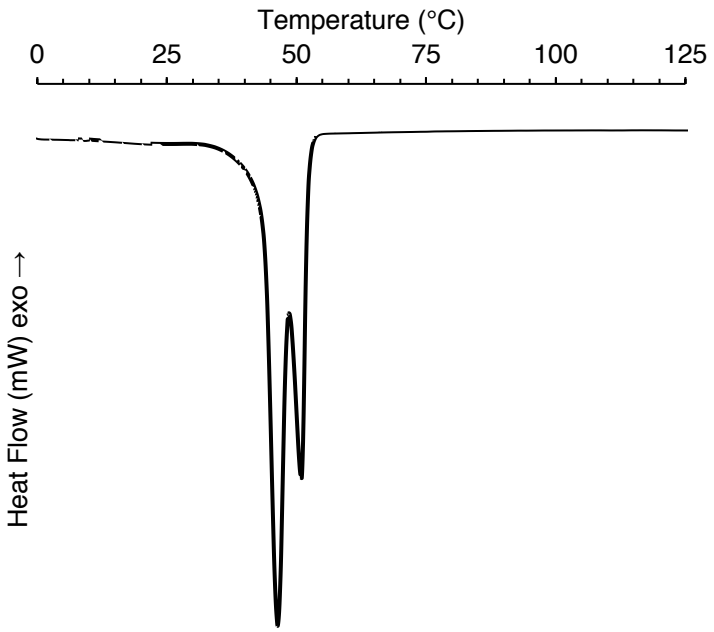

Figure S68. DSC thermogram of PO-CL copolymer from Supplementary Table 1, Entry 7.

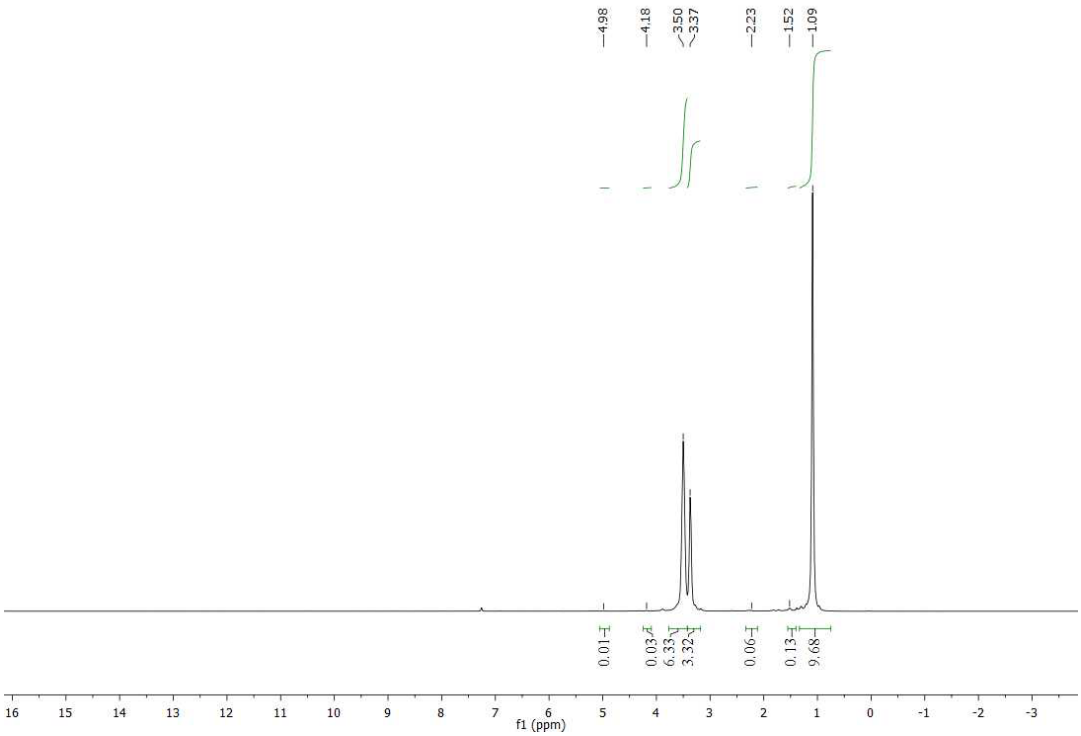

Figure S69. ^{1}H NMR spectrum of PO-CL copolymer from Supplementary Table 1, Entry 8.

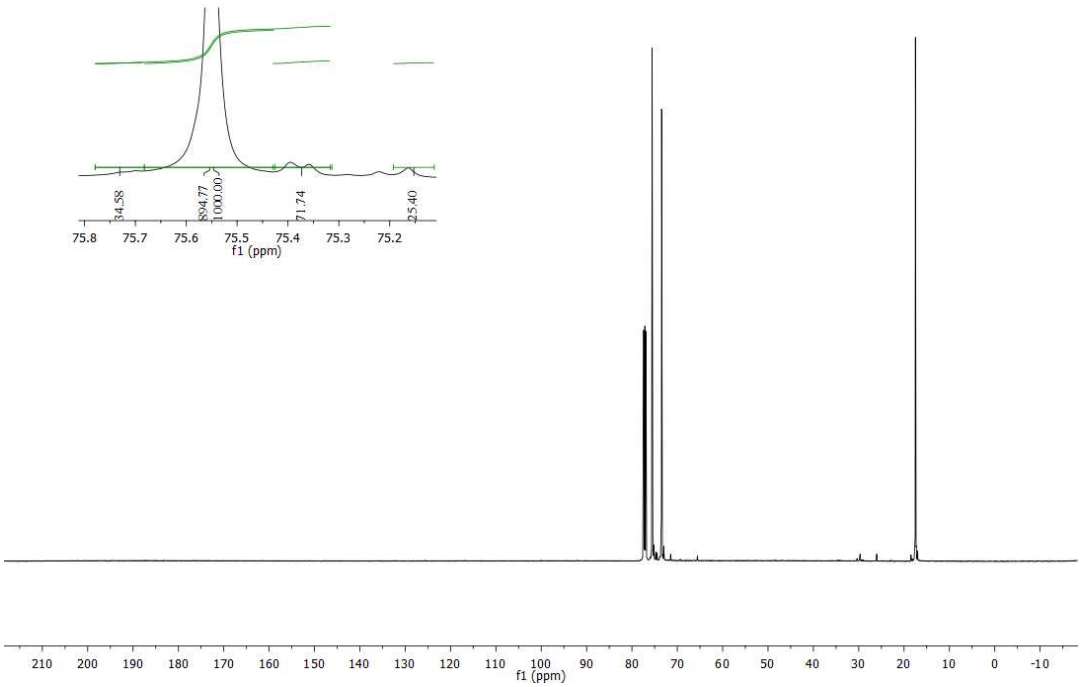

Figure S70. ^{13}C NMR spectrum of PO-CL copolymer from Supplementary Table 1, Entry 8.

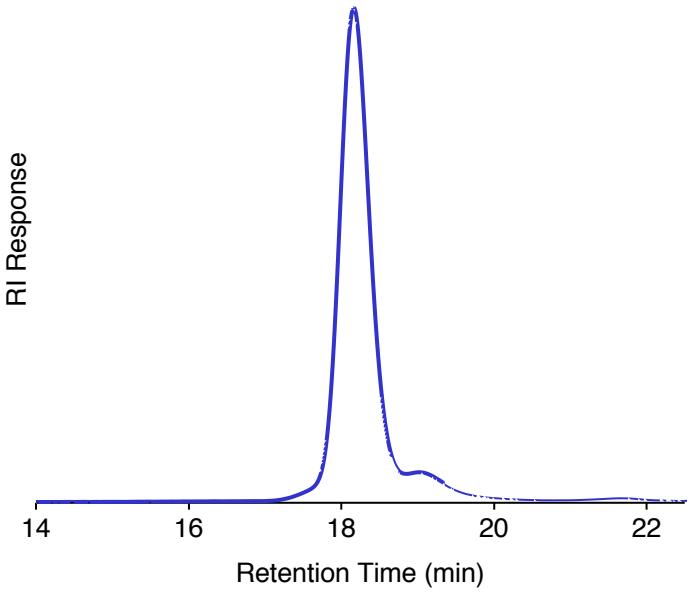

Figure S71. GPC chromatogram of PO-CL copolymer from Supplementary Table 1, Entry 8.

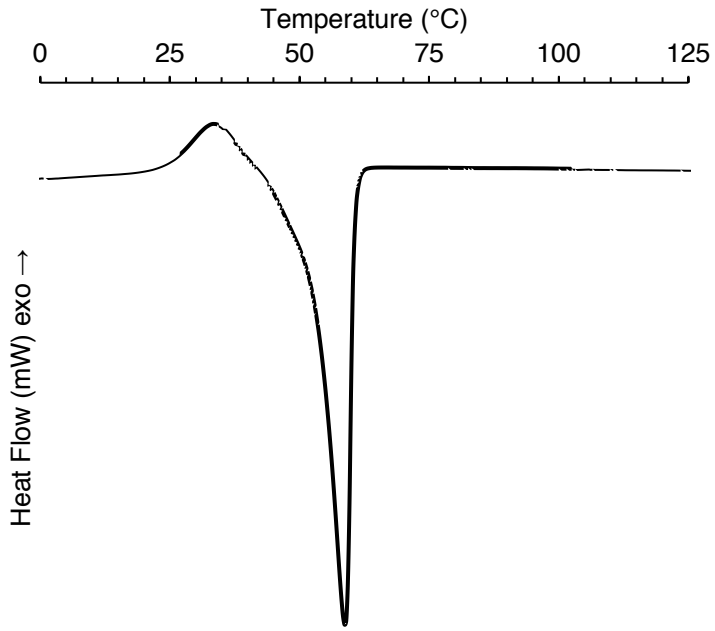

Figure S72. DSC thermogram of PO-CL copolymer from Supplementary Table 1, Entry 8.

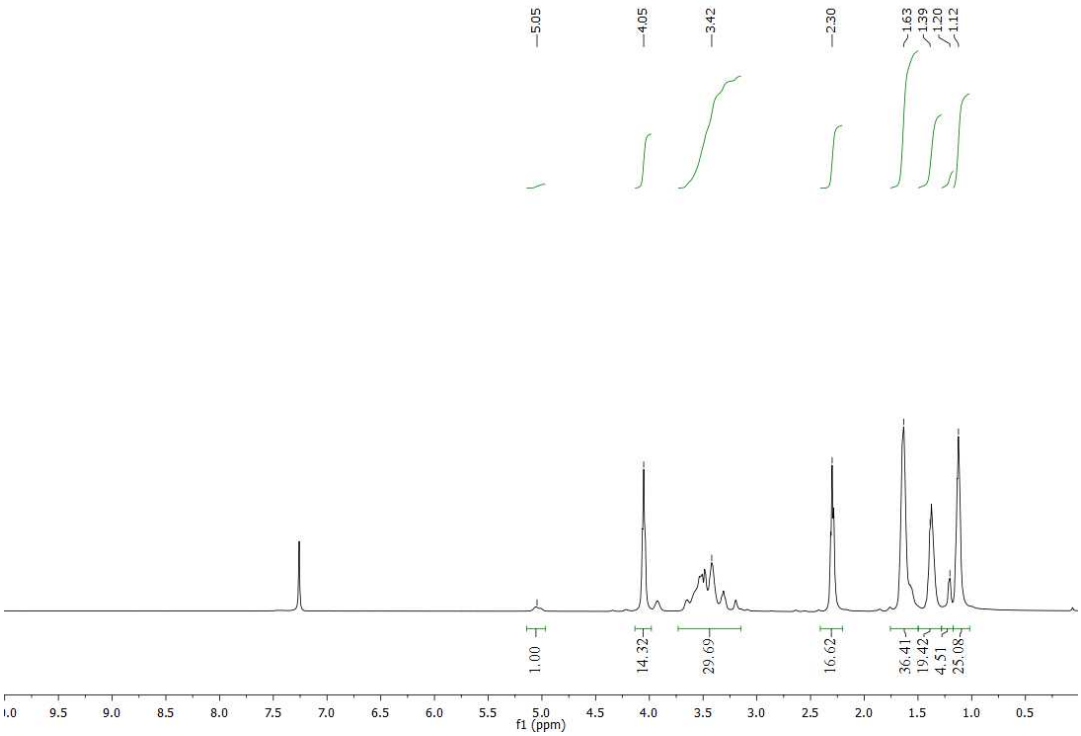

Figure S73. [1]H NMR spectrum of PO-CL copolymer from Supplementary Table 1, Entry 9.

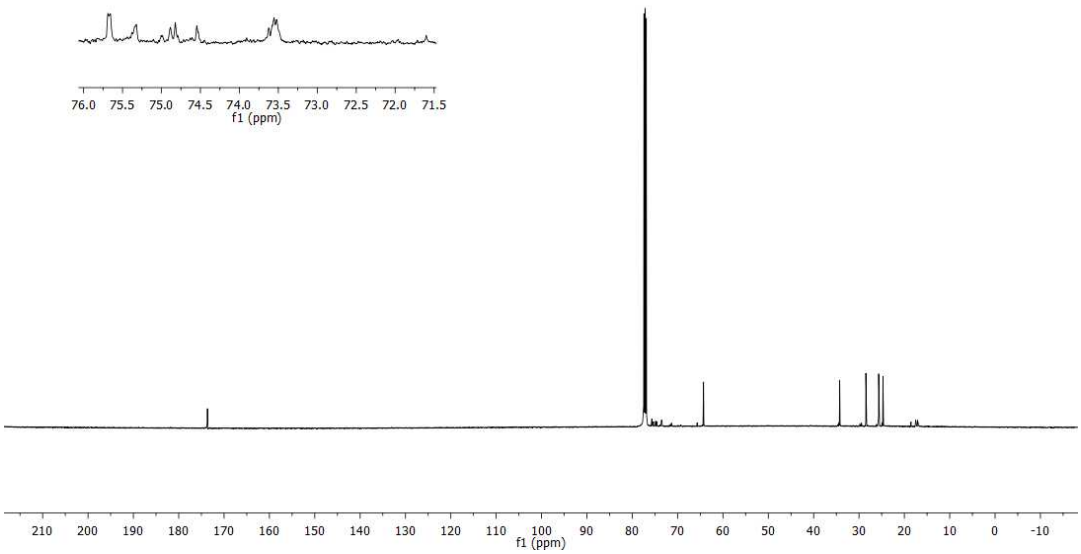

Figure S74. [13]C NMR spectrum of PO-CL copolymer from Supplementary Table 1, Entry 9.

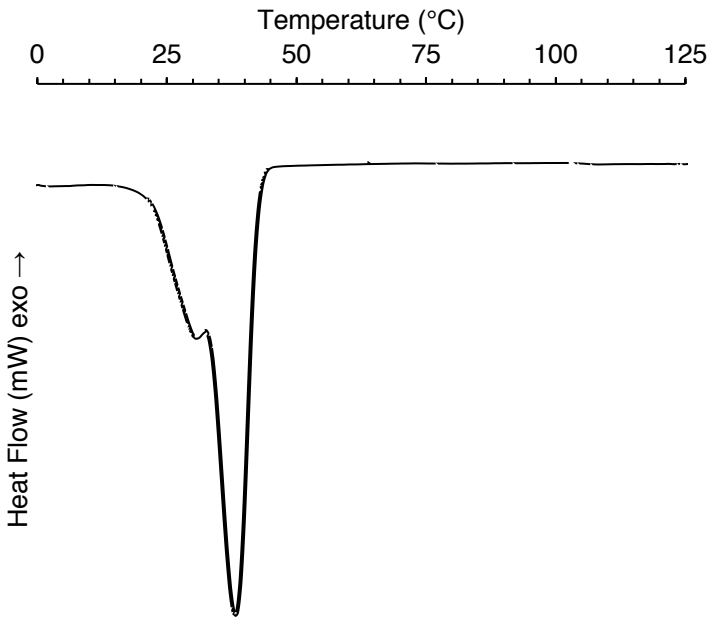

Figure S75. DSC thermogram of PO-CL copolymer from Supplementary Table 1, Entry 9.

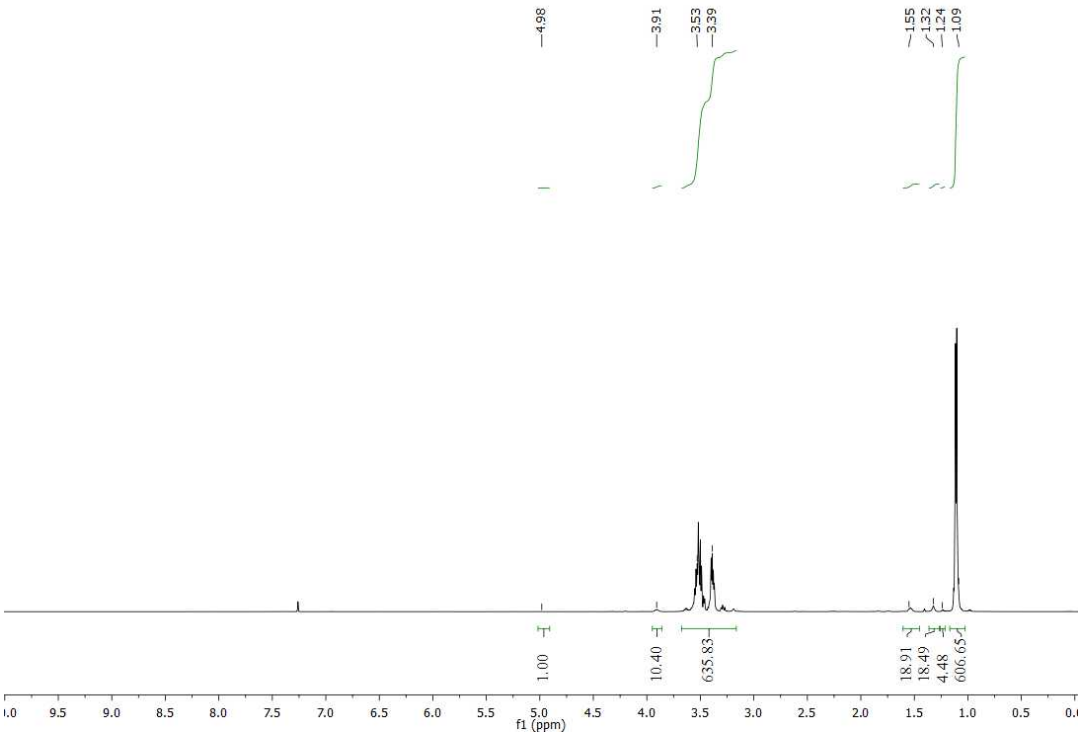

Figure S76. [1]H NMR spectrum of PO-CL copolymer from Supplementary Table 1, Entry 10.

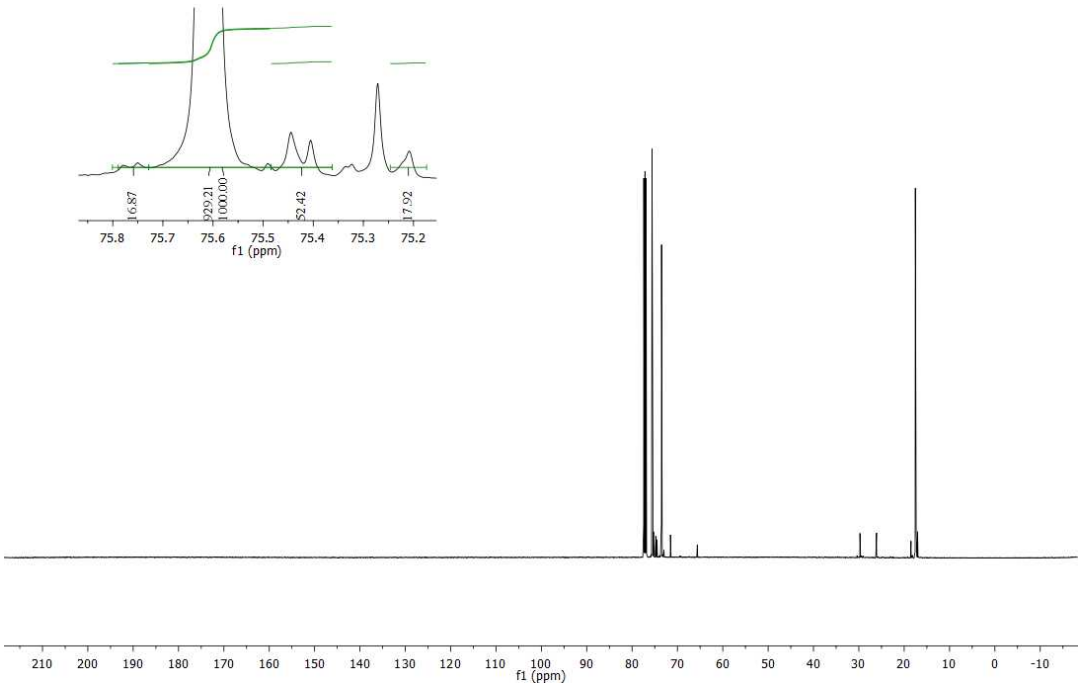

Figure S77. [13]C NMR spectrum of PO-CL copolymer from Supplementary Table 1, Entry 10.

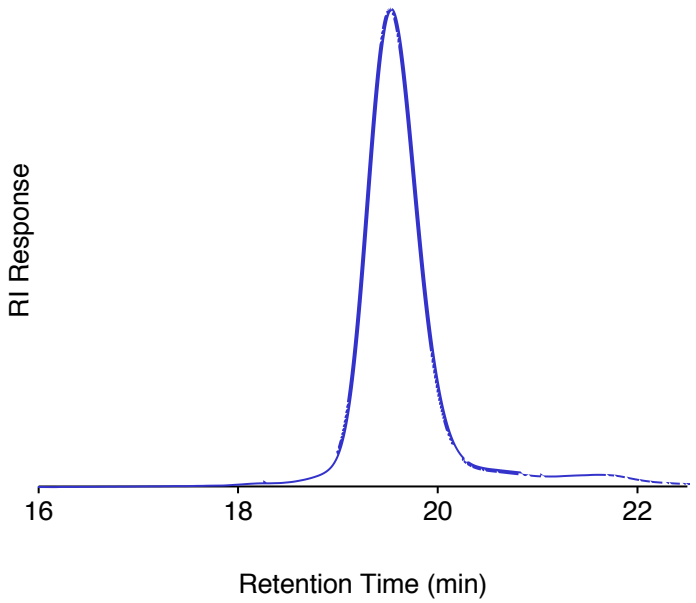

Figure S78. GPC chromatogram of PO-CL copolymer from Supplementary Table 1, Entry 10.

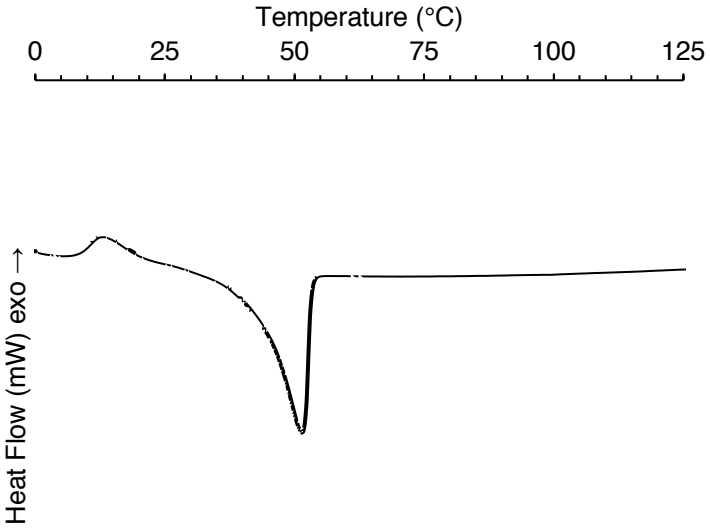

Figure S79. DSC thermogram of PO-CL copolymer from Supplementary Table 1, Entry 10.

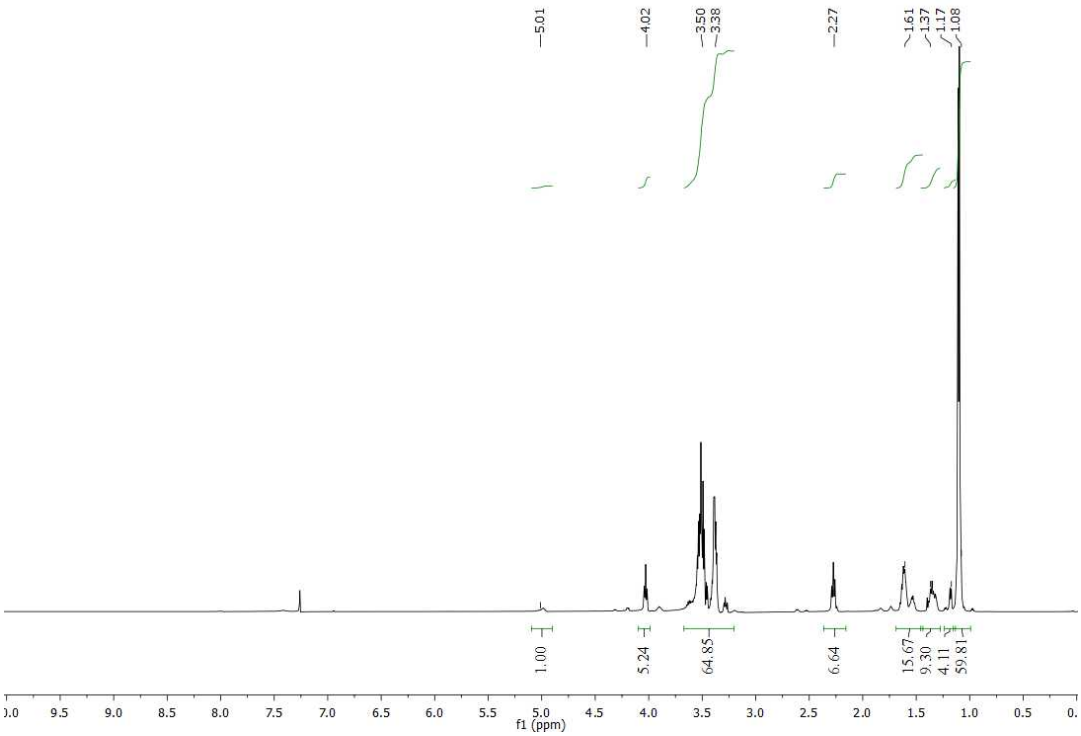

Figure S80. [1]H NMR spectrum of PO-CL copolymer from Supplementary Table 1, Entry 11.

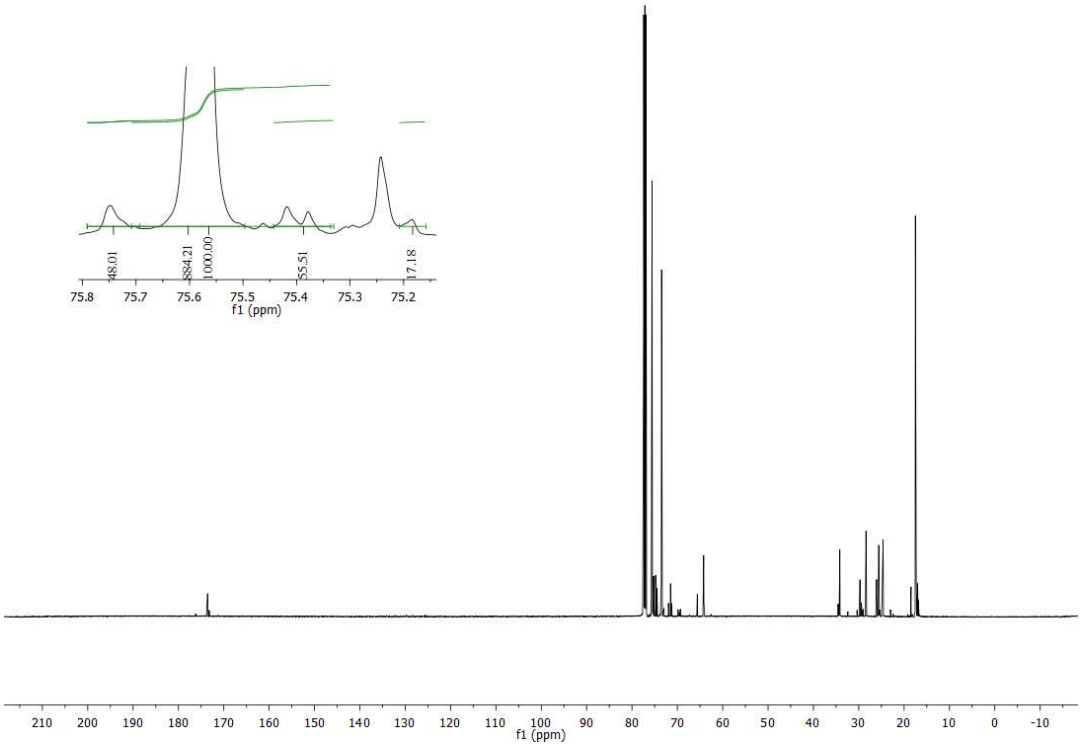

Figure S81. [13]C NMR spectrum of PO-CL copolymer from Supplementary Table 1, Entry 11.

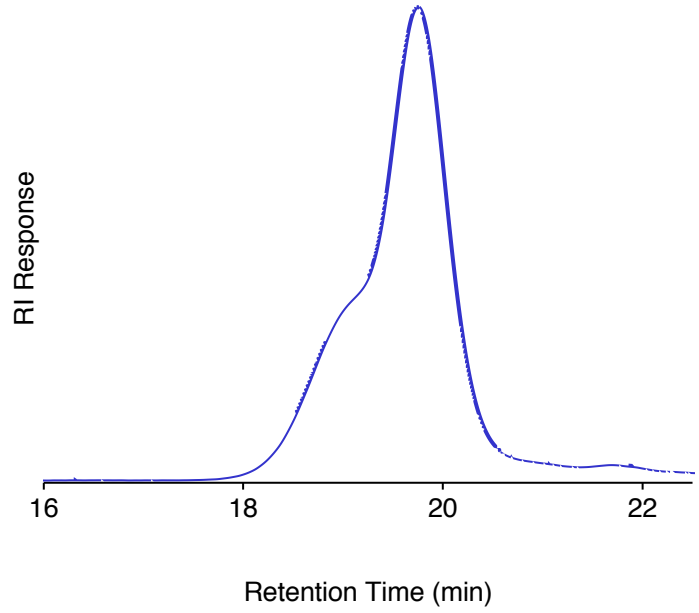

Figure S82. GPC chromatogram of PO-CL copolymer from Supplementary Table 1, Entry 11.

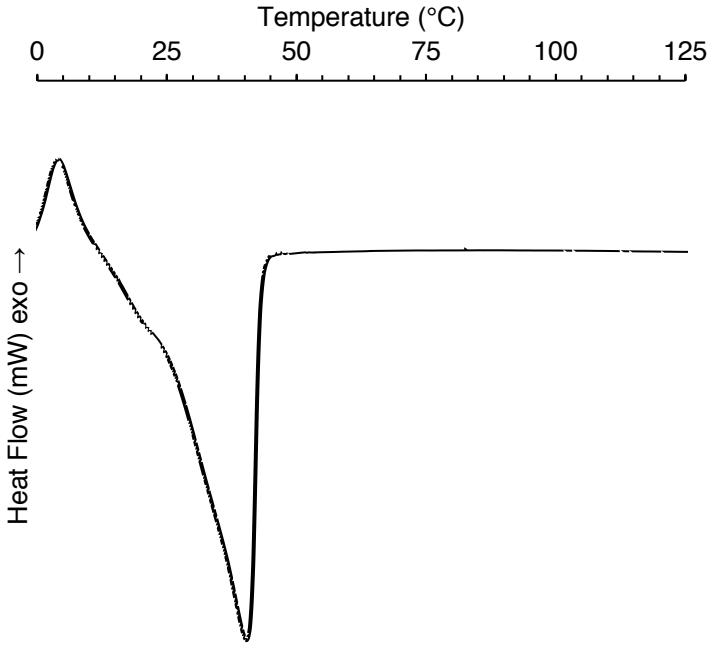

Figure S83. DSC thermogram of PO-CL copolymer from Supplementary Table 1, Entry 11.

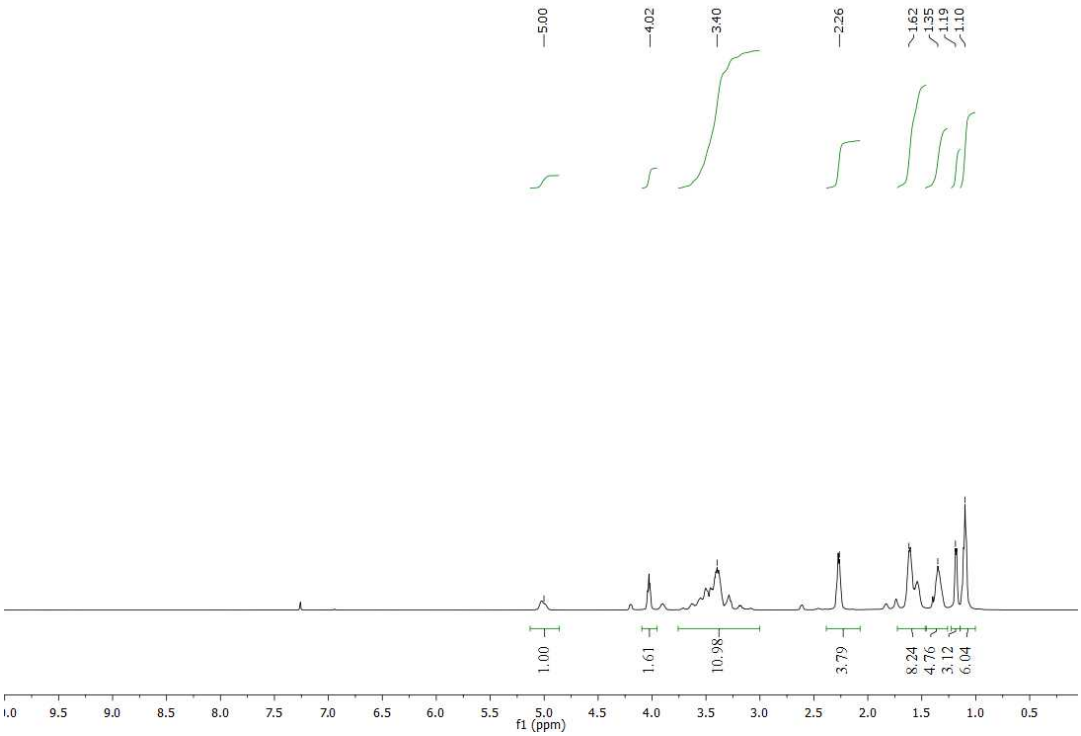

Figure S84. ^{1}H NMR spectrum of PO-CL copolymer from Supplementary Table 1, Entry 12.

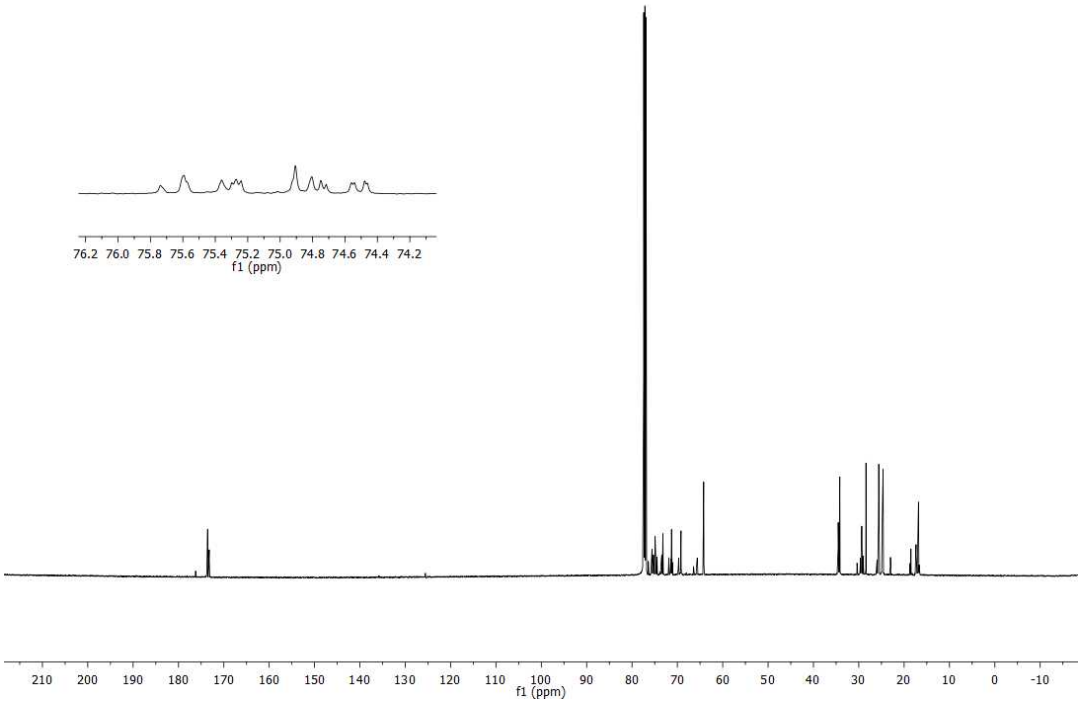

Figure S85. ^{13}C NMR spectrum of PO-CL copolymer from Supplementary Table 1, Entry 12.

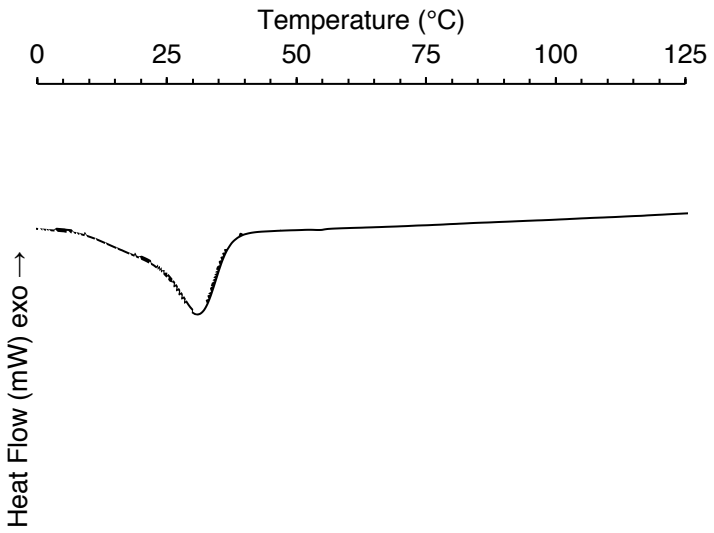

Figure S86. DSC thermogram of PO-CL copolymer from Supplementary Table 1, Entry 12.

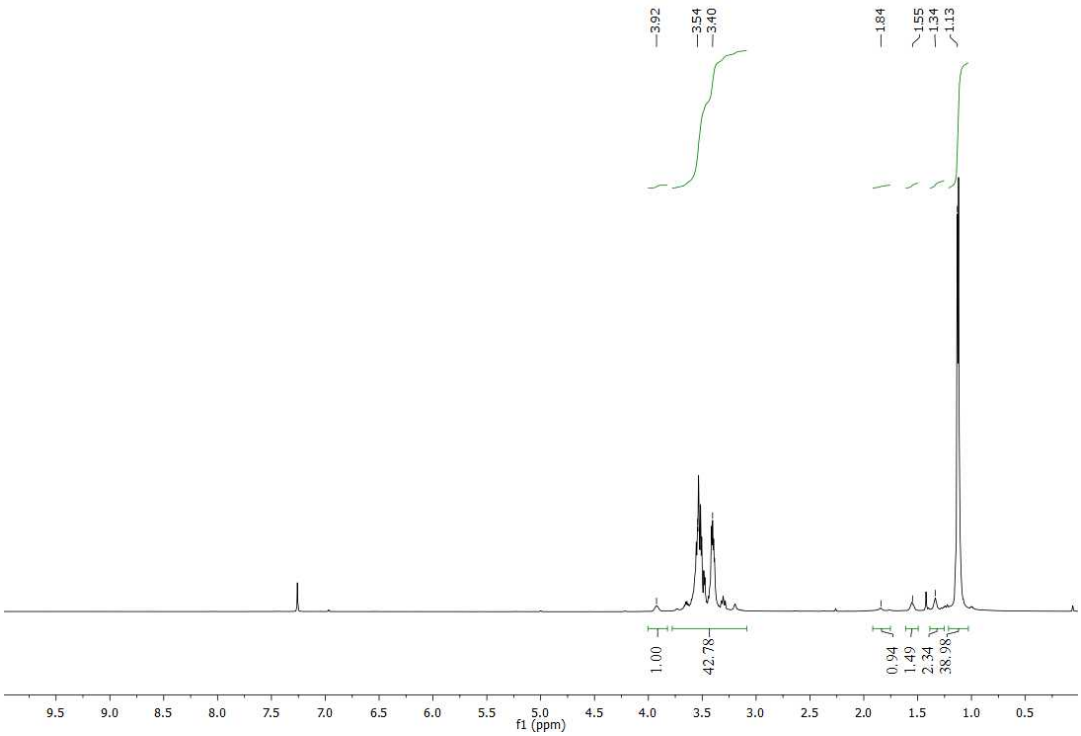

Figure S87. ^{1}H NMR spectrum of PO-BL copolymer from Supplementary Table 1, Entry 13.

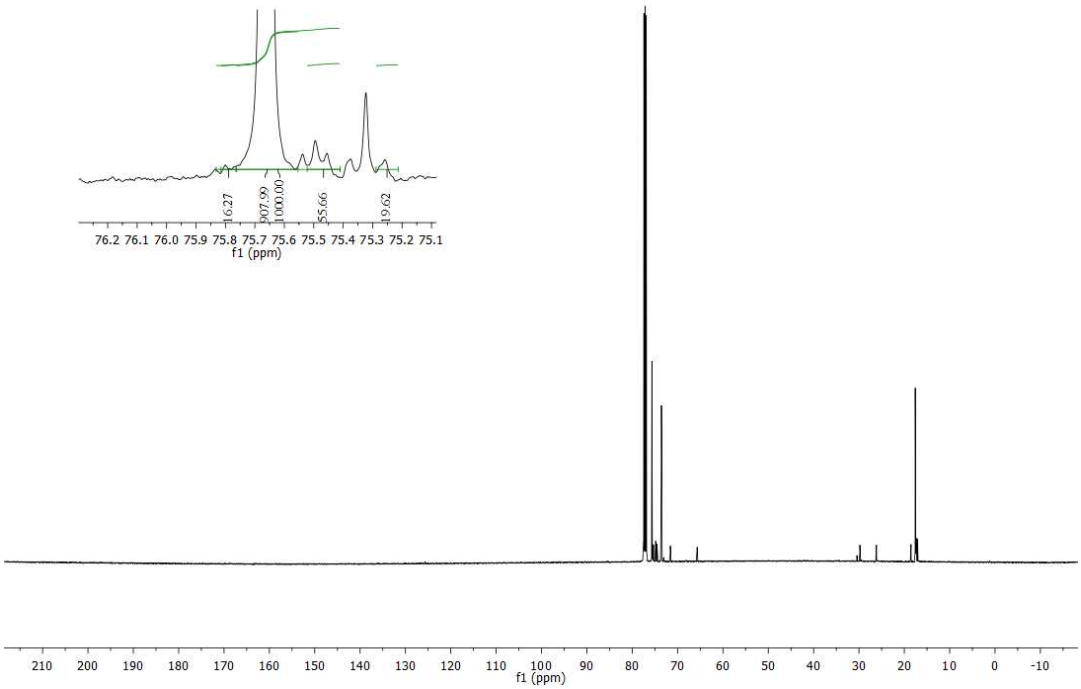

Figure S88. ^{13}C NMR spectrum of PO-BL copolymer from Supplementary Table 1, Entry 13.

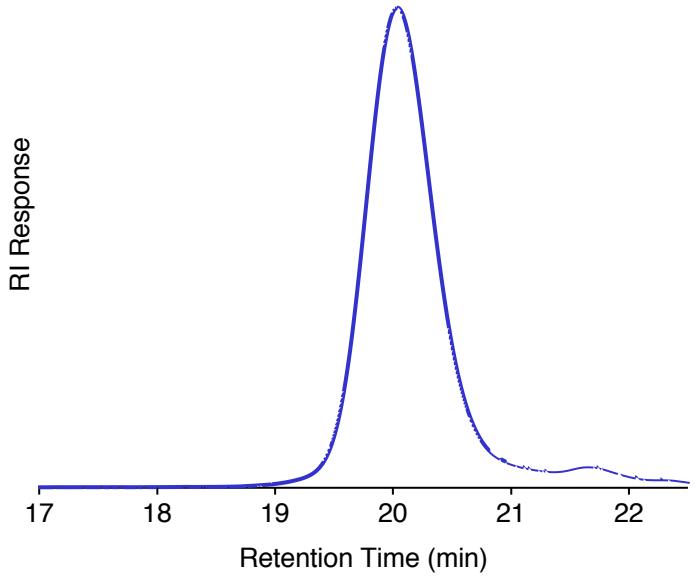

Figure S89. GPC chromatogram of PO-BL copolymer from Supplementary Table 1, Entry 13.

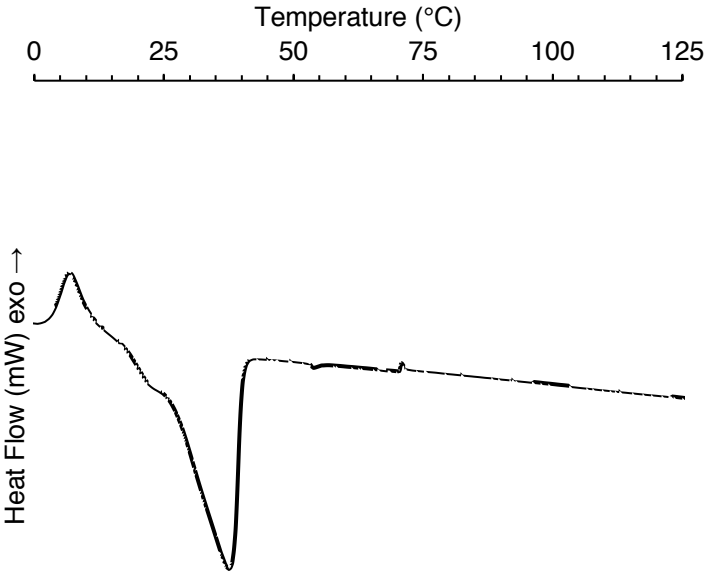

Figure S90. DSC thermogram of PO-BL copolymer from Supplementary Table 1, Entry 13.

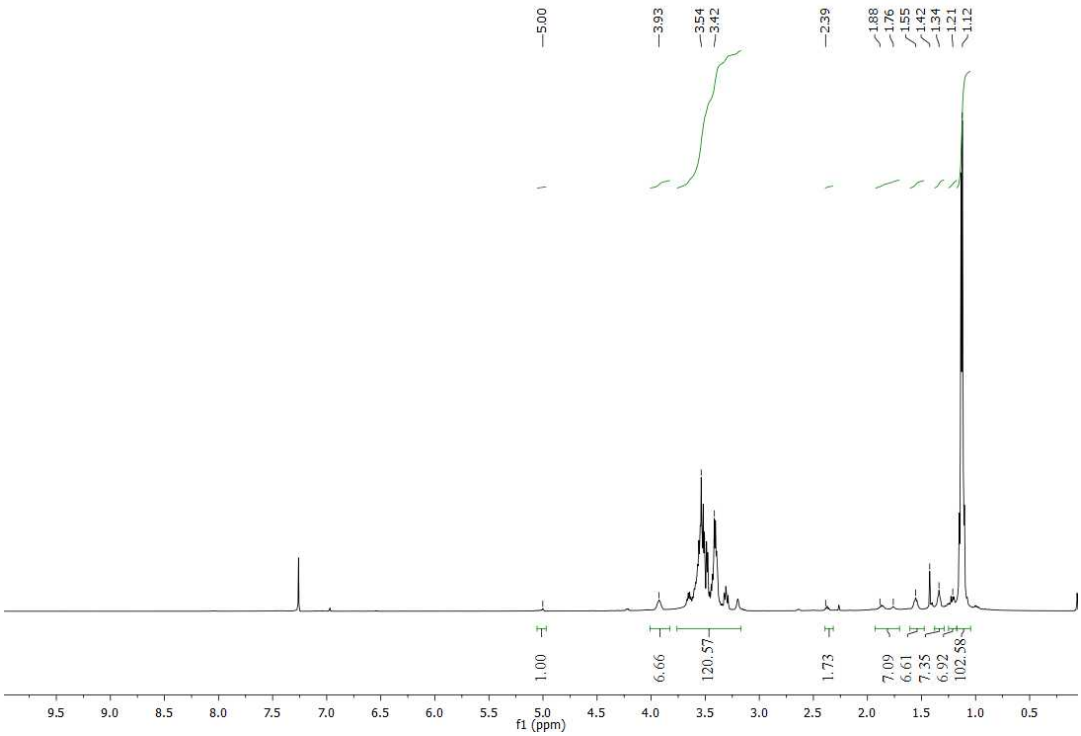

Figure S91. ^{1}H NMR spectrum of PO-BL copolymer from Supplementary Table 1, Entry 14.

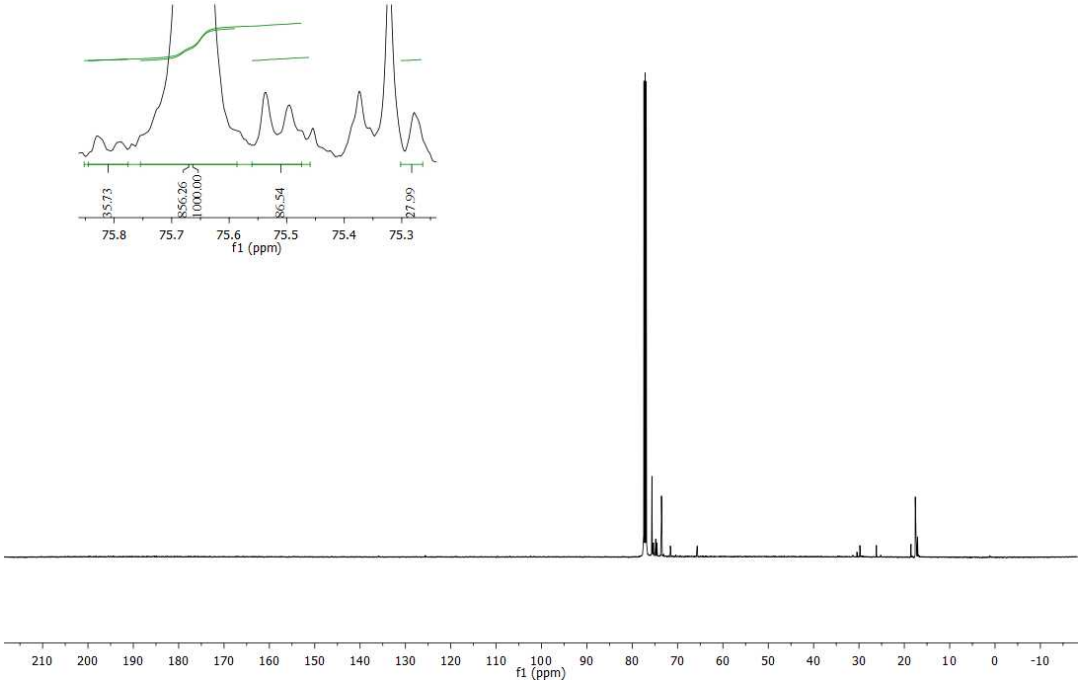

Figure S92. ^{13}C NMR spectrum of PO-BL copolymer from Supplementary Table 1, Entry 14.

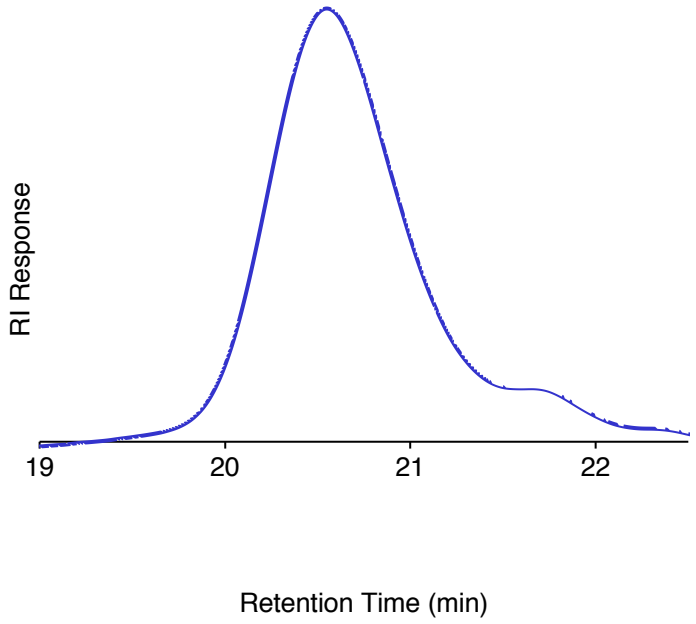

Figure S93. GPC chromatogram of PO-BL copolymer from Supplementary Table 1, Entry 14.

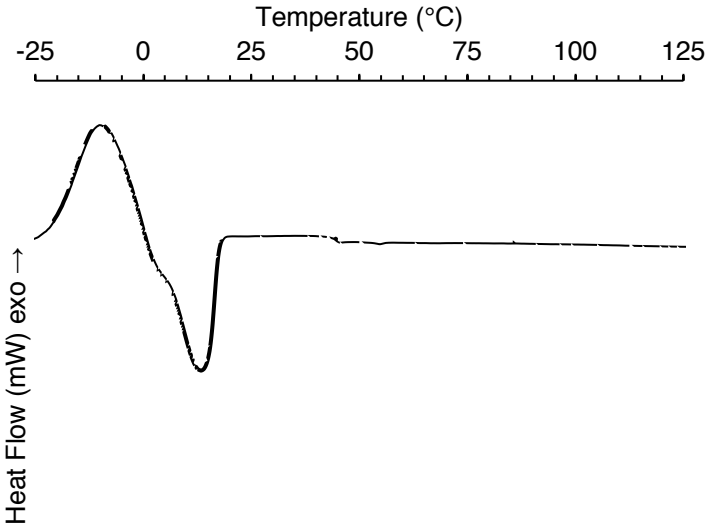

Figure S94. DSC thermogram of PO-BL copolymer from Supplementary Table 1, Entry 14.

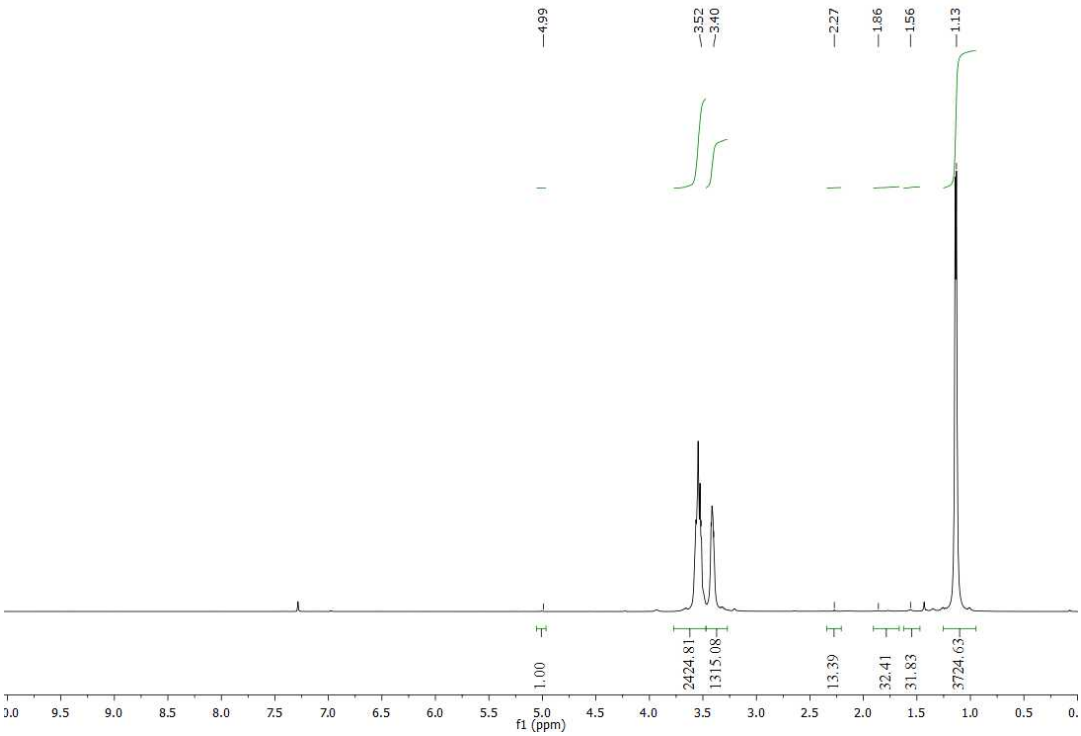

Figure S95. [1]H NMR spectrum of PO-BL copolymer from Supplementary Table 1, Entry 16.

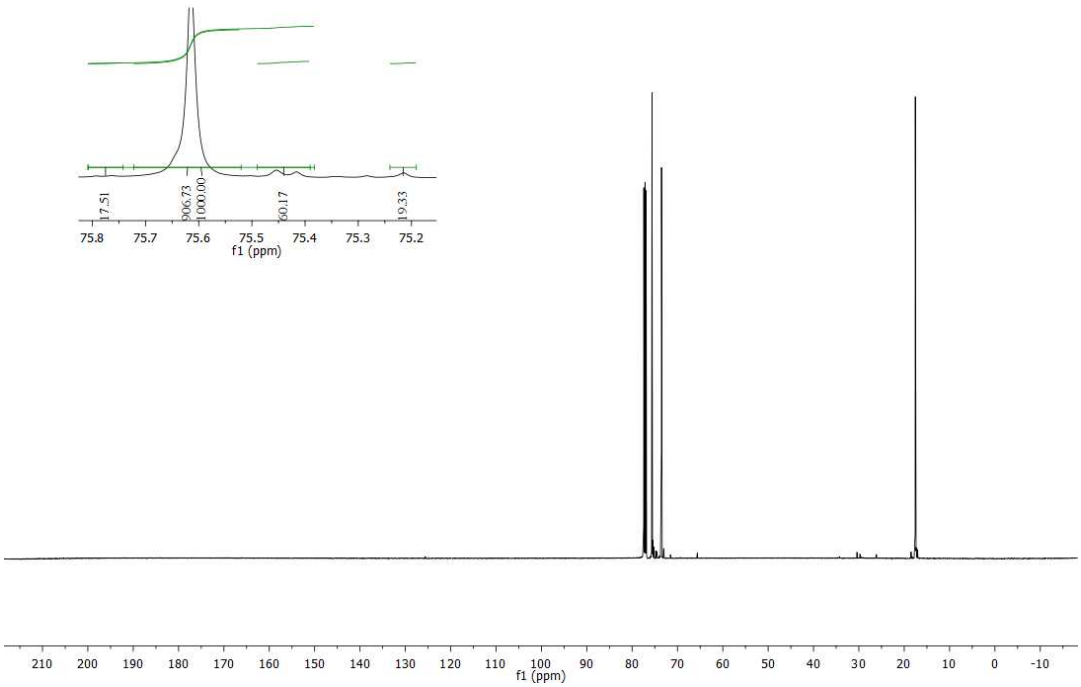

Figure S96. [13]C NMR spectrum of PO-BL copolymer from Supplementary Table 1, Entry 16.

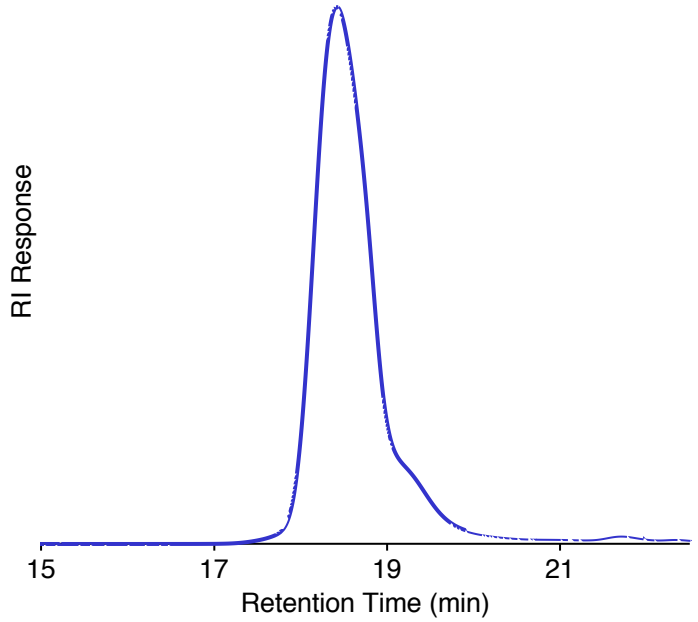

Figure S97. GPC chromatogram of PO-BL copolymer from Supplementary Table 1, Entry 16.

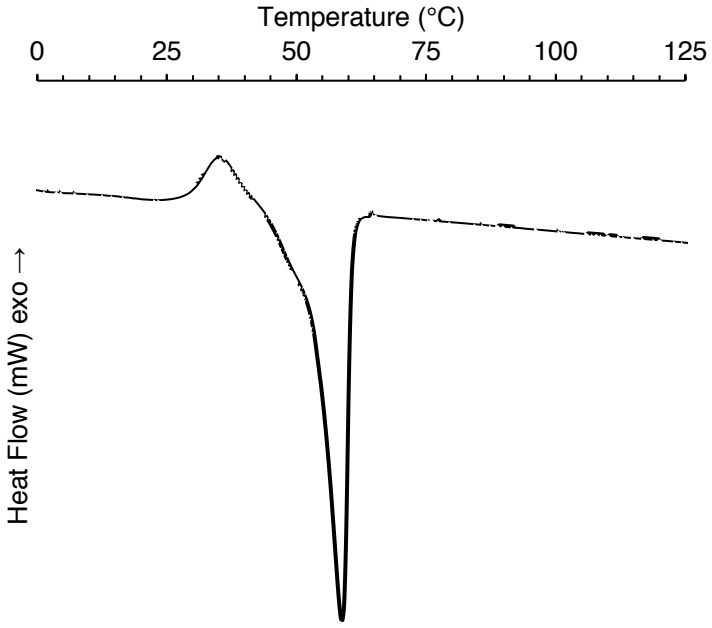

Figure S98. DSC thermogram of PO-BL copolymer from Supplementary Table 1, Entry 16.

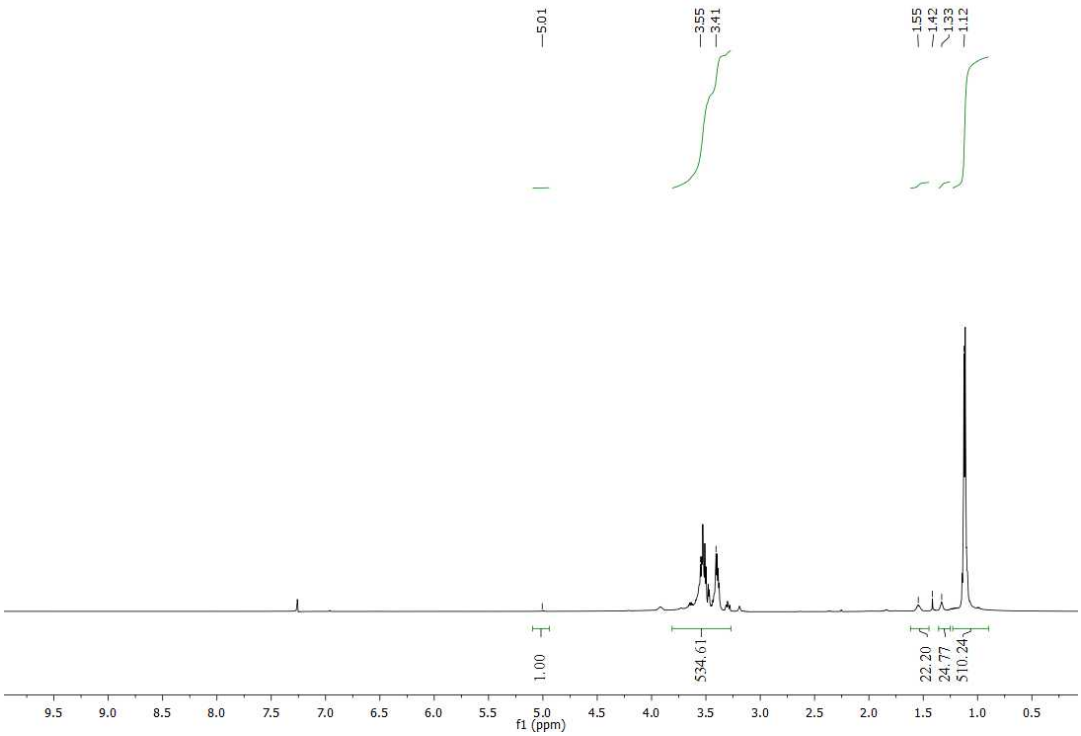

Figure S99. ^{1}H NMR spectrum of PO-BL copolymer from Supplementary Table 1, Entry 18.

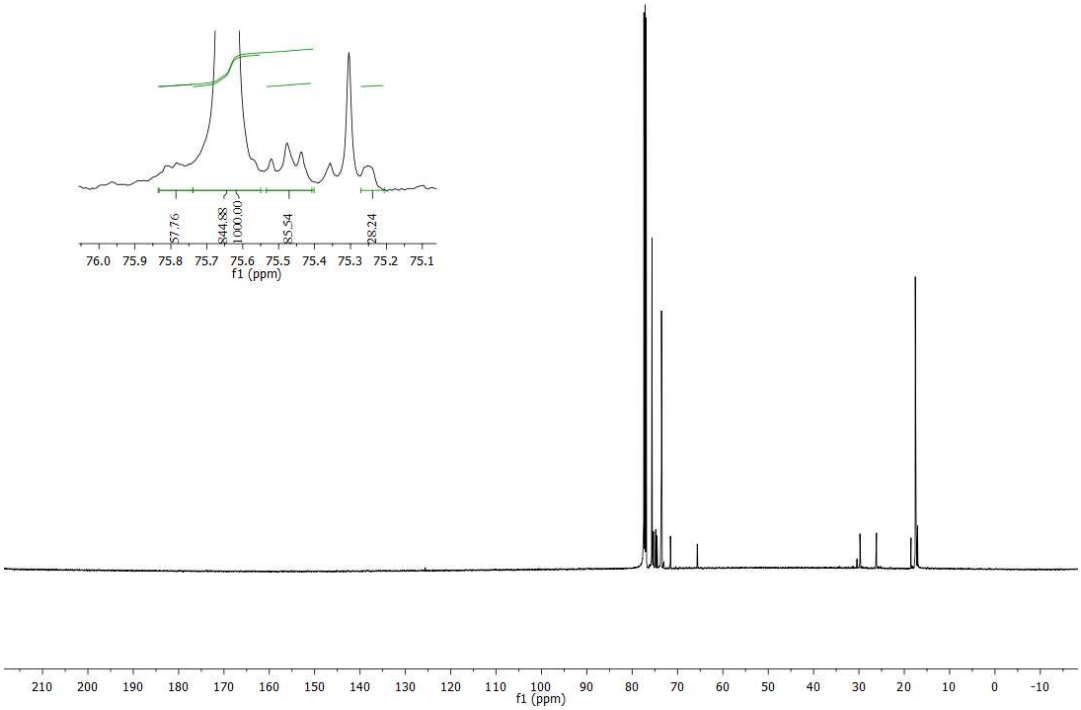

Figure S100. ^{13}C NMR spectrum of PO-BL copolymer from Supplementary Table 1, Entry 18.

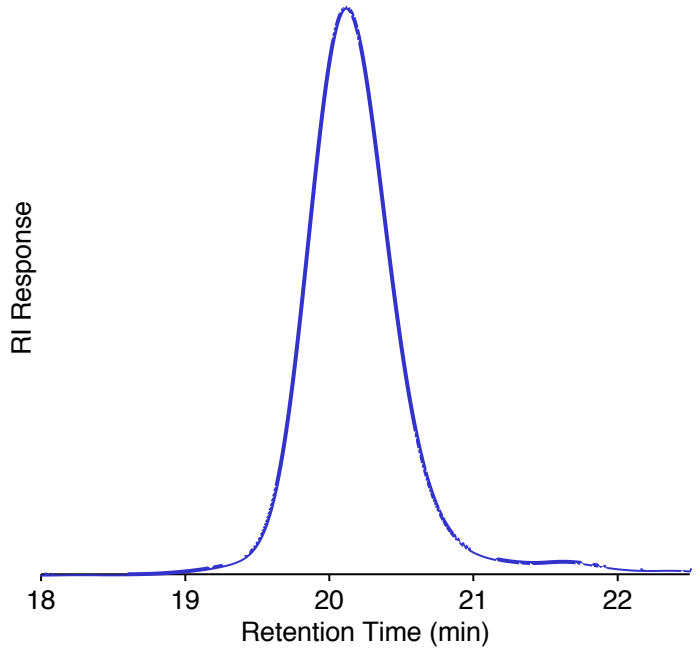

Figure S101. GPC chromatogram of PO-BL copolymer from Supplementary Table 1, Entry 18.

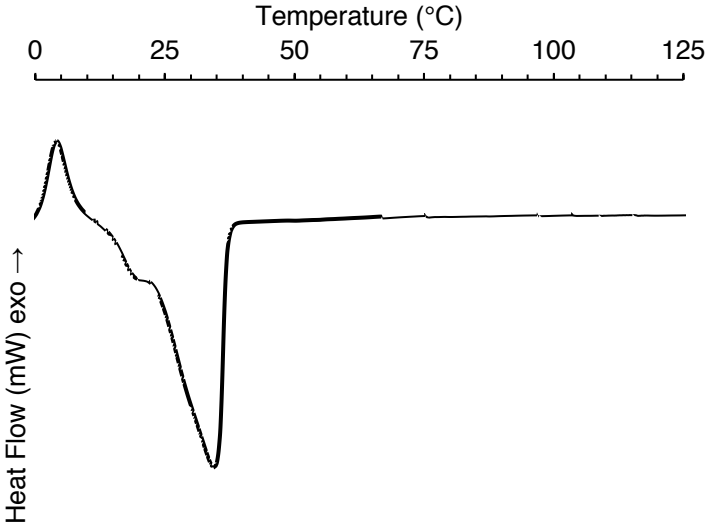

Figure S102. DSC thermogram of PO-BL copolymer from Supplementary Table 1, Entry 18.

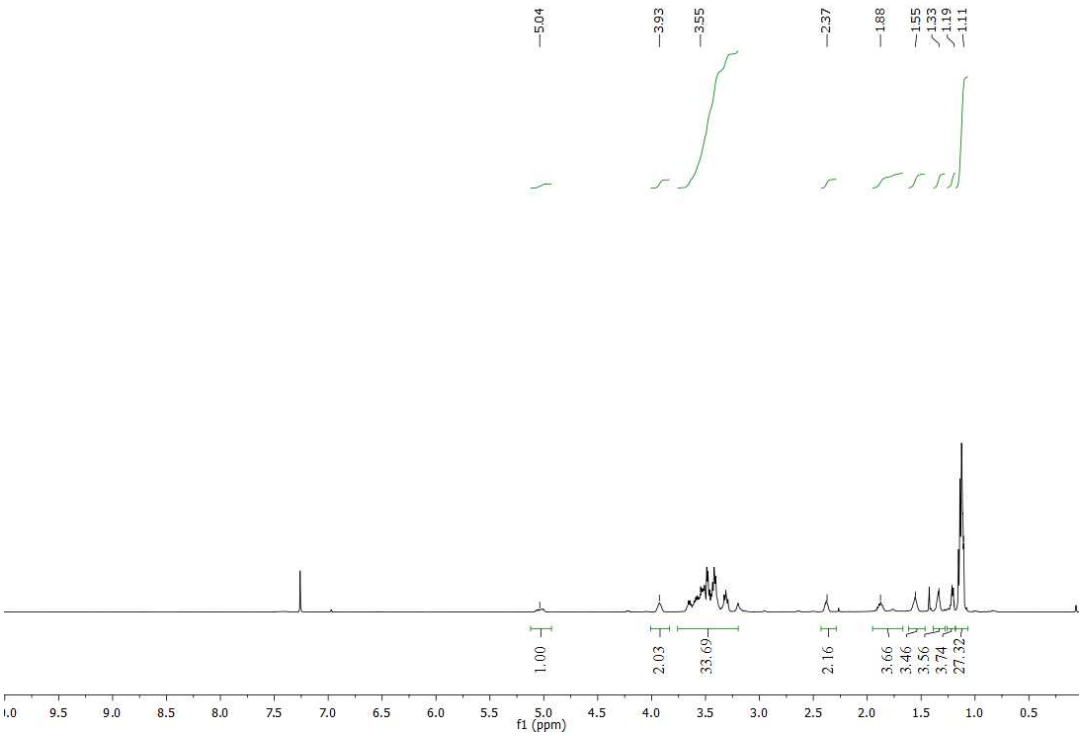

Figure S103. ^{1}H NMR spectrum of PO-BL copolymer from Supplementary Table 1, Entry 19.

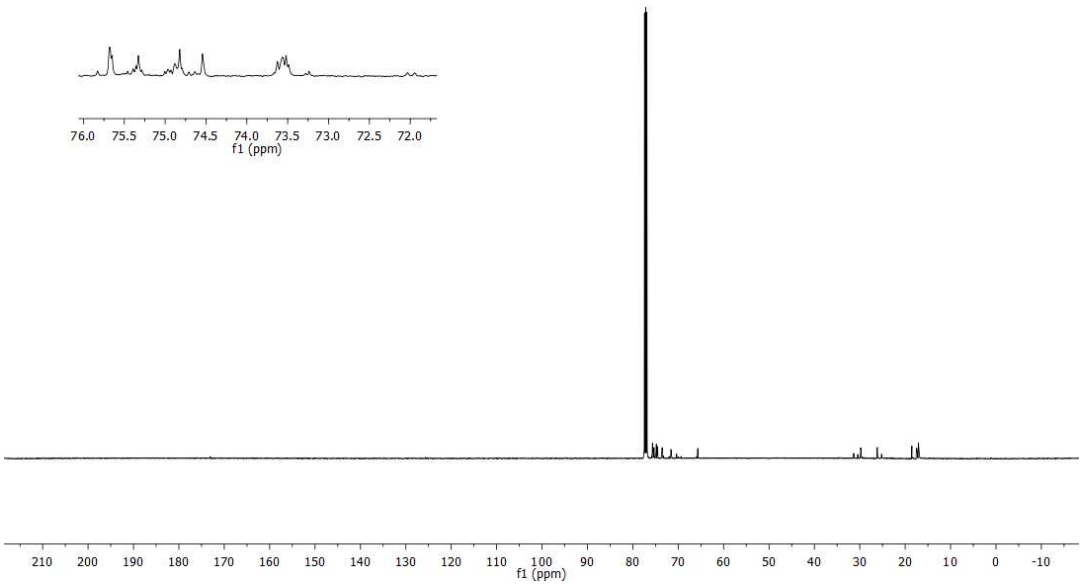

Figure S104. ^{13}C NMR spectrum of PO-BL copolymer from Supplementary Table 1, Entry 19.

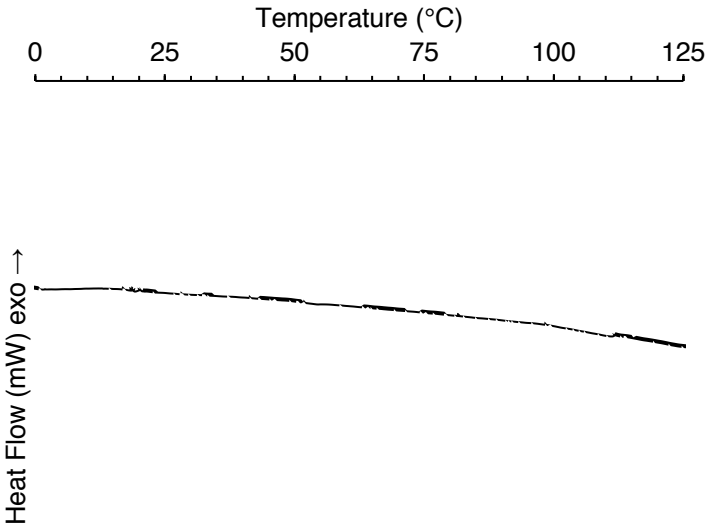

Figure S105. DSC thermogram of PO-BL copolymer from Supplementary Table 1, Entry 19.

References

1. M. I. Childers, A. K. Vitek, L. S. Morris, P. C. B. Widger, S. M. Ahmed, P. M. Zimmerman and G. W. Coates, *J. Am. Chem. Soc.,* 2017, **139**, 11048–11054.
2. L. S. Morris, M. I. Childers and G. W. Coates, *Angew. Chem. Int. Ed.*, 2018, **57**, 5731–5734.
3. B. Antalek and W. Windig, *J. Am. Chem. Soc*., 1996, **118**, 10331–10332.
4. L. Castañar, G. Dal Poggetto, A. A. Colbourne, G. A. Morris, M. Nilsson, *Magn. Reson. Chem.*, 2018, **56**, 546–558.
5. B. Antalek, L. Slater, G. Bennett, *Macromolecules*, 2019, **52**, 1025–1032.